REPORT NO. P66-66
HAC REFERENCE NO. A1859

SPACECRAFT ANTENNA SYSTEMS

FINAL ENGINEERING REPORT

OCTOBER 1963 – JANUARY 1966
NAS 5-3545

COMMUNICATIONS RESEARCH BRANCH
CODE 733
GODDARD SPACE FLIGHT CENTER
GREENBELT, MARYLAND

BY
- W.H. KUMMER
- R.A. BIRGENHEIER

AEROSPACE GROUP
RESEARCH AND DEVELOPMENT DIVISION

HUGHES

HUGHES AIRCRAFT COMPANY
CULVER CITY, CALIFORNIA

Report No. P66-66
HAC Ref. A1859

FINAL ENGINEERING REPORT

for

STUDY OF SPACECRAFT ANTENNA SYSTEMS

(October 1963 - January 1966)

March 1966

Contract No. NAS 5-3545

W.H. Kummer and R.A. Birgenheier

Prepared by

Antenna Department
Hughes Aircraft Company
Culver City, California

APPROVED:

L. L. Bailin

L. L. Bailin, Manager
Antenna Department

for

Goddard Space Flight Center
Greenbelt, Maryland
Communications Research Branch Code 733
Louis J. Ippolito, Technical Officer

CONTENTS

ILLUSTRATIONS

TABLES

SUMMARY

A two-year study (October 1963 to January 1966) of Spacecraft Antenna Systems was performed by the Hughes Aircraft Company for the NASA/Goddard Space Flight Center. Objective of the program was the recognition of advanced antenna techniques that would provide spacecraft communication systems that were highly reliable and low in power consumption. An intensive Phase I survey of the state-of-the-art in antenna techniques, especially beam-steering concepts, identified several promising self-steering techniques for Phase II implementation. Two specific techniques were designed and built as breadboards; a multiple-beam transdirective concept developed at Hughes and a self-phasing retrodirective concept. Both had 10-MHz bandwidths with center frequencies of 6.301 GHz for the up-link and 4.081 GHz for the down-link.

The multiple-beam breadboard used two separate 4-by-4 arrays and two beam-forming matrices, one to form multiple beams to receive an information signal from one arbitrary direction and the other to form beams for retransmission in response to a pilot signal from another arbitrary point. This system performed satisfactorily on both receive and transmit and met most design objectives. Gain of the 6-GHz receiving section was 20.8 at the peak of a center beam and 15.0 db at the crossover of two outside beams. Predicted values were 21 and 14 db, respectively.

The self-phasing breadboard used the same 4-GHz array for transmitting as the multiple-beam system and automatically formed a high-gain beam in response to a pilot signal to relay information previously received. The receiving antenna was one helical element with a 50-degree beamwidth. Self-phasing was accomplished by phase reversal through mixing. Antenna patterns of the breadboard were as predicted, and measured signal levels were close to those predicted. Gain of the

4-GHz transmitting array at broadside was 21 db compared with a predicted 21.75. Minimum gain was 18 db.

It is believed that these breadboards represent the first time these beam-steering concepts have been implemented in functioning systems. Both designs appear feasible for application to satellite antenna communication systems. It is recommended that engineering models of each technique be designed and constructed and that study of new and advanced components for self-steering arrays be continued.

ACKNOWLEDGMENTS

This program involved the participation and cooperation of many individuals. The contributions of the following Hughes Aircraft Company personnel are acknowledged:

M. C. Behnke, G. Brand, M. T. Delzell, B. J. Forman, J. Howard, A. P. King, F. A. Lauriente, C. H. Nonnemaker, Jr., A. F. Seaton, S. S. Shapiro, E. D. Shaw, F. G. Terrio, P. Umphres, A. T. Villeneuve, and O. C. L. Witte.

The interest, support, and suggestions of the Technical Officers from NASA/Goddard Space Flight Center should also be mentioned. These officers included A. Kampinsky, D. Backus, J. Driver, and L. Ippolito.

1.0 INTRODUCTION

1.1 PROGRAM OBJECTIVES

A two-year survey of Spacecraft Antenna Systems was performed in two phases from October 1963 to January 1966 by the Hughes Aircraft Company for the NASA/Goddard Space Flight Center. Objective of the program was the recognition of techniques that would provide spacecraft antenna systems capable of optimum reliability with least power consumption. Primary emphasis was placed on electronic beam-steering techniques. Phase I consisted of an intensive study of advanced antenna techniques that could be applied to spacecraft systems; it included a literature search, a field survey, and a critical analysis of many possible electronic scanning and steering techniques. Results were published in an Interim Engineering Report, Phase I - Final report (Kummer and Villeneuve, 1965).

From the most promising antenna techniques identified in the Phase I survey, several were chosen as being particularly applicable to satellite communications, and two specific configurations were recommended for further study and for implementation. These configurations were designed, fabricated, and tested in the second phase of the Spacecraft Antenna Systems program. The present report constitutes the Final Program Report, but it is mainly concerned with the implementation of the two breadboard systems.

1.2 IMPLICATIONS OF HIGH-GAIN ANTENNAS

The antenna in present-day satellite communication systems is primitive. Any improvement in this component would substantially increase the overall capability of the entire communication system. The immediate area for potential antenna improvement lies in a substantial increase in gain. At the present time, this improvement could be realized without undue difficulty. The implications of increased gain

are so important that a consideration of antenna techniques must be part of any overall system design for a mission. These techniques form an essential part of the trade-offs in weight, accuracy, and reliability.

The pertinent characteristics of an antenna are closely interrelated. High gain implies a beam from the satellite antenna that is narrower than a beam that would subtend the earth, an aperture that is large compared with wavelength and thus is physically large at the lower frequencies but small at the higher frequencies, and a steering mechanism that can point the antenna beam continuously at one or more selected locations on earth. The degree of pointing accuracy required of a satellite antenna increases as its directivity is increased. Two limitations are encountered here, one in the capability of a vehicle to control its mechanical orientation and the other in the accuracy with which this orientation may be determined at any given time. In addition, a question also exists of the extent to which control of the vehicle attitude is advisable in any given set of circumstances. The answers entail practical compromises and depend on the techniques available for directing or steering the antenna beam as compared with those for controlling the vehicle attitude.

Three types of steering mechanisms are possible for satellite antenna systems: mechanical, including large appendage antennas; electromechanical; and electronic or inertialess. The electronic techniques offer the greatest versatility with regard to communications between satellites and earth, between satellites and airborne vehicles and ships at sea, and between satellites themselves. Once implemented in some form and with the appropriate components, they also provide a simplicity of operation that increases system reliability. There are two generic types: those that require external controls to properly phase the elements and those that are self-steering. The externally controlled systems such as the conventional phased array need an external sensor (i-r, r-f, or ground station) to point the beam and a computer, phasing network, and attitude sensing device to point the beam appropriately. In a self-steering system, however, attitude information is presented to the antenna system by a pilot beam from

a ground station, and electronic circuitry senses the phase of incoming pilot signals to position a beam in that direction.

1.3 SELF-STEERABLE ANTENNAS

Three general groups of self-steerable antennas were analyzed in Phase I of the Spacecraft Antenna Systems program as potentially capable of fulfilling the characteristics dictated by a space mission: switched multiple-beam antennas, self-phased arrays, and adaptive arrays. Special configurations in each of the first two groups were designed and built as breadboard models during Phase II of the program.

1.3.1 Switched Multiple-Beam Antennas

This type of self-steerable system uses multiple-beam antennas with appropriate switching and control circuitry to select the proper beam either on command from the transmitter station or as indicated by a pilot signal from the receiver station. Several configurations are possible, including multiple feed lenses, reflectors, and beam-forming matrices.

The multiple-beam antenna breadboarded at Hughes was a special configuration called the Transdirective Array. It utilizes one hybrid beam-forming matrix and array elements to form a high-gain antenna that receives incident signals from arbitrary directions and processes them to have arbitrary amplification and frequency before reradiating the signals from the same or another matrix toward arbitrary, desired directions. The system selects the signals from the stations, which identify themselves with unique pilot tones, and reradiates these signals toward other stations. The redirecting is accomplished either through the use of pilot tones transmitted from the desired receiving station or by a command signal from the transmitter. The participating stations all utilize the high gain and directivity of the Transdirective Array as they simultaneously communicate with one another through the spacecraft.

Some of the more important characteristics of switched multiple-beam antennas are listed below.

Advantages

a) They do not require variable phase shifters to scan the beam.
b) Their gain is not limited by the requirement that each beam cover the entire visible earth.
c) They are applicable to both nonsynchronous and synchronous gravity-gradient stabilized orbits.
d) They require no earth sensor and no preprogrammed controls.
e) They utilize inherently reliable r-f components (matrix or lens).
f) They have satellite attitude information inherently available.
g) They readily lend themselves to control by command.

Disadvantages

a) They require large numbers of couplers or hybrids (array with beam-forming matrix).
b) They require generation of pilot signal at the receiver.
c) Their weight may be a problem, depending on the configuration (use of a lens, for instance).
d) They require electronically controlled r-f switches and switch control circuitry.
e) Switching among the beams may result in switching transients in the information signal.
f) The minimum useful signal is determined by the gain at the switch-over point. For smooth transfer, variable power dividers instead of switches may have to be used between beams (additional circuitry and control circuitry).

1.3.2 Self-Phased Arrays

This group of self-steerable antennas is composed of conformal arrays of elements, each of which has its own electronic circuitry that automatically phases the elements to produce a beam in the direction

dictated by a pilot signal from a station desiring to communicate with a transmitting station.

In the simplest form of the self-phasing or retrodirective array, the needed phase inversion is derived from a mixing action. A c-w signal received by the nth element of an array is subtracted from (mixed with) a common local oscillator to obtain a transmit signal which is nearly of the same frequency as the received signal except that it has an inverted phase angle. The phase angle is similarly inverted at every element to create the condition by which the transmit signal is amplified and formed into a beam in essentially the same direction as the received signal. A circulator or branching filter is used to separate the transmit and receive signals at the antenna elements. A slight frequency shift is used to improve isolation between transmitted and received signals. A design of this type was breadboarded in the second phase of the program.

In a more advanced form of the idea, the total incoming signal at the nth element consists of a narrow band pilot signal (ω_{p1}), offset from a broad information band (ω_m). The signals are subtracted from a suitable offset frequency (ω_1) and the difference frequencies are filtered, separately amplified, and mixed once more. The signal at the last difference frequency ($\omega_m - \omega_{p1}$) which is independent of the incoming interelement phase shift, is summed with all similar outputs from the other elements. At this point, the total array gain is realized.

A pilot (ω_{p2}) transmitted from the receiving ground station is also processed to form a beam toward that station. The information which is summed is amplified, frequency-translated, and added to the pilot signal (ω_{p2}) to send the information toward the receiving station. Thus a complete communication channel is established.

The various types of self-phased arrays, arrays whose beams are steered automatically by use of the interelement phase shift of an incident pilot signal, have certain properties in common.

Advantages

a) The array is made up of independent channels so that failure of one is not catastrophic.

b) Controlled phase shifters are not required to steer the beam.

c) Their gain is not limited by the requirement that the beam cover the entire visible earth.

d) They are applicable to nonsynchronous, synchronous, stabilized, or unstabilized systems.

e) They require no earth sensor and no preprogrammed controls.

f) They are also applicable to satellite-to-satellite communications.

g) They are capable of being enlarged (growth potential).

h) They require no switches or switch controls.

i) Satellite attitude information is inherently available.

Disadvantages

a) The components needed for implementation in flight-qualified, lightweight form need further development (essentially true of most systems).

b) They require generation of pilot signal at receiver.

c) An N element array requires N phase-matched channels.

d) Each channel requires a complete receiver and transmitter.

1.3.3 Adaptive Arrays

This class of arrays is closely related to the self-phasing arrays but uses phase-locked loops at each element to accomplish the appropriate phasing across the antenna aperture. The term adaptive comes from certain properties of the loops which adjust the phase at each element to realize the maximum gain of the array regardless of the direction of the incoming signal. An adaptive array is a receiving antenna system employing a phase-locked loop at each active element which automatically adjusts the electrical phases of the signals received by each element to obtain antenna directivity. The basic operation of these arrays uses the phase-locked loop to lock the phase of the signal received by each element to that of a common reference signal. Thus the output of each element is in phase and can be added directly to realize the array gain

for any angle of signal incidence. Adaptive arrays can be made to transmit retrodirectively by appropriate additions to the circuitry at each element.

Advantages and disadvantages of adaptive arrays are similar to those of the self-phased arrays except for certain specific variations.

Advantages

a) The use of servo-controlled phase shifts can achieve very low tracking errors.
b) Phase shifters can handle large transmitted powers.
c) Satellite attitude information is inherently available.

Disadvantages

a) A servo loop and a controlled-phase shifter are required for each element in the array.
b) A trade-off is required between pointing accuracy and rapidity of beam positioning.
c) The beams which are formed cannot be split into several arbitrary beams for multiple access.
d) The circuitry for phase locking is complicated in practice.

1.4 EXPERIMENTAL IMPLEMENTATIONS

The two beam-steering techniques judged the best adapted for the present satellite programs are the multiple-beam array and the self-phasing array. Each concept was implemented by a breadboard design which is described in detail in this Final Report.

In general, a 6,000 n. mi. altitude was chosen for both configurations, with the angle subtended being 42 degrees. A gravity-gradient stabilization system was chosen for the satellite model. Because of the unknown librations in the gravity-gradient system, a coverage angle of 50° was used. Both systems had a bandwidth of 10 MHz with center frequencies of 6.301 GHz for the up-link and 4.081 GHz for the down-link. The pilot frequencies for the multiple-beam system were 6.310 GHz

for the receiving pilot and 6.313 GHz for the transmitting pilot. For the self-phasing system, the pilot frequency was 4.159 GHz.

Both systems utilized the same 4-by-4 array of helical elements at 4 GHz as their high-gain transmitting antenna. The multiple-beam system, in addition, had a similar 4-by-4 receiving array scaled to 6 GHz. The self-phasing system used one helical element with a 50° beamwidth at 6 GHz.

The multiple-beam antenna system used a transdirective concept developed at Hughes. One beam-forming matrix forms multiple beams to receive an information signal from one arbitrary direction while a separate matrix forms beams for retransmission in response to a pilot signal from another arbitrary point. The breadboard consisted of an r-f unit, an i-f unit, a logic unit, and a power supply unit. The 6-GHz receiving portion of the system processed both receiving and transmitting logic. I-f switches were used to select discrete beam positions for the receiving system, and ferrite digital switches and variable power dividers, in conjunction with the 4-GHz beam forming matrix, were used to form a continuum of beam positions for the transmitting section.

The system was rather bulky and complex due largely to the complexity of the logic circuitry; for example, over 1000 transistors alone were used. However, it did perform satisfactorily on receive and transmit, and it did meet most design objectives in signal levels, signal-to-noise ratios, shape of beam, and crossover points. Gain of the 6-GHz array measured at the beam ports of the beam-forming matrix was 20.8 db at the peak of a center beam and 15.0 db at the crossover of two outside beams. Predicted gain values were 21 db and 14 db, respectively. The gain on transmit was designed to be 18 db minimum with a ripple of 2 db and a 3-db fall off at the edges of coverages. (Maximum gain would be 21 db.) In certain instances the logic selected incorrect beams which degraded the minimum gain by 3 db. This problem is not inherent in the transdirective concept but lies only in the logic implementation. Recommendations for an improved logic are included.

The retrodirective system which was implemented used the self-phasing concept. One 50° beamwidth antenna receives information and another antenna, an array, automatically forms a high-gain beam in response to a pilot signal to relay the information received. Self-phasing is accomplished by phase reversal. This breadboard was constructed as one unit which contained the r-f and i-f components, the only external equipment being the power supplies and the local oscillators. A conventional receiver was used for the information channel; it directed the information to the 16 channels of the system by way of a 16-way power divider. Phase reversal was accomplished by mixing the pilot signal for each channel with a common local oscillator. This phase information was then applied to the information signal by an up-converter to enable retransmission of the information in the desired direction.

Antenna patterns of the self-phasing system breadboard were as predicted; sidelobe levels and beamwidth were approximately as calculated. Measured signal levels throughout the system were close to those predicted except for a conversion loss through the up-converters. These devices, however, were designed as low-level mixers for the multiple-beam system and did not function efficiently as high-level up-converters. The S/N of the pilot signal at the i-f amplifier outputs was 28.4 db compared with a predicted value of 29 db. Gain of the 4-GHz array at broadside was measured at 21 db. Predicted gain was 21.75 db. Gain decreased from this value by about 3 db at ±25°, as predicted, to give a minimum gain of 18 db.

1.5 ORGANIZATION OF FINAL ENGINEERING REPORT

This first section of the Final Engineering Report for the Spacecraft Antenna Systems program has been intended to provide a summary of the importance of improved antennas to spacecraft communication systems. Especially noted were the implications of an improved gain figure. One of the basic conditions governing the gain of a spacecraft communications antenna is the beam-steering technique

utilized. Of the techniques applicable, the self-steerable ones are considered the most versatile and promising for spacecraft. Two specific self-steerable configurations, a multiple-beam (transdirective) and a self-phased retrodirective, were developed as breadboard models during the second phase of the program.

A discussion of the helical antenna elements utilized in both breadboard systems is presented in Section 2. Detailed descriptions of the system and the system operation of the multiple-beam array are given in Section 3 and of the self-phased array in Section 4. Section 5 is the New Technology section. It is believed that each breadboard model represents a first implementation in system form of that particular configuration; thus, both systems are essentially New Technology. To avoid repetition, however, only generalized summaries of the systems are given in Section 5.

The conclusions and recommendations derived from the two-year program are presented in Section 6. Included among others are recommendations for implementation of engineering models and an evaluation of the application of self-steering techniques to millimeter wavelengths. A list of the references used in the report forms the concluding section.

A complementary report is also being issued by the Hughes Aircraft Company: Technical Report -- Feasibility Models (1966). This report includes developmental data such as gain figures, patterns, system gain, and noise data, r-f losses, channel phase shifts, power consumption, and an overall assessment of the two models. Engineering sketches will be provided to permit duplication of the circuits and systems illustrated. All these items except the engineering sketches are given in this report in Sections 3 and 4.

2.0 ANTENNA ELEMENTS AND ARRAY DESIGN

It was desirable for both breadboards to utilize the same antenna to make more valid a comparison of the two different system concepts. Accordingly, the transmitting antenna for each system was a 4-by-4 array of helical elements. The same array was also scaled for use as the receiving portion of the multiple-beam transdirective array, and one of the elements was used as the receiving portion of the self-phased array. Choice of the helix and design of the elements were governed by the available aperture space, the desired shape of the element beam, and a circular polarization requirement. The importance of these factors and the performance of the array are discussed in this section.

2.1 INTERELEMENT SPACING

A self-steered array that utilizes a conventional Butler matrix array or a self-phased array has an interelement spacing of approximately $0.5\lambda_o$. With this spacing a number of beam directions are generated which completely fill visible space without the presence of grating lobes, and the number of beams is equal to the number of elements in the Butler matrix array. In some applications it is desirable to fill most of space to obtain wide angle coverage. For communication satellites, however, a much smaller angle of coverage is required, particularly at or near synchronous altitude. This limited angle of coverage permits the use of a larger interelement spacing and an element that has directivity. In this manner a higher gain array is achieved from a limited number of modules or from a matrix of a given number of terminals.

In an alternative means of achieving increased gain, the interelement spacing is maintained at $0.5\lambda_o$, but the number of elements is increased. This procedure yields the best array with few compromises in performance for a small angle of coverage. However, the

number of elements is quite large and the complexity of the system becomes prohibitive. For example, to achieve 35-db gain after nominal losses have been accounted for, a 35-by-35 λ_o aperture would be required. With an interelement spacing of 0.5 λ_o, the array would have approximately 5000 elements and a 70-by-70 Butler matrix would be required. Not only is a matrix of this size completely beyond the state-of-the-art but the internal losses would probably reduce the increased gain to a fraction of the increased theoretical aperture gain. Of necessity, then, larger interelement spacings have to be used.

The use of larger interelement spacings raises some problems and necessitates a compromise in the array design. The severity of the compromise depends on a number of parameters in the system such as the gain required, the coverage angle required, and the size of the largest number of modules or the largest Butler matrix which is within the state-of-the-art and has reasonable loss. The main compromise results from the fact that the array generates grating lobes whenever the interelement spacing exceeds 0.5 λ_o.

Grating lobes are actually new beams that arise to fill the space left when increased interelement spacing causes the beams from a given array to become narrower and the primary set of beams formed by the array or matrix to decrease in coverage angle. Each new beam or grating lobe shares a terminal with one of the original beams at the bottom of the Butler matrix as shown in Figure 2-1. These grating lobes decrease the gain of the desired beams and must be suppressed as completely as possible. Hence the gain of the element must be increased and its beamwidth reduced as much as possible without cutting down on the gain of the outermost desired beams. The ideal element pattern would be a sector beam which must cover all the desired beams and then abruptly drop to zero to suppress all the grating lobes. However, it takes a very large element aperture to create even a poor approximation to a sector beam — much more than the aperture available to each element even though they have been spread apart considerably.

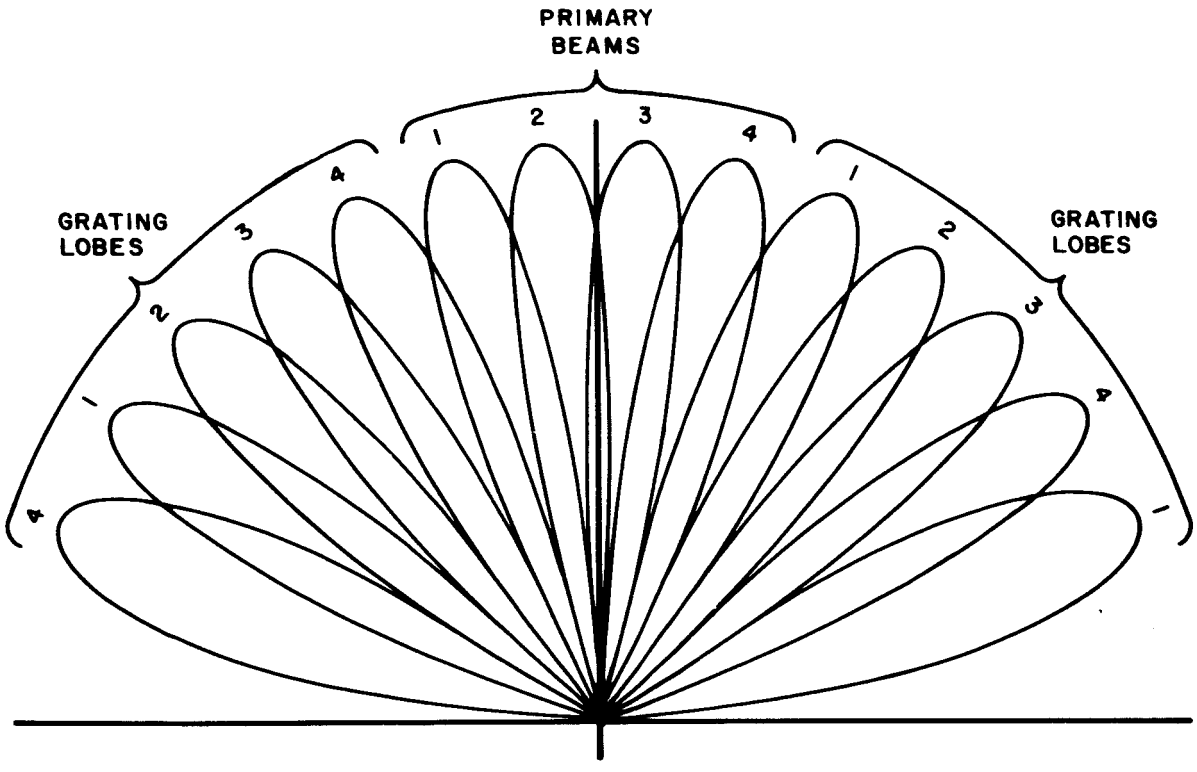

Figure 2-1. Generation of grating lobes by Butler matrix that uses interelement spacing considerably larger than $\lambda_o/2$.

A straightforward solution to the problem is to assume that the portion of the aperture available to each element is uniformly illuminated and to determine the element beamwidth from the applicable equation. It can then be shown that the 3-db point of the element pattern always coincides with the outside 3-db point of the outermost principal beam. Thus, the outside beams will be reduced in amplitude by 3 db compared with those in the center of the cluster.

For the multiple-beam breadboard antenna system, the objective was to provide 16 distinct beams on receive and a continuously variable beam on transmit which would fill a cone that subtended a total angle of 50 degrees. The element pattern was calculated with the assumption that it was essentially that of a uniformly illuminated segment of the

aperture. With this assumption, the pattern would have the form

$$\frac{\sin\left(\frac{kL}{2}\sin\theta\right)}{\frac{kL}{2}\sin\theta}$$

where

k = the free space propagation constant

L = the edge length of the element area

θ = the angle off broadside in the principal plane.

At $\theta = \theta_o = 25$ degrees, this pattern must be down 3 db from its maximum value. This requirement means that

$$L/\lambda = 1.05$$

where λ = the free space wavelength

For the arrays built for the breadboard, L was made equal to one wavelength.

2.2 ELEMENT DESIGN

A promising approach to the element design was the use of endfire elements such as helices. Experimental evidence showed that endfire elements might be capable of producing a better compromise than the uniformly illuminated small apertures mentioned above. No space limitation was involved since these elements can be made as long as desired. The limitation is rather one of mutual coupling or mutual interaction between the elements if they are spaced too closely together in relation to their equivalent area gain. The simple helix with a circumference of about one wavelength radiates circular polarization in the axial or endfire mode over a wide range of frequencies. The beamwidth of such a device varies with the number of turns--much as does the beamwidth of a linear array with the number of elements involved. A six- or seven-turn helix normally has beamwidths of 40 to 60 degrees and first null locations at angular offsets of 50 degrees.

In view of the requirements for the elements of the feasibility models, the helix seemed to be most nearly suited to modification to produce a flat-topped beam with low sidelobes at the desired locations. The optimum helix has a pitch angle of about 14 degrees and contains six turns. These physical characteristics combine electircally to produce a circularly polarized radiator with a beamwidth of about 40 degrees. An optimum helix element was designed and built to illustrate the feasibility of the endfire element for both the multiple beam and the self-phasing arrays.

Several attempts were made to modify the optimum configuration to produce a distorted pattern that would have a flat or concave top with steep slopes on the main lobe and minimum sidelobes beyond 30 degrees. Aperture blockage through the use of metal discs added to the end of the element was very effective but degraded the axial ratio.* Another interesting approach involved two independent helices wound on the same axis and connected in parallel. Rotation of one helix caused a differential phase shift, and an ideal pattern could be obtained for one principal plane and one polarization of incident energy. Axial ratio worsened, however, and patterns became asymmetrical for other cuts and polarizations. As a compromise between pattern shape and repeatability, the basic helix was used.

The first models of the element were wound of plexiglass rods grooved with a helical thread and plugged into a coaxial line terminated by an OSM miniature connector. Pitch and diameter were determined by the relationship shown in Figure 2-2.

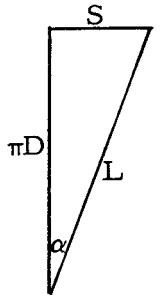

where S = spacing between turns
(L sin α)
D = diameter of helix
α = pitch angle
L = length of one turn

Figure 2-2. Determination of helix parameters.

*Axial ratio is defined as the ratio of the major to the minor axes of the polarization ellipse.

If the length of one turn is to be one wavelength at the center frequency of 6.301 GHz, then

$\alpha = 14^{o}$ (optimum helix pitch)

L = 1.875 inches (λ_o at 6.301 GHz)

$S = 1.875 \sin 14^{o}$

$D = S/\pi \tan \alpha$

and

S = 0.454 inch or 0.242 λ_o

D = 0.580 inch or 0.31 λ_o

The helical element designed from these calculations is shown schematically in Figure 2-3a and as an array in Figure 2-3b. Diameter of the conductor was 0.032 inch or 0.017 λ_o.

Several of these elements varying in length from 6 to 10 turns were tested, and the 8-turn model was chosen for study. Patterns showed an axial ratio of about 2 db and pattern degradation which gave rise to beam-pointing differences as the orientation of the helix was changed or as polarization of incident energy varied. Further checks indicated that the presence of the dielectric rod was affecting the phase velocity of the energy propagated down the helix; the rods were bored out to provide a minimum dielectric shell for the windings. The addition of a cup at the base of the helix provided an additional degree of beam shaping and reduced the axial ratio to less than 1 db. The λ_o spacing of elements allowed the use of a large cup, whose aperture was greater than cut-off wavelength. Patterns of a typical element are shown in Figure 2-4. The 8-turn helix with cup produced a pattern with nulls in the vicinity of $\pm 40^{o}$ (the locations of the close-in grating lobes of the array) and sidelobe levels about 13 db down at $\pm 60^{o}$ (the locations of the next grating lobes). The half-power points occur at $\pm 20^{o}$. A perfect flat-topped beam was not realized; however, the helix was easy to reproduce and the patterns were consistent. It is felt that this breadboard model indicates the usefulness of such an element.

Since the terminal impedance of this type of helix is on the order of 100 to 150 ohms, an impedance matching device was built to provide

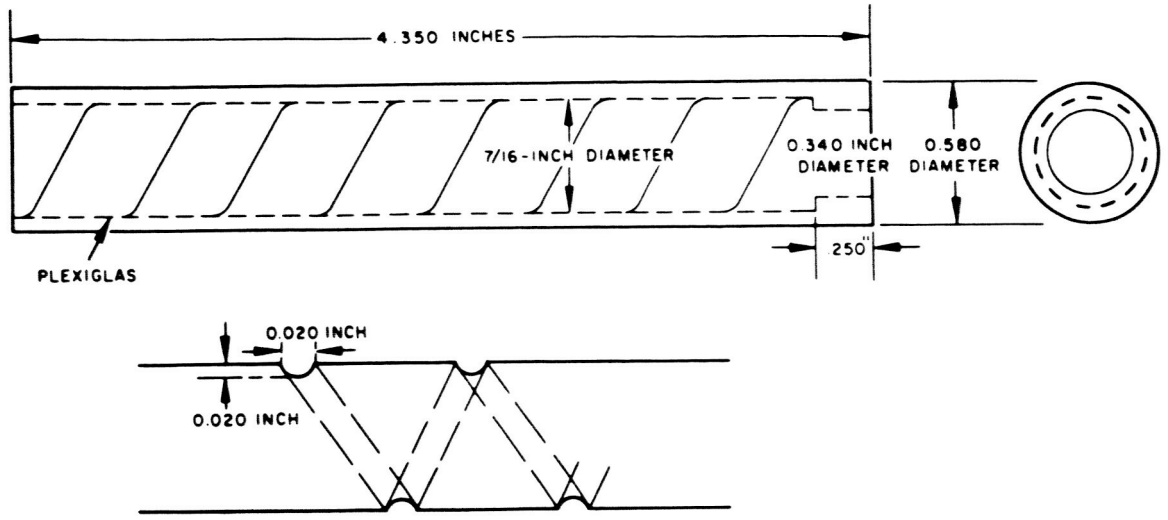

a) Element schematic

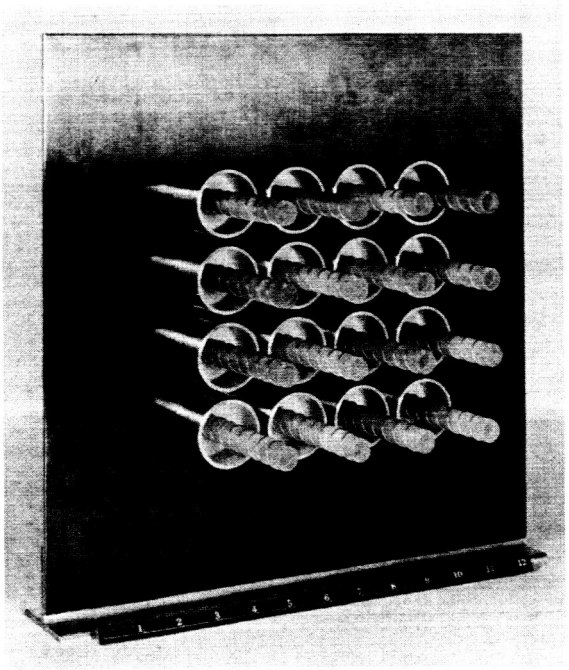

b) Elements arrayed.

Figure 2-3. Four-by-four array of helical elements.

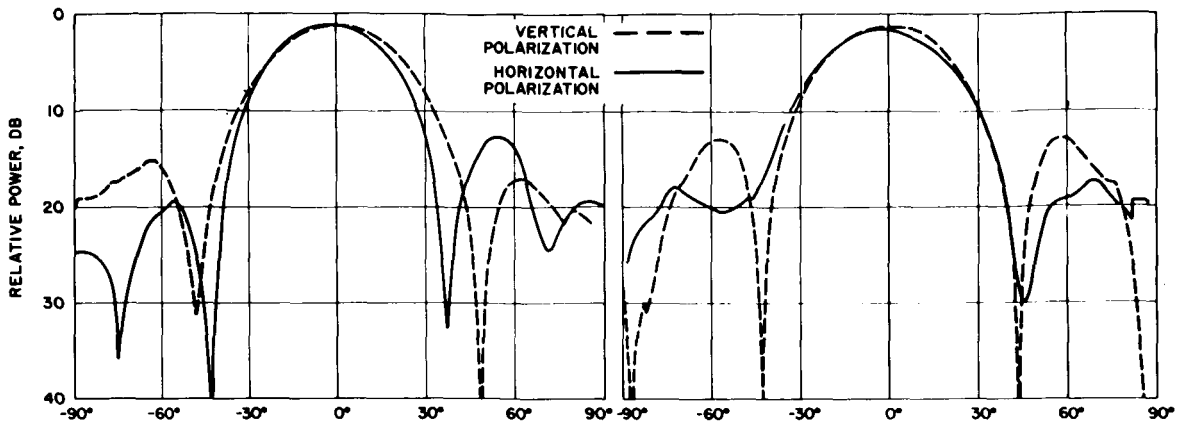

Figure 2-4. Patterns of helical element.

a match to the 50-ohm RG141/U coaxial line. The transformer consisted of two $\lambda_o/4$ stages of coaxial line with an air dielectric. The center pin was of uniform diameter through both sections while the diameter of the outer conductor changed to form 72-ohm and 106-ohm steps. A plot of the VSWR versus frequency is shown in Figure 2-5. Across the operating band of 6301 ± 150 MHz, the VSWR was 1.1:1 or less with 1.03:1 at the center frequency.

2.3 ARRAY DESIGN AND EVALUATION

A 4-by-4 array of the helical elements was built for use as the transmitter of both the multiple-beam transdirective array and the self-phased array. A similar array was scaled for use as the receiver of the transdirective array. The two arrays can be seen mounted on their groundplanes in the transdirective breadboard in Figure 2-6.

The array pattern for the breadboards had the form

$$\frac{\sin 2(kd \sin\theta + \alpha)}{\sin\frac{(kd \sin\theta + \alpha)}{2}} \frac{\sin 2(kd \sin\theta + \gamma)}{\sin\frac{(kd \sin\theta + \gamma)}{2}}$$

where

k = the free space propagation constant

d = the interelement spacing

θ = the azimuthal angle from broadside

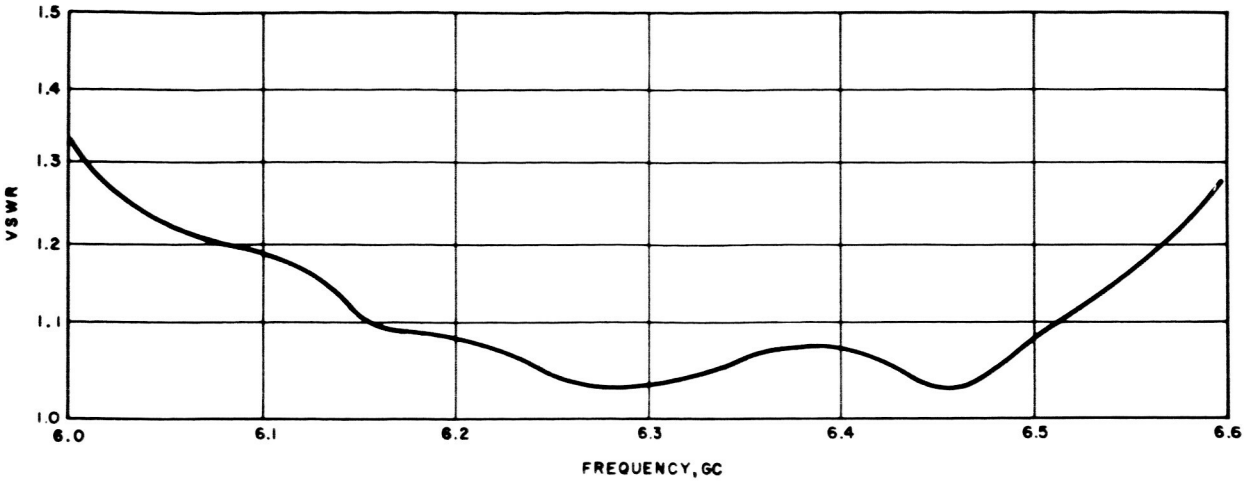

Figure 2-5. Measured VSWR of helical element.

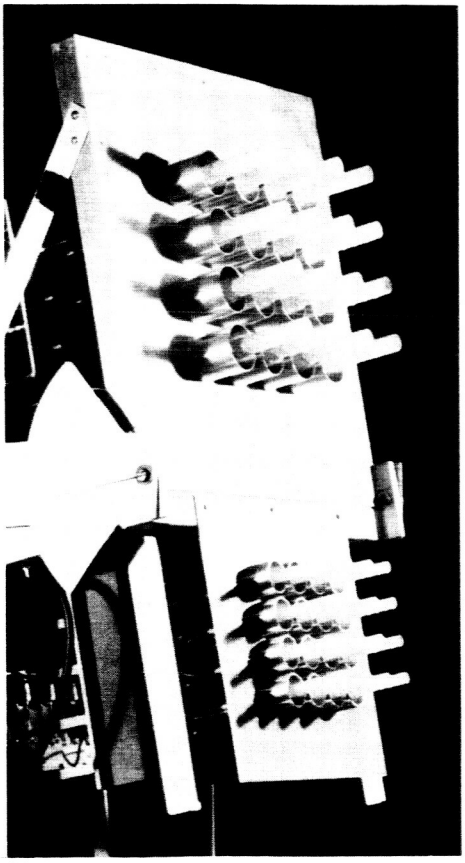

Figure 2-6. Transmitting and receiving arrays of the transdirective multiple-beam breadboard (HAC Photo No. R107505).

ϕ = the elevation angle from broadside

α = the horizontal interelement phase shift

γ = the vertical interelement phase shift

} These assume that the plane of the array lies in a vertical plane.

For a conventional 4-by-4 Butler matrix, such as was used for the multiple-beam breadboard, $|\alpha|$ = 45 degrees for a beam scanned off 1 right or 1 left* from broadside, and $|\alpha|$ = 135 degrees for a beam scanned off 2 right or 2 left from broadside. Similarly, $|\gamma|$ = 45 degrees for a beam scanned 1 up or 1 down from broadside and $|\gamma|$ = 135 degrees for a beam scanned 2 up or 2 down from broadside. The positions of the peaks of the discrete beams for both the transmitting and receiving arrays of the transdirective breadboard are shown in Figure 2-7.

The theoretical aperture gain of the arrays was calculated under the assumption of uniform aperture illumination:

$$G = \frac{4\pi A}{\lambda^2} = \frac{4\pi 16\lambda^2}{\lambda^2} = 23 \text{ db}$$

Assumed aperture efficiency	-1.0 db
Cable	-0.25 db
Butler matrix loss	-0.75 db
Element factor fall-off for outside beams	-3 db
Theoretical antenna gain: inside beams	21 db
outside beams	18 db
Loss due to circularly polarized elements when used with linearly polarized waves (no ellipticity assumed)	-3 db
Theoretical antenna gain (as tested with the linearly polarized waves): inside beams	18.0 db
outside beams	15.0 db

*1 left, 1 right, etc. describes the beam position from a field point located at broadside as one faces the array. For example, "1 right 1 up" or "1R1U" means the first beam position to the right and the first position up.

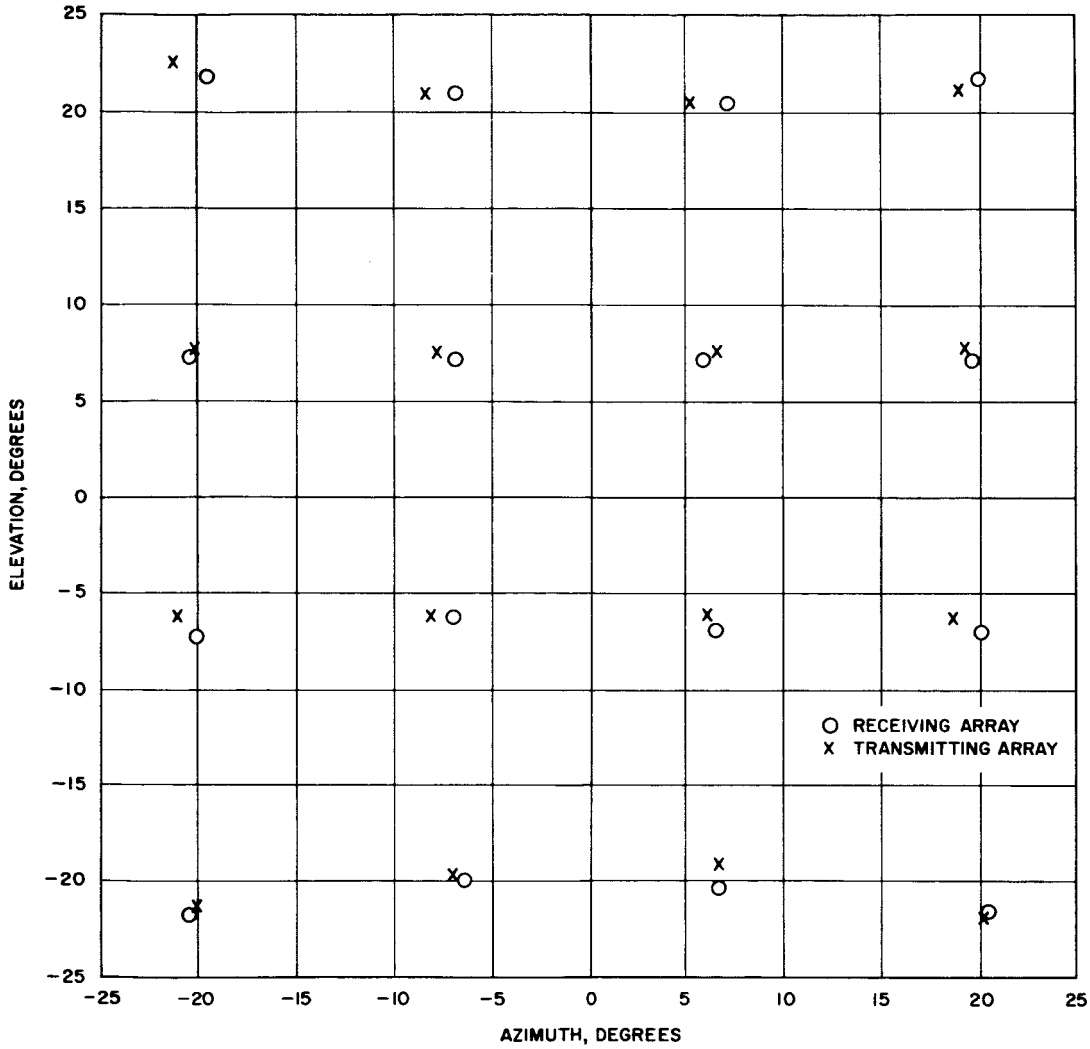

Figure 2-7. Beam-pointing directions for transdirective multiple-beam breadboard arrays.

For the theoretical gain characteristics, it was assumed also that the element factor suppressed the outside beams by 3 db.

The calculated characteristics of the antenna patterns are listed in Table 2-1. It may be noted that the outside beam positions that appear in Figure 2-7 are not as far from broadside as predicted by the array factor (Table 2-1). This difference can be attributed to the fact that the beams are compressed somewhat toward broadside by the

element factor; the latter was not taken into account in the calculations of the beam pointing directions.

Representative measured power patterns* for both the arrays are shown in Figure 2-8. The measured characteristics of these arrays, taken at the beam ports of the Butler matrices, are listed in Table 2-1 for comparison with the calculated data. As the patterns show, the element factor after the elements were placed in the array, did flatten somewhat about the normal direction because of mutual coupling effects. This distortion caused the gain of the outside beams to be slightly more than had been predicted.

*The patterns were taken by tilting the antenna with respect to the pedestal to obtain the desired elevation angle, and rotating it about the axis of the pedestal. For an elevation angle other than 0 degrees, this procedure results in a change of this angle as the patterns are taken; however, the change is small until the azimuthal angle becomes larger than $\pm 25^{o}$ because of the small elevation angles involved.

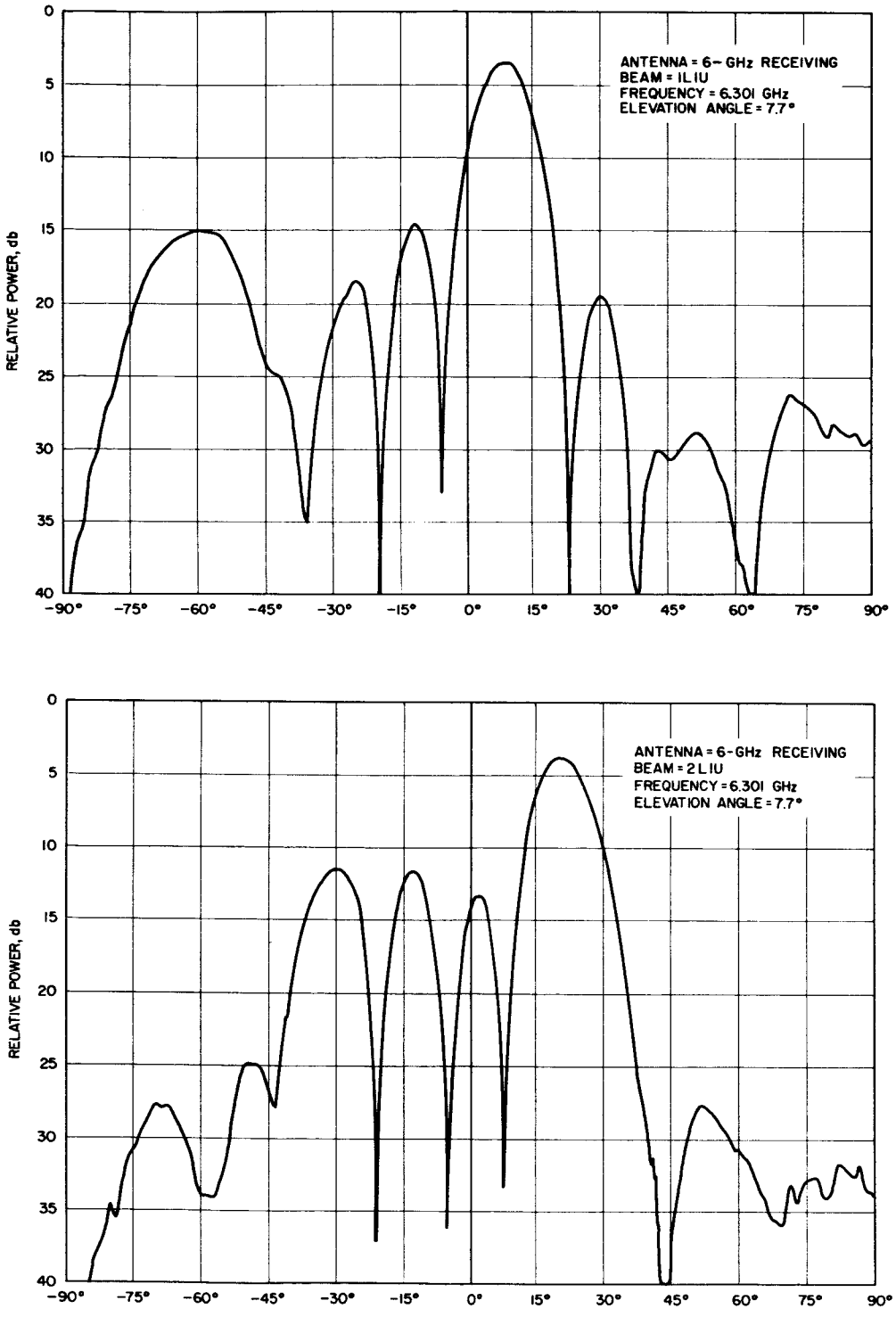

Figure 2-8. Power patterns of the 4-GHz and 6-GHz arrays as measured at the beam ports of the beam-forming matrices. (See Table 2-1 for absolute gain)

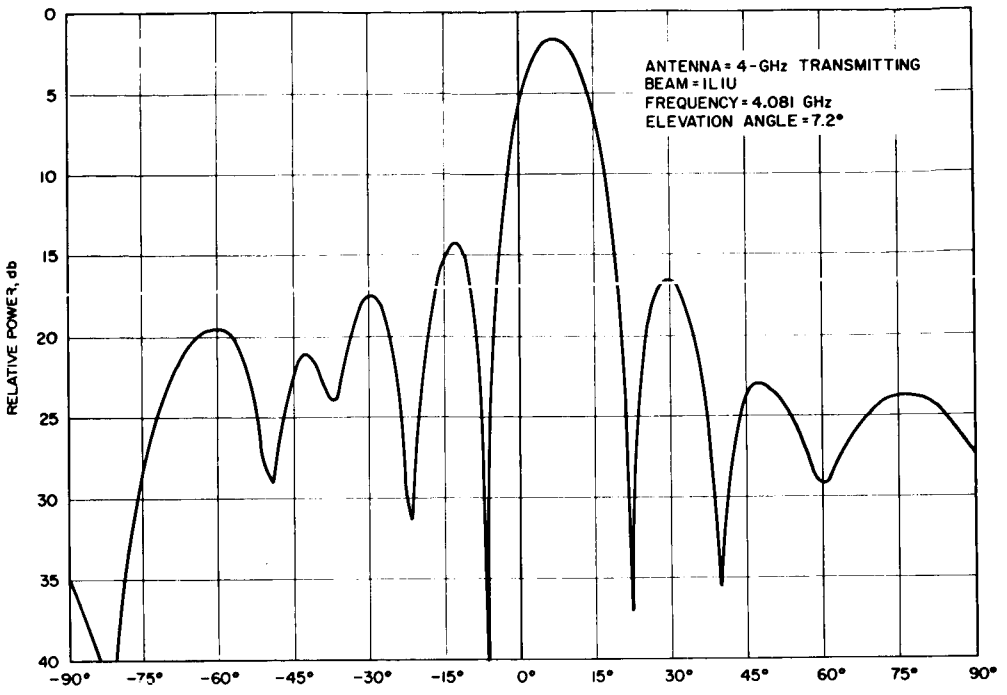

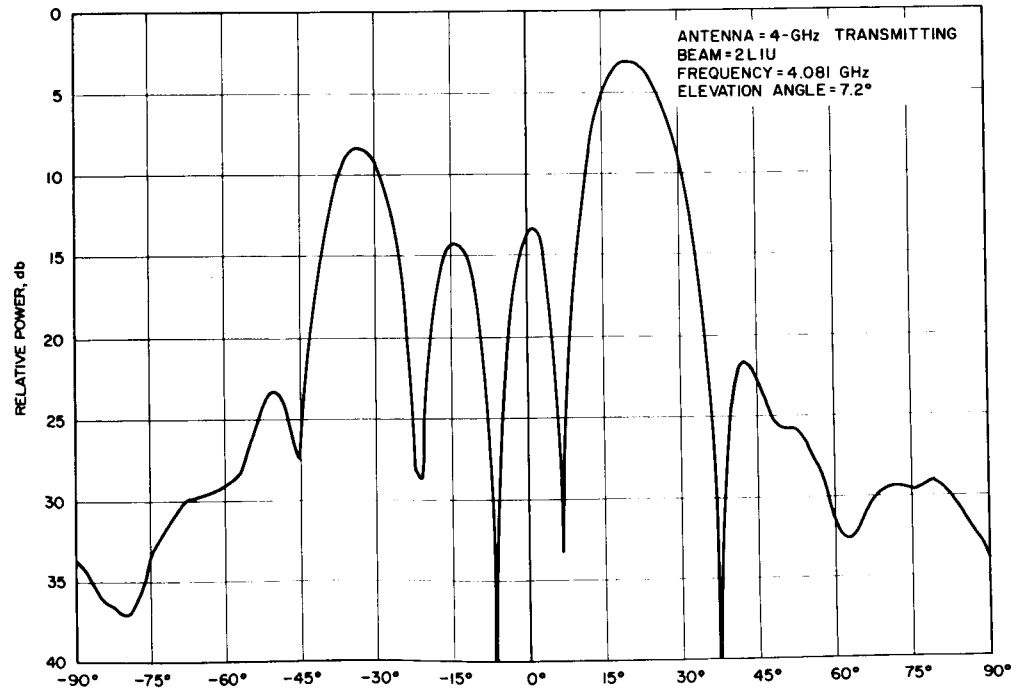

Figure 2-8. (Continued)

	Beam Designation ①	Principal Beam Position (A_z) ② (degrees)	Second Order Beam Position (A_z) ② (degrees)	Location of Nulls ③ (degrees)						3 db Beamwidth of Principal Beam (degrees)	Sidelobe Level from Peak of Principal Beam (db)	Second Order Beam Level from Peak of Main Beam (db)	Gain (db) ④
Theoretically Predicted Characteristics	2L2U	-22	32	-61	-38.8	- 7.18	7.18	22	61	14.2	-10	-5	18
	1L2U	- 7.18	61	-61	-38.8	-22	7.18	22	38.8	13.2	-13	-15	18
	1R2U	7.18	-61	-38.8	-22	- 7.18	22	38.8	61	13.2	-13	-15	18
	2R2U	22	-32	-61	-22	- 7.18	7.18	38.8	61	14.2	-10	-5	18
	2L1U	-22	32	-61	-38.8	- 7.18	7.18	22	61	14.2	-10	-5	18
	1L1U	- 7.18	61	-61	-38.8	-22	7.18	22	38.8	13.2	-13	-15	21
	1R1U	7.18	-61	-38.8	-22	- 7.18	22	38.8	61	13.2	-13	-15	21
	2R1U	22	-32	-61	-22	- 7.18	7.18	38.8	61	14.2	-10	-5	18
	2L1D	-22	32	-61	-38.8	- 7.18	7.18	22	61	14.2	-10	-5	18
	1L1D	- 7.18	61	-61	-38.8	-22	7.18	22	38.8	13.2	-13	-15	21
	1R1D	7.18	-61	-38.8	-22	- 7.18	22	38.8	61	13.2	-13	-15	21
	2R1D	22	-32	-61	-22	- 7.18	7.18	38.8	61	14.2	-10	-5	18
	2L2D	-22	32	-61	-38.8	- 7.18	7.18	22	61	14.2	-10	-5	18
	1L2D	- 7.18	61	-61	-38.8	-22	7.18	22	38.8	13.2	-13	-15	18
	1R2D	7.18	-61	-38.8	-22	- 7.18	22	38.8	61	13.2	-13	-15	18
	2R2D	22	-32	-61	-22	- 7.18	7.18	38.8	61	14.2	-10	-5	18
Measured 4 Gc Array Characteristics	2L2U	-19.7	32	-48	-38	- 7	7	22	65	13	- 9.8	- 5.5	19.1
	1L2U	- 6.9	44	-58	-40	-22	7	21	37	13	-11.5	-19.7	20.5
	1R2U	7.05	-58	-37	-22	- 7	22	39	55	12	-10.7	-21.8	19.8
	2R2U	19.8	-32	-53	-22	- 7	7	37	53	12.5	- 9.8	- 5.1	18.8
	2L1U	-20.3	33	-61	-38	- 7	7	22	45	13.5	-10.2	- 5.3	19.2
	1L1U	- 7.0	61	-59	-39	-22	7	22	37	13	-12.3	-17.8	20.4
	1R1U	5.8	-60	-38	-22	- 7	22	39	61	12.5	-10.7	-11.8	20.1
	2R1U	19.3	-32	-57	-22	- 7	7	37	61	14	- 8.1	- 4.8	18.1
	2L1D	-20.05	32	-63	-37	- 7	7	22	58	14	- 9.6	- 4.8	18.5
	1L1D	- 7.2	62	-60	-38	-22	7	23	38	12.5	-11.8	-16.2	20.5
	1R1D	6.4	-61	-38	-23	- 7	22	39	61	13	-11.2	-14.3	20.1
	2R1D	20.05	-33	-56	-22	- 7	7	37	61	14	- 8.8	- 5.3	18.7
	2L2D	-20.5	32	-58	-39	- 8	6	21	54	13	- 9.3	- 5.3	17.8
	1L2D	- 6.75	58	-59	-38	-22	7	20	38	12	-11.7	-19.8	19.1
	1R2D	6.6	-47	-38	-22	- 8	23	37	47	13	-10.7	-19.3	19.4
	2R2D	20.1	-33	-60	-22	- 8	7	37	58	13	- 8.4	- 4.5	18.0
Measured 6 Gc Array Characteristics	2L2U	-21.25	30		-43	- 8	7	18	54	13	- 8.8	- 6.7	19.9
	1L2U	- 8.5	42	-62	-42	-24	4	20	35	12	- 9.8	-19.5	20.4
	1R2U	5.05	-56	-38	-22	- 8	21	38	58	12	-13.2	-17.8	19.5
	2R2U	18.75	-33	-69	-23	- 7	7	38	52	12.5	- 7.3	- 6.8	18.8
	2L1U	-20.25	30	-68	-43	- 8	6	21	43	12	- 7.7	- 7.8	20.8
	1L1U	- 7.8	58	-63	-38	-23	6	19	37	12	-11.0	-11.3	21.2
	1R1U	6.45	-57	-38	-23	- 7	22	37	62	12	- 9.2	-12	21.2
	2R1U	19.15	-32	-45	-22	- 8	7	42	57	12	- 8.8	- 7.6	20.7
	2L1D	-21.1	30	-58	-42	- 8	5	20	43	13	- 9.0	- 7.0	20.5
	1L1D	- 8.2	58	-61	-37	-23	6	20	38	12.5	-10.0	- 8.2	20.8
	1R1D	6.15	-56	-38	-22	- 7	20	38	58	12	-11.2	-12.3	20.5
	2R1D	18.65	-32	-64	-22	- 7	7	41	60	12.5	- 7.7	- 7.0	20.6
	2L2D	-20.1	32	-54	-40	- 8	6	22	46	13.0	- 8.0	- 5.8	18.6
	1L2D	- 7.1	57	-58	-36	-22	7	20	39	12	-12.6	-16.2	19.5
	1R2D	6.55	-53	-37	-22	- 7	22	42	66	12	-10.5	-15.6	19.5
	2R2D	20.1	-32	-58	-22	- 8	7	39	61	13	- 8.1	- 6.5	19.1

1 The beam positions are defined looking from the field to the array; 1L1U means one left one up, 1R1D means one right one down, etc.

2 For the theoretically predicted characteristics beam, compression due to the element factor was not taken into account except for the second order beams located at $\pm 32^{\circ}$. For these second order beams, the element factor caused a significant effect; therefore it had to be accounted for. The beam compression due to the element factor actually caused the outside beams and second order beams to move in toward broadside.

3 The theoretically predicted null locations are given only for the array factor. The element factor would also cause nulls at approximately $\pm 50^{\circ}$.

4 It was assumed that the element factor was down by 3 db for all outside beams, but actually the corner beams should be down more than the other outside beams. Also, it was assumed that there was no ellipticity when determining the experimental values for gain. These gain measurements were made by measuring gain referenced to a linearly polarized gain standard and adding 3 db to account for the circularly polarized elements. Some ellipticity does exist which accounts for the gain of some beams to appear greater than theoretically predicted.

Table 2-1. Theoretically predicted and measured characteristics for the 4-by-4 antenna arrays through principal plane cuts of constant elevation angle.

3.0 THE MULTIPLE-BEAM TRANSDIRECTIVE ANTENNA BREADBOARD SYSTEM

A multiple-beam antenna system that implemented a transdirective self-steering concept was designed and built in a breadboard model. The system had two 4-by-4 arrays of helical elements and two separate r-f sections, one for transmitting and one for receiving; similarly, there were two matrices for the formation of the multiple beams. A detailed discussion of the operation of this type of self-steering technique and a performance evaluation of the system follows. A physical description of the breadboard is also given.

3.1 SYSTEM OPERATION

The operation of the multiple-beam antenna system breadboard is described with reference to the schematic diagram of Figure 3-1. The system used two beam-forming matrices for the formation of the multiple beams, one for the transmitting frequency and one for the receiving frequency.

3.1.1 Component Functions

The 6-GHz receiving system processed both the receiving and transmitting logic. Proper operation of the transmitting system requires that the receiving and transmitting antenna beams be identical. In the antenna design, the arrays and elements were scaled appropriately. The transmitting array could have been used for the logic for the transmitting mode, but such a design would have necessitated that the transmitting pilot be in the 4 GHz frequency region and that the transmitting logic have a complete receiver and a separate logic, as well as critical filters, to prevent overloading of the 4-GHz received signals by the 4-GHz transmitted signal.

In operation, two c-w pilot signals are generated from the ground stations, 6.310 GHz from the transmitting station and 6.313 GHz

from the receiving station. These c-w signals are received by the 6-GHz array and its beam-forming matrix which has an output port for each of the antenna beams. Following the outputs of the matrix are high pass filters which prevent saturation of the balanced mixers from the coupling of power from the transmitting array. The signals from each beam port of the receiving matrix are down-converted to i-f by the balanced mixers. From the outputs of the balanced mixers, the pilot signals pass through i-f buffer amplifiers to i-f switches. The buffer amplifiers serve to isolate the pilot and information channels and prevent noise from entering the information channel from the pilot i-f switches which time share the 16 i-f signals (one for each beam of the antenna system). If time-sharing were not used, the system would require 16 high-gain i-f amplifiers (which gain track) and 32 filters to amplify and separate the pilot signals. The outputs of the pilot i-f switches are directed to the common input of an i-f amplifier which is used to isolate the inputs of the two i-f pilot filters and which has sufficient gain to compensate for the insertion loss of these i-f filters.

The pilot i-f signals, which have now been separated by the pilot i-f filters, are directed to high-gain i-f amplifiers whose output is video detected. Following the video detectors are video amplifiers which boost the signal level to that required for sample hold circuits; at this point the signal-to-noise ratio of the pilot signals is increased because of the narrow bandwidth used (100 KHz). A representative waveform at the video amplifier outputs is shown in Figure 3-2 for a case in which the pilot is located at 0^{o} elevation and 0^{o} azimuth from the antenna system. Because the beam-forming matrices, filters, r-f mixers, i-f amplifiers, and video amplifiers are linear over about a 25-db dynamic range and the video detectors are approximately square law, the relative amplitudes of the voltage steps at the output of the video amplifiers are approximately proportional to the relative power levels of the pilot signals in the respective beams of the antenna system.

Following the video amplifiers are sample-hold circuits -- one for each beam of the antenna system. These sample-hold circuits are synchronized with the i-f sampling switch so that a particular sample-hold circuit samples the video amplifier output voltage during the time

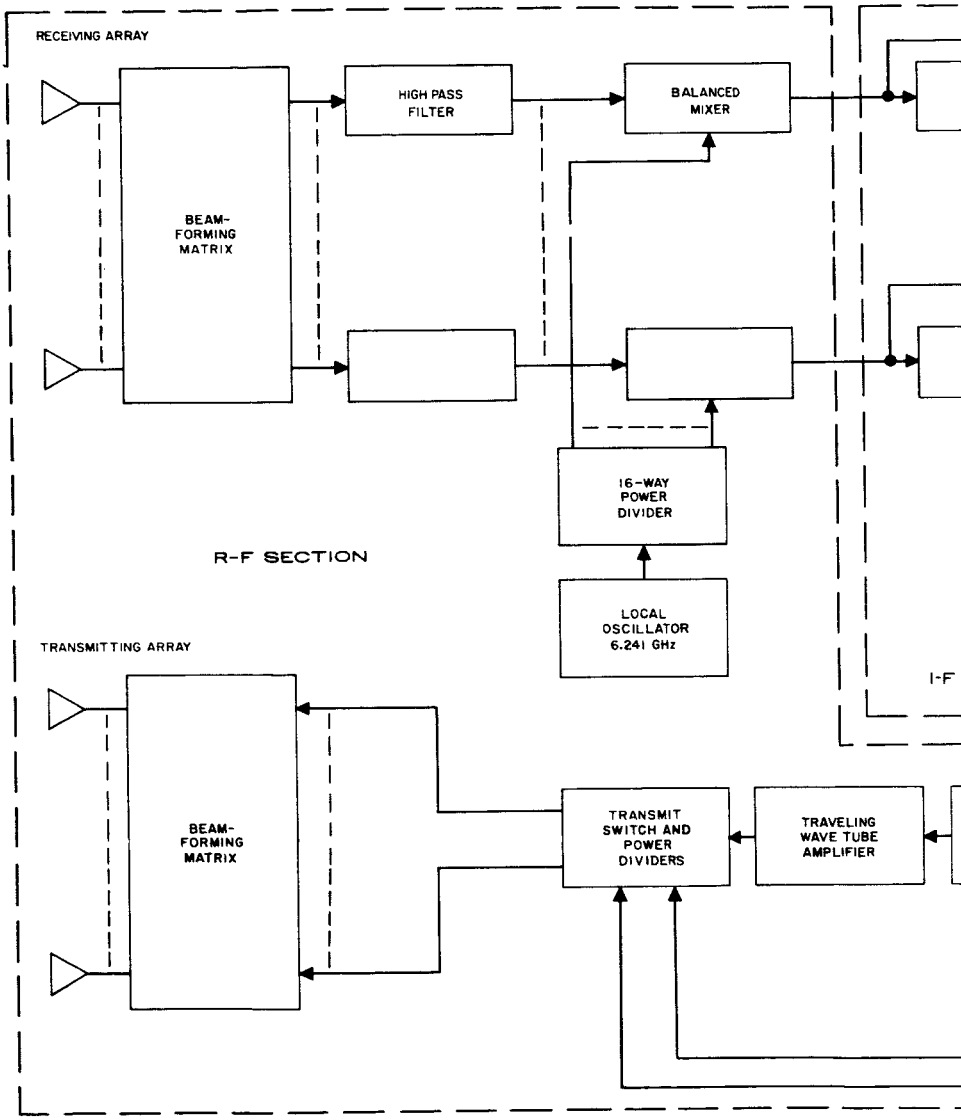
RECEIVING ARRAY
BEAM-FORMING MATRIX
HIGH PASS FILTER
BALANCED MIXER
16-WAY POWER DIVIDER
R-F SECTION
LOCAL OSCILLATOR 6.241 GHz
TRANSMITTING ARRAY
BEAM-FORMING MATRIX
TRANSMIT SWITCH AND POWER DIVIDERS
TRAVELING WAVE TUBE AMPLIFIER
I-F

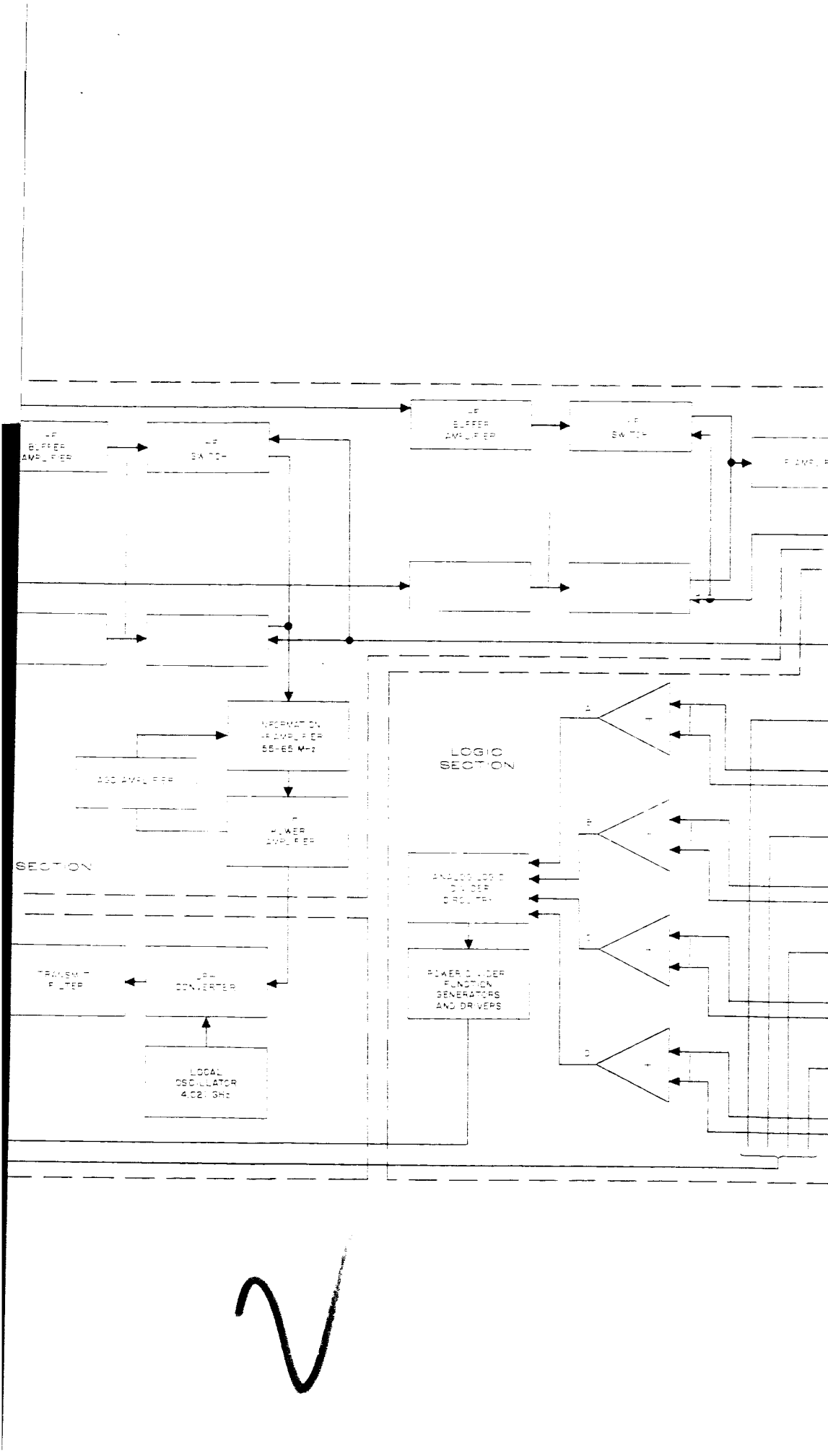
LOGIC
SECTION
LOCAL
OSCILLATOR
4.021 GHz

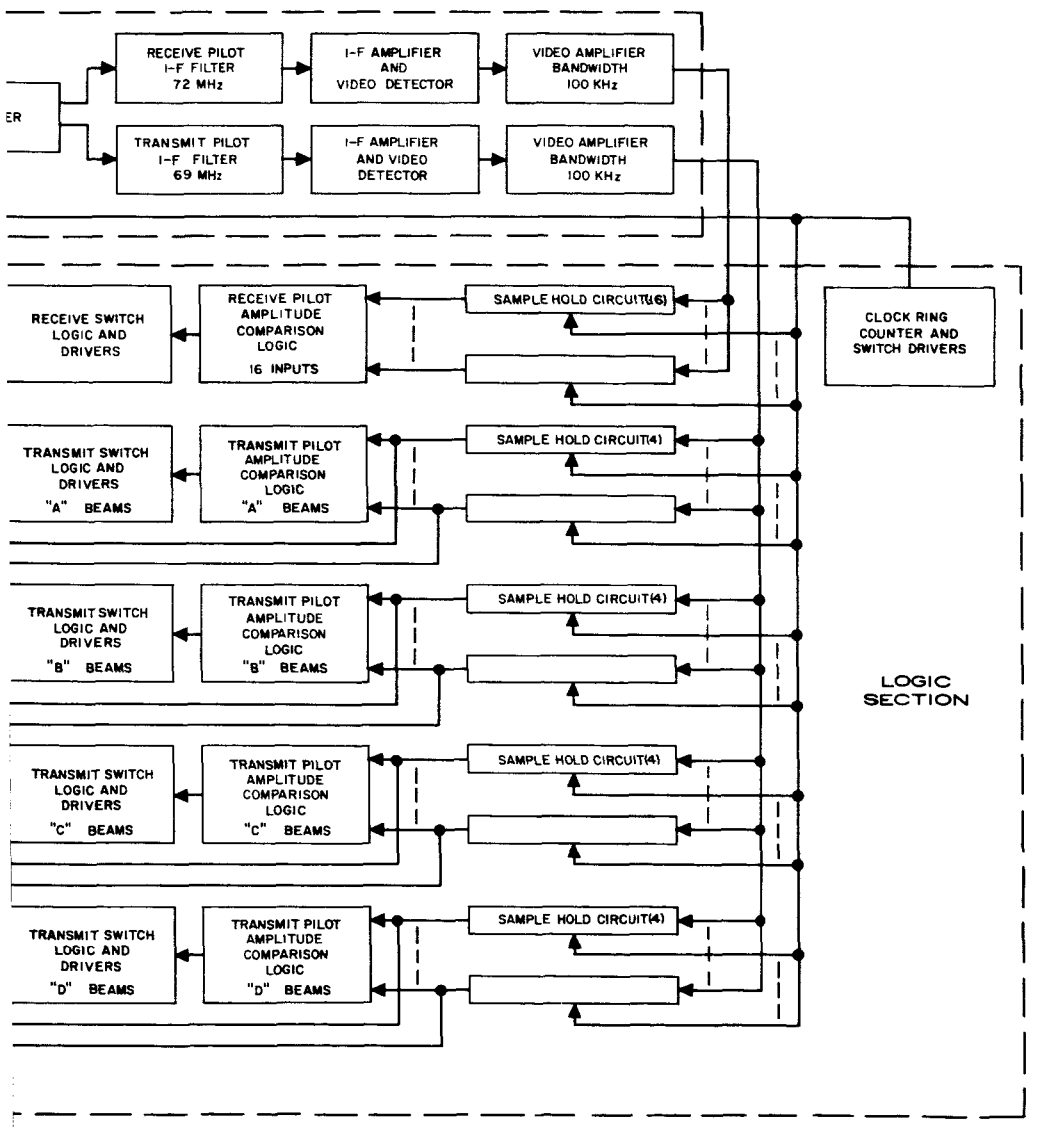

Figure 3-1. Multiple-beam antenna system schematic.

3

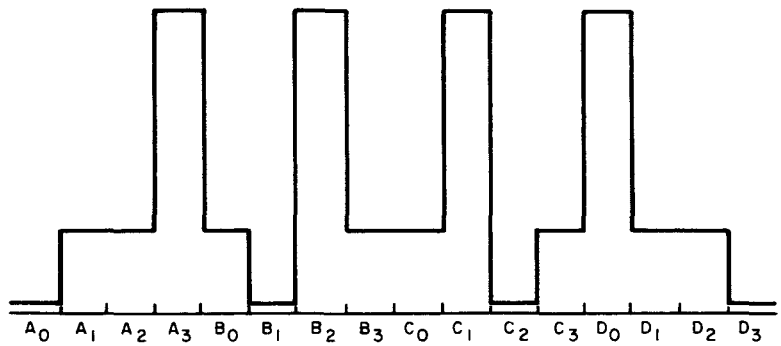

Figure 3-2. Video amplifier output voltage waveform.

in which the i-f switch is switched to the same channel. The sample-hold circuit then holds this voltage until this channel is again sampled. At the output of the sample-hold circuits are 16 d-c voltages, one for each pilot signal, proportional to the power received by that particular antenna beam.

The frequency of the driver for the sampling circuits was chosen on the basis of the response time required. There are two conflicting requirements. The sample rate should be as slow as possible so that a long rise time may be obtained. A long rise time will reduce the effects of transients in the information channel. On the other hand, the sample rate must be fast enough to allow adequately fast beam switching. The speed here is related to the motion of the satellite with respect to the earth station, including changes in attitude. A frequency of 1000 Hz was chosen; it gives a sample rate per beam of 62.5 samples per second of 1 millisec sample time which will result in a switching response time of greater than or equal to 32 milliseconds and a pulse width much greater than the switching time.

The function of the receive logic is to determine the antenna beam with the largest receiving pilot signal and to switch the information channel into this channel by the application of a voltage to the appropriate i-f switch connected to the information channel. The information then received by the antenna beam with the highest signal is down-converted to i-f and directed to the information i-f amplifier. The function of the information i-f amplifier is to give a large gain and

to establish the 10-MHz bandwidth of the antenna system. Also incorporated with the information i-f amplifier is an automatic gain control which maintains a constant output signal level for a large range of signal input levels. This AGC is necessary to maintain a constant signal level into the upconverter for greatest upconverter efficiency and to prevent saturation of the TWT amplifier. From the output of the information i-f amplifier, the signal is up-converted by mixing the information i-f signal with a local oscillator at 4.021 GHz. The upper sideband is then passed by the transmit filter to the input of the traveling-wave tube amplifier. The TWT amplifier raises the signal level up to that required for transmitting from the antenna system.

The function of the transmit logic is to use the information contained in the voltages at the sample-hold outputs to determine the direction of incidence of the transmit pilot and thus control the transmit switch and variable power dividers which, in conjunction with the transmit beam-forming matrix, form a beam that points in the desired direction.

The principal feature of a 4-by-4 beam forming matrix is the availability of 16 distinct beams or beam-pointing directions, any one of which can be selected by feeding energy into the appropriate beam port. The beams overlap to form in space the "4-by-4" cluster which is symmetric about broadside, as shown in Figure 3-3. There

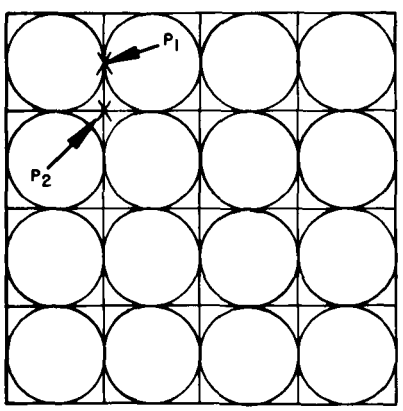

Figure 3-3. Four-by-four symmetrical beam cluster. (Circles represent 4-db contours.)

are, however, two disadvantages in the use of distinct beams: a non-constant gain and switching transients. These problems are resolved to a great extent for the transmitting antenna of the multiple-beam antenna system by a continuous scanning process that utilizes digital switches and variable power dividers.

3.1.2 Continuous Beam Scanning

Because the constant amplitude plane for each beam forms a circle, it can be deduced from Figure 3-3 that the gain will not be constant everywhere within one of the squares. At points at which two adjacent overlapping beams are of equal gain, such as point P_1 in Figure 3-3, the gain is down ~4 db from the peak. At points at which four adjacent overlapping beams are of equal gain, such as point P_2, the antenna gain is down about 8 db from the peak gain. The system margin is determined by the 8-db figure.

In addition to the non-constant gain feature, the use of distinct beams gives rise to noticeable switching transients as the antenna system switches from one beam to another. To eliminate the effect of amplitude variations between adjacent beams and switching transients, the transmitting beam is continuously scanned. The distinct but overlapping beams are utilized to form one continuously moving beam. This improvement is accomplished by using four adjacent overlapping beams with appropriate weightings to form a new beam which continuously scans to track the transmitting pilot. While this scanning beam will have minor amplitude variations with scan, it will have no noticeable holes. Since power is continuously decreased or increased to the beam ports with scan, there are also no noticeable switching transients in its coverage.

It is possible to remove this disadvantage in the receiving mode also. The method of implementation would be similar. Since satellite power and weight are limited, the weakest communication path is from satellite to earth. It was therefore felt appropriate to demonstrate the technique on transmitting only.

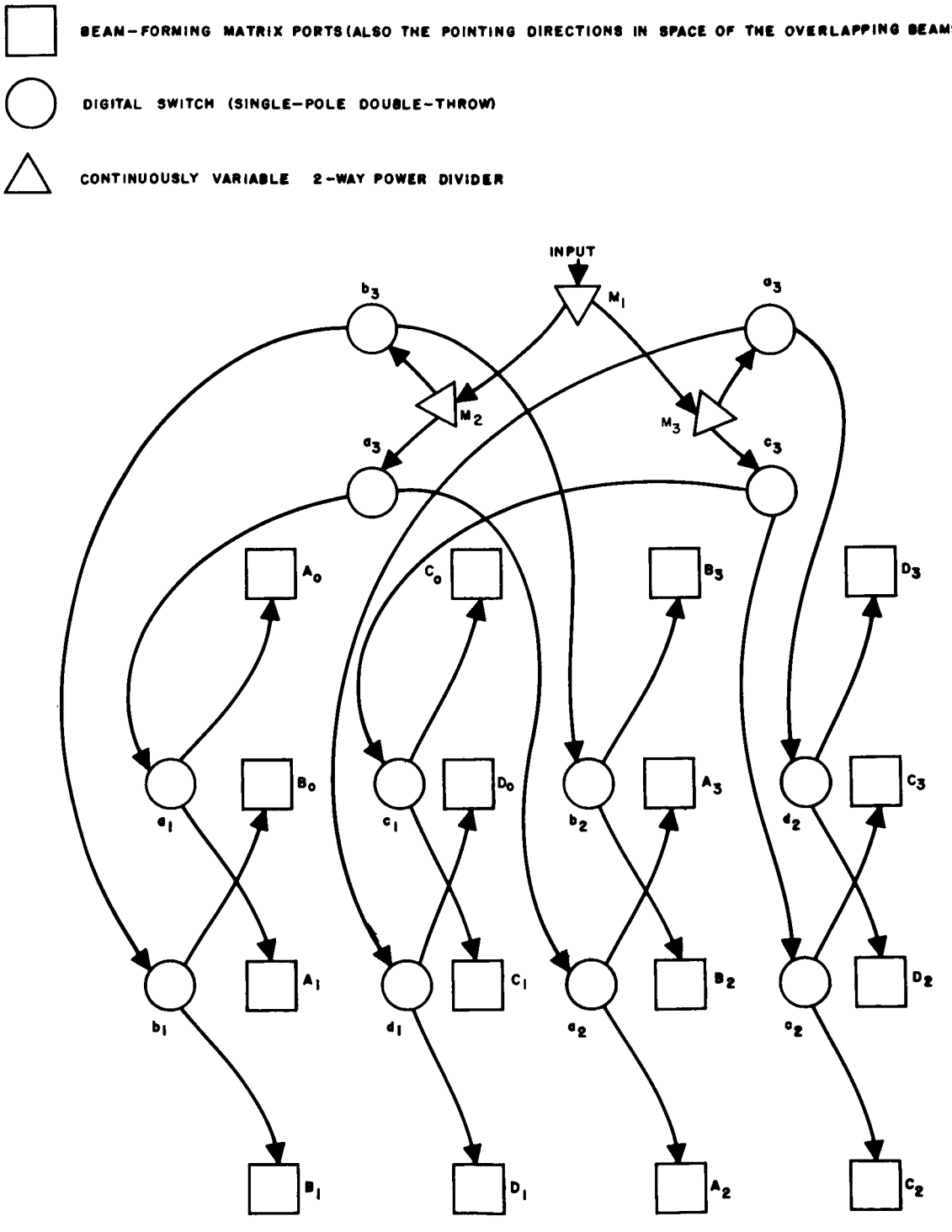

Figure 3-4. Transmitting switch and power dividers.

The beam direction is controlled by digital switches and power dividers as indicated in Figure 3-4. The beam ports (and beams in space) are arranged to form a 4-by-4 cluster as in a discrete switching system but with the sixteen beam ports divided into four sets of four beams each. Any four adjacent overlapping beams (ports) which form a square are made up of one beam from each of the four sets of beams. Determining the beam with the largest transmitting pilot signal in each of the four sets enables the system to locate the position of the transmitting pilot within four adjacent beams. Then, by a comparison of the relative amplitude of the pilot signals in these four adjacent beams, the precise position of the receiving station can be determined.

3.1.3 Operation of Transmitting Switch and Power Divider Logic and Driver Cricuitry

The digital microwave switches which are used for the system are ferrite latching circulators; the power dividers are also ferrite devices which can be controlled electronically to give a precise power division. The function of the switch and power divider can be described by outlining the transmitting logic (Figure 3-5).

1) Determine "A" output with highest level transmit pilot signal. Call this output A'.
2) Connect the channel with the highest level "A" output through the "A" switch matrix.
3) Simultaneously repeat 1) and 2) with B, C, and D. (At this time the digital microwave switches are correctly programmed.)
4) Determine A' + B' and C' + D'.
5) Set power divider M_1 (Figure 3-5A) to divide the power between dividers M_2 and M_3 approximately in proportion to

$$\frac{A' + B'}{C' + D'} .$$

6) Set power divider M_2 to divide the power (it receives from M_1) between switches a_3 and b_3 approximately in proportion to A'/B'.

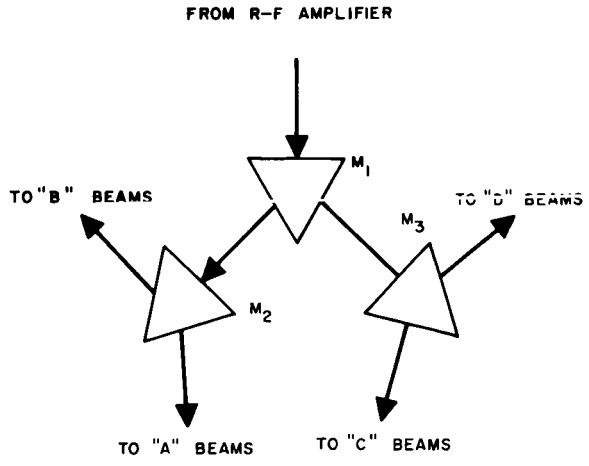

A) Power dividers.

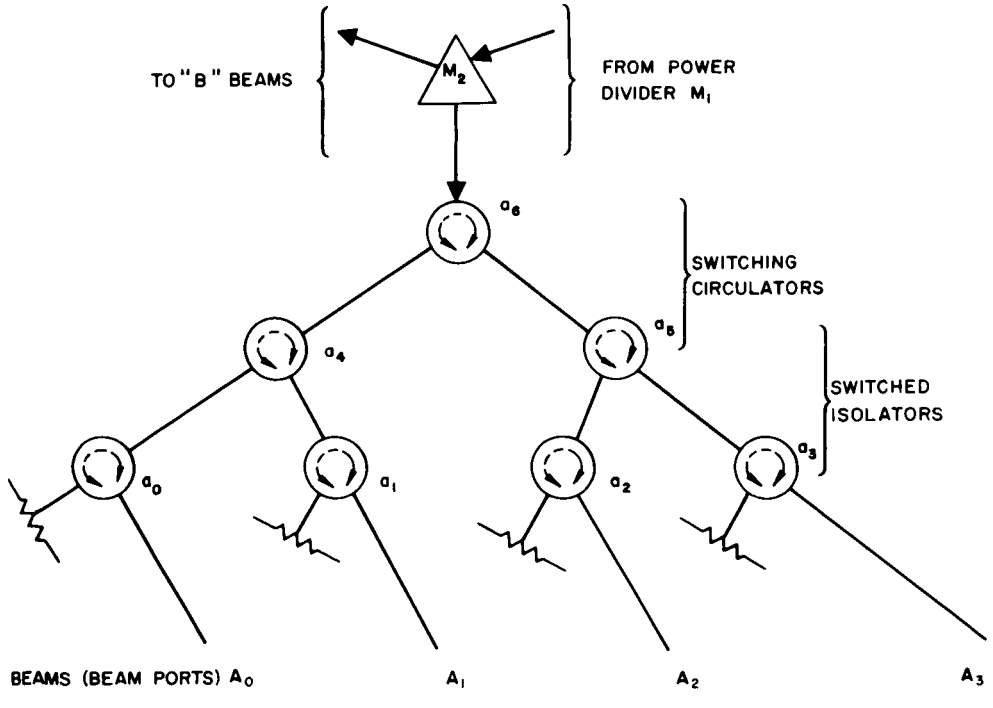

B) Set of "A" beams.

Figure 3-5. Transmitting switch and logic.

7) Set power divider M_3 to divide the power (it receives from M_1) between switches c_3 and d_3 approximately in proportion to C'/D'.

8) The beam has now been formed in the direction of the transmitting pilot signal.

3.1.4 Description of Transmitting Logic for Switch

A single-pole four-throw switch fed from a power divider that is shown in the block diagram of Figure 3-5A is a building block for the transmitting switch. The seven digital switches shown in Figure 3-5B are latching type switching circulators of which a_o through a_3 are used as isolators. Switched isolators are necessary because of the high isolation (greater than 30 db) required between beam ports to prevent degradation of the antenna pattern and because of the limitations in the VSWR and isolation obtainable with present state-of-the-art circulators.

The switch is set to transmit on beam a_o (Figure 3-5B). Circulators a_1, a_2, a_3, a_4 and a_6 will be set to transfer power in the counterclockwise direction and a_o will be set in the clockwise direction. Switched circulator a_5 may be set in either direction. The VSWR of each circulator port is less than 1.2:1, isolation is greater than 20 db, and insertion loss is less than 0.25 db. For the case at hand, leakage to switch output a_1 will be caused by leakage of power in the clockwise direction in circulators a_4 and a_1 and reflection of power from the input of a_o which will go back through a_4 and will be attenuated by 20 db at a_1. The worst case will result when the contribution from these sources of leakage are in phase. The case of worst isolation from A_o to A_1 is 34.4 db. Similarly, the worst case isolation to both A_2 and A_3 is also 34.4 db.

By the use of this switch configuration, the required isolation is obtained. Since the circulators are of the latching type, they require only a pulse of current of short duration to perform the switching; thus the power consumption is quite low. The reliability of the transmitting switch is very good, because of the nature of ferrite devices.

The operation of the digital portion of the transmit logic can be described with the aid of Figure 3-6 which presents a block diagram

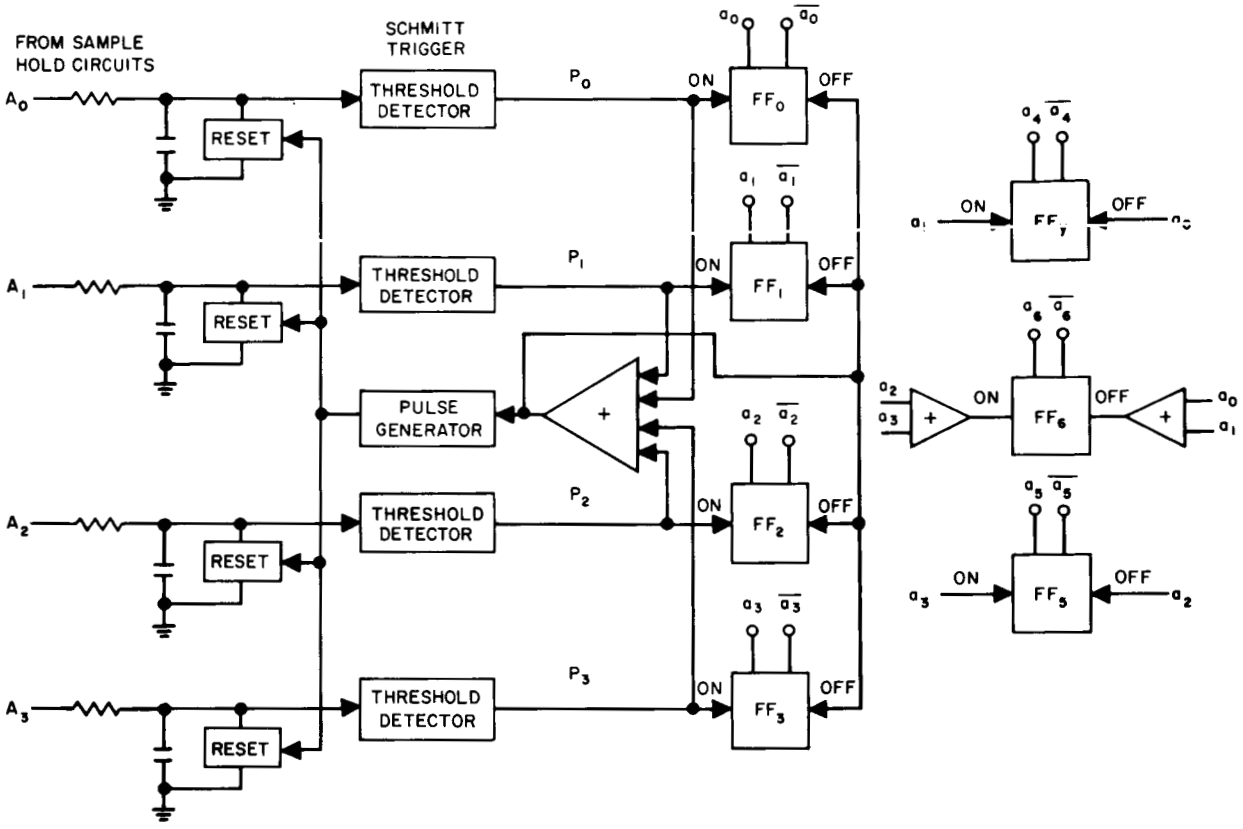

Figure 3-6. Transmitting logic for digital switches.

of the digital transmitting logic of the "A" beams. The logic of the "B", "C", and "D" beams is identical.

The input to the transmitting logic is a d-c voltage which is obtained from the sample-hold circuits for each channel of the antenna system. These voltages are proportional to the power in the transmit pilot signals from the respective receiving matrix output ports. The capacitors in the RC networks at the input to the transmitting logic are considered initially discharged, and four d-c voltages are applied to A_0 through A_3. The capacitors charge, at a rate depending on the magnitude of the d-c voltage input, until one of the threshold detectors is triggered. This threshold detector emits a pulse which resets all the charging circuits and the charging cycle is repeated.

There is a train of pulses at the output of the threshold detector for the channel with the largest signal level while the other threshold detectors have no output. These pulses are used in turn to switch the appropriate flip-flops "ON" or "OFF." For example, if the signal for a_o is the largest of the "A" beams, a train of pulses will be present at P_o and the "ON" input of FF_o. These pulses will also be present at FF_o through FF_3 through an "OR" gate. Therefore, FF_1, FF_2, and FF_3 will be turned "OFF." Since FF_o has both an "ON" and "OFF" input and the flip-flops are designed so that the "ON" input overrides the "OFF" input, FF_o will be turned on.

If the flip-flops are in the proper state, an incoming pulse has no effect. Now if the signal level in one of the other beams becomes the largest (for example a_1), a train of pulses becomes present at P_1. The first pulse of this train turns FF_1 "ON" and FF_2 "OFF."

Flip-flops FF_4 through FF_6 are connected to FF_o through FF_3 as shown in Figure 3-7 to form the proper logic for the digital switches. The output of each flip-flop is connected to a pulse generator via an "OR" gate as shown in Figure 3-7. The pulse generator emits a pulse whenever its associated flip-flop changes state. This pulse is directed to the appropriate input of the switch driver by "AND" gates at the switch driver input. Since the output power required from each flip-flop is very low and the switch drivers consume power only during a change of state of their associated switches, the total power consumption for the transmitting digital logic is very low.

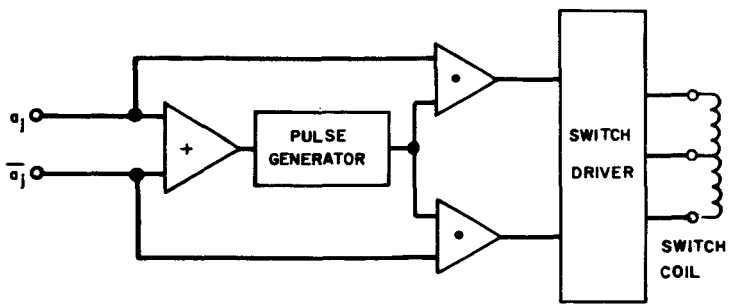

Figure 3-7. Pulse generators and switch driver for one digital switch.

3.1.5 Description of Transmitting Logic for Power Divider Control

The operation of the power divider control of the transmitting logic can be explained with the aid of Figure 3-8. Again the input is taken from the output of the sample-hold circuits, but now the inputs are four d-c voltages proportional to the signal power levels of the four beams with transmitting pilot signals of the largest amplitude. The function of this part of the transmitting logic was given in (4) through (8) in the outline of transmitting logic in Section 3.1.3. Sample-hold signals A' + B' and C' + D' are determined and fed into a logarithmic amplifier and the difference taken by means of a difference amplifier. This difference, which is proportional to log (A' + B')/(C' + D'), is fed to an antilog amplifier to obtain an output proportional to (A' + B')/(C' + D'). This signal is then used to drive a sine-cosine function generator.

The sine-cosine voltage relationship is generated to control the variable power dividers.* Two control voltages, both sinusoidal and 90 degrees different in phase, are required to produce in the power dividers a magnetic field which is constant in magnitude but variable in sense. Varying the sense of this magnetic field varies the ratio of power coupled to the output ports of the power dividers. The outputs of the sine-cosine function generator, proportional to $\cos[f(A' + B')/(C' + D')]$ and $\sin[f(A' + B')/(C' + D')]$, are fed to the power divider M_1 via a power divider driver which will give power division by the divider proportional to (A' + B')/(C' + D'). The power divider controls for M_2 and M_3 are similar.

This method of power divider control is relatively simple and straight-forward. Continuously variable ferrite power dividers are presently available, and the components for the power divider controls are standard analog building blocks which can be obtained with highly precise performance and very good reliability.

*This power divider is the same as the synchronous ferrite phase shifter described by Kummer and Villeneuve (1965, p. 44) except for the output section.

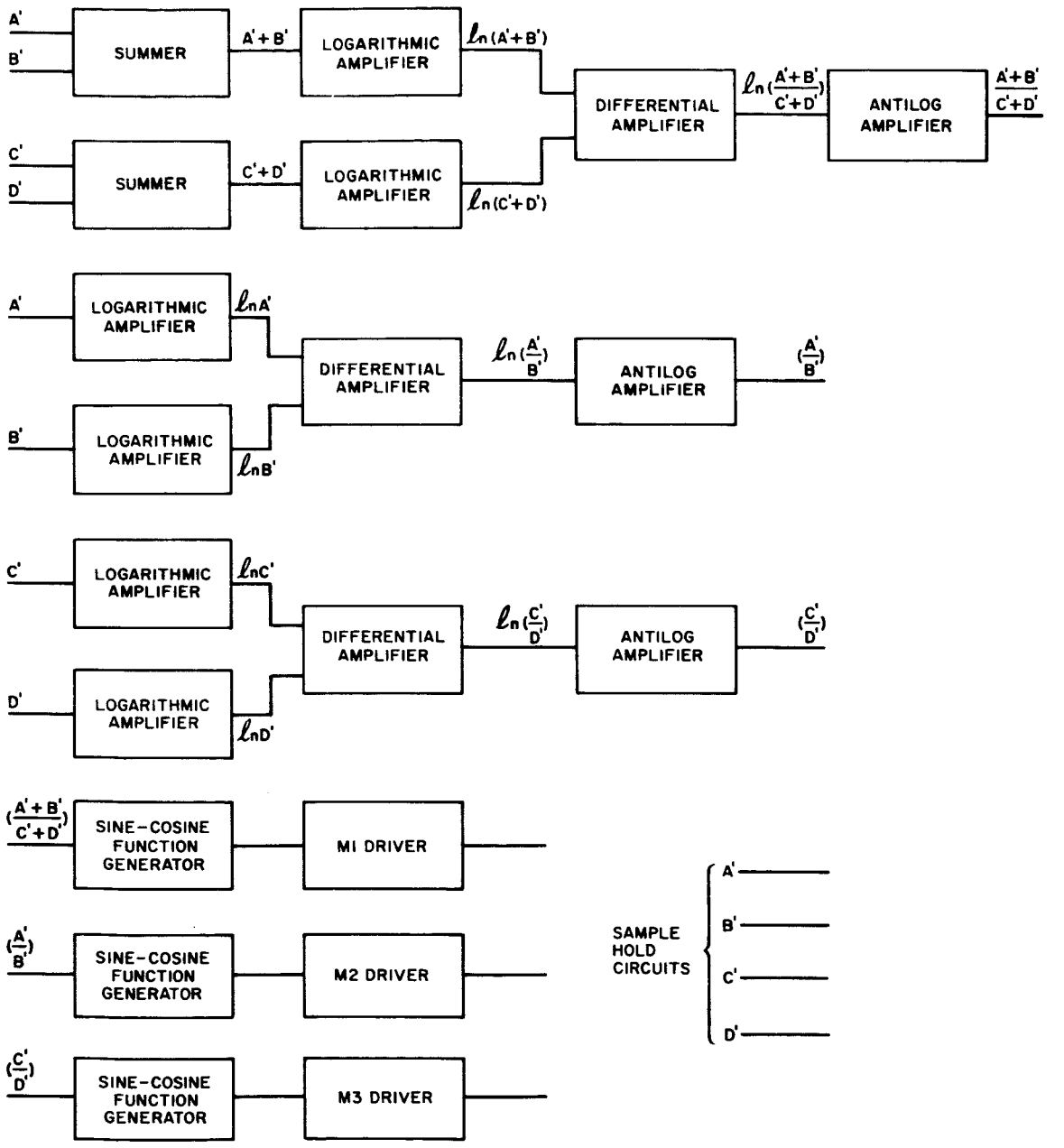

Figure 3-8. Transmitting logic for power divider control.

Information Channel				
Parameter	Component Gain (db)	Minimum Antenna Gain (db)	Signal Level (dbw)	S/N (db)
Effective radiated power			18.9	22
Theoretical peak aperture gain	23			
Element factor falloff on edge of coverage	+3			
Beam ripple on transmit	-2			
Cable loss	+0.25			
Beam-forming matrix loss	+0.75			
Minimum gain at beam ports		17	1.9	
Transmit switches, 0.20 db each	-0.60			
Continuously variable power dividers (1.5 db each)	-3.0			
Minimum system antenna gain*		14.4		
Traveling-wave tube gain and power output	35		5.5	
Transmitting filter insertion loss	-2.5			
Upconverter conversion loss	-10			
I-f amplifier output signal level			-17	
I-f amplifier gain and input signal level	89		-106	25
I-f buffer and i-f switch (including -3 db at buffer input)	-1.5			
Signal level at buffer amplifier input			-104.5	
Balanced mixer conversion loss	-6			
High pass filter loss	-0.5			
Minimum gain at beam ports		12		
Cable loss	-0.25			
Beam-forming matrix loss	-0.75			
Element factor falloff on edge of coverage	-3 -6**			
Additional crossover loss in non-principal plane	-4			
Beam crossover loss in principal plane	-4			
Loss when using linearly polarized waves	-3***			
Theoretical peak aperture gain		23		
Received signal level (isotropic) (linear polarization)			-107	
Pilot Channels				
Video amplifier output signal level			-13	27.5
Video amplifier gain	30			
I-f amplifier gain and input signal level	77.5		-120.5	17.5
Pilot i-f filter and i-f amplifier	0			
I-f buffer and i-f switch (including -3 db at buffer input)	-1.5			
Pilot signal level at buffer amplifier input			-119.0	
Antenna gain at balanced mixer output	2.5			
Received pilot signal level (isotropic)			-121.5	

*Gain measured at the power divider input.
**During the initial phase of the system design, it was assumed that the element factor was flattened and the edge of coverage raised 1 db.
***Not included in gain figures.

Table 3-1. Design objectives for multiple-beam antenna breadboard.

3.1.6 Signal and Noise Levels

For the receiving portion of the system, the signal levels are somewhat arbitrary. During the initial stages of the system design, the signal levels were determined on the basis of a 25-db signal-to-noise ratio at the input to the information i-f amplifier* based on a 10-MHz bandwidth and a signal-to-noise ratio greater than 25 db at the video amplifier outputs. The design objectives for the gain and noise figures of the components and the signal and noise levels through the system are presented in Table 3-1.

3.2 PHYSICAL DESCRIPTION

The multiple-beam antenna system breadboard (Figure 3-9) consited of four major units which were interconnected electrically with cables: an r-f unit, an i-f unit, a logic unit, and a power supply unit.

3.2.1 R-f Unit

The r-f unit (see Figure 3-9) contained the 4-GHz transmitting and the 6-GHz receiving arrays, two beam-forming matrices, ferrite digital switches, variable power dividers, a transmit band pass filter, a traveling-wave tube amplifier, an up-converter, 16 highpass filters and 16 r-f mixers. The components were supported structurally by a section of plywood, 3/4 inch by 22 inches by 34 inches, with a peripheral frame made from a 2-by-4. The two arrays were mounted at one end of the frame with the transmitting array above the frame and the receiving array below.

The arrays consisted of ground planes made from 1/8-inch aluminum plates, 22 inches square for the 4-GHz transmitting array and 14 inches square for the 6-HGz receiving array, and 16 helical radiating elements in a 4-by-4 arrangement. Element spacing was one wavelength. The elements were 8-turn helices with a circumference of 1 wavelength, which were wound on hollow plexiglass rods. At the base of the rods were aluminum cups.

*There will be a decrease in signal-to-noise in the first stages of the i-f amplifier.

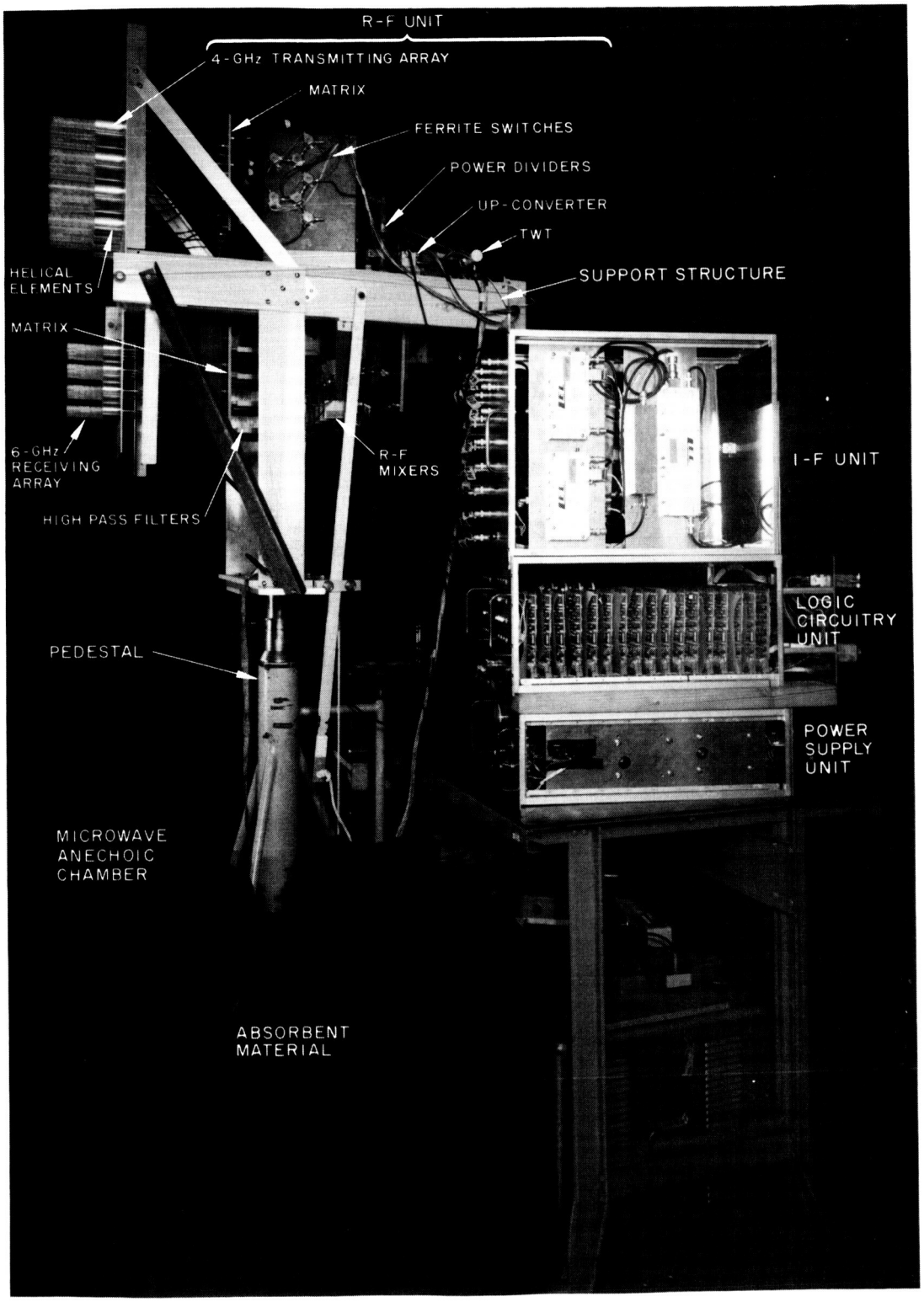

Figure 3-9. Multiple-beam antenna system breadboard.

Behind each array was a beam-forming matrix, a strip transmission line device that was ten inches square by 3/8 inch thick. For the transmitting array, this matrix was mounted 8 inches from, and parallel to, the ground plane of the array. The matrix was connected to the array and supported by semi-rigid coaxial cables with OSM connectors.

Following the transmitting section matrix were ferrite digital switches arranged on four cards (one for each set of beams) in such a way that they fanned out toward the matrix. The cards were positioned vertically behind the matrix. Connections from the switch outputs to the beam ports of the matrix were semi-rigid coaxial cables and OSM connectors.

Three variable power dividers, cylindrical in shape with dimensions of about 8 inches in length and 2-1/2 inches in diameter, were mounted behind the ferrite switches. One power divider was in a horizontal position in the center of the board with the other two vertically on either side. The power dividers are connected electrically with coaxial cables to the switches. Both switches and dividers were connected by cables to a control box at the rear of the support structure and, through a multi-lead cable, to the logic unit.

Behind the power dividers at the rear of the supporting structure were a traveling-wave tube amplifier, a transmitting filter, and an up-converter.

The 6-GHz receiving portion of the r-f section was mounted on the bottom of the supporting frame below the transmitting components (see Figure 3-9). The array was at the front of the frame directly below the transmitting array. Behind the receiving array was its beam-forming matrix, positioned about 8 inches behind and parallel to the array. Again, interconnections were made with semi-rigid cable that also supported the matrix.

Behind the matrix were balanced mixers, mounted across the width of the supporting structure. One port of the balanced mixers was connected to the beam ports of the matrix by way of a coaxial high pass filter and a semi-rigid coaxial cable; another port was connected to a 16-way power divider located vertically behind the balanced mixers. The output

ports of the mixers had BNC connectors leading to the input ports of the i-f section of the breadboard system by means of RG58 coaxial cables.

3.2.2 I-f Unit

The i-f unit of the breadboard system (Figure 3-10) was a standard 19-inch panel that could be rack mounted. On the front of the panel were BNC connectors for the inputs and i-f and video outputs. The components were mounted vertically in this section with each component packaged in a nickel-plated box. The components included buffer i-f amplifiers and i-f switches, two pilot i-f filters, two pilot i-f amplifiers, two pilot video amplifiers, an information i-f amplifier, an information power i-f amplifier and an AGC amplifier, and the i-f section power supply.

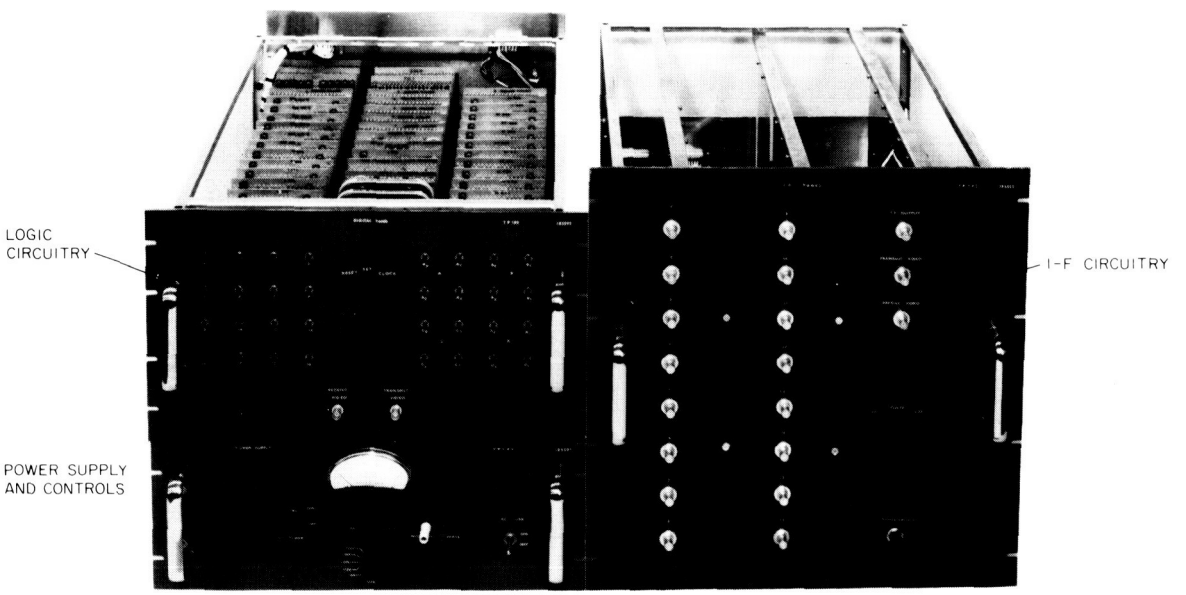

Figure 3-10. Logic, i-f, and power supply units.

3.2.2 Logic Unit

The logic unit was also a standard 19-inch panel that could be rack mounted (see Figure 3-10). The electronics were packaged on 35 pin cards mounted vertically in the panel. The front of the panel contained two BNC jacks for the video input and two 4-by-4 arrays of lights to indicate which beam had been selected by the receiving section and which four beams had been selected by the transmitting section.

3.2.4 Power Supply Unit

The power supply unit was a 19-inch panel that contained modular power supplies for the logic unit of the system (Figure 3-10). The front of this panel had two "ON-OFF" switches for a-c and d-c power, respectively; a SET-RESET switch for the ring counter; a meter to monitor the power supply voltages; and a switch to select the voltage to be monitored.

3.3 PERFORMANCE AND EVALUATION

Extensive measurements were performed with the multiple-beam breadboard. These tests included patterns of both transmitting and receiving sections, signal levels at various parts of the system, noise levels, and power consumption.

3.3.1 Antenna System Patterns

To obtain patterns of the receiving section, the system was operated in an anechoic chamber at a distance of 35 feet from the receiving pilot and information transmitters and rotated in azimuth while the signal strength at the input to the information i-f amplifier was measured. Patterns were taken for seven positions in elevation, of which a typical pattern is shown in Figure 3-11. The absence of any discontinuity in the patterns at the switching position indicates that the system switched beams at the beam crossover points, as it should have. Some variation in the gain of the beams did occur.

In this system, to prevent jitter between beams when the pilot is exactly at the crossover of two beams, some hysteresis must be

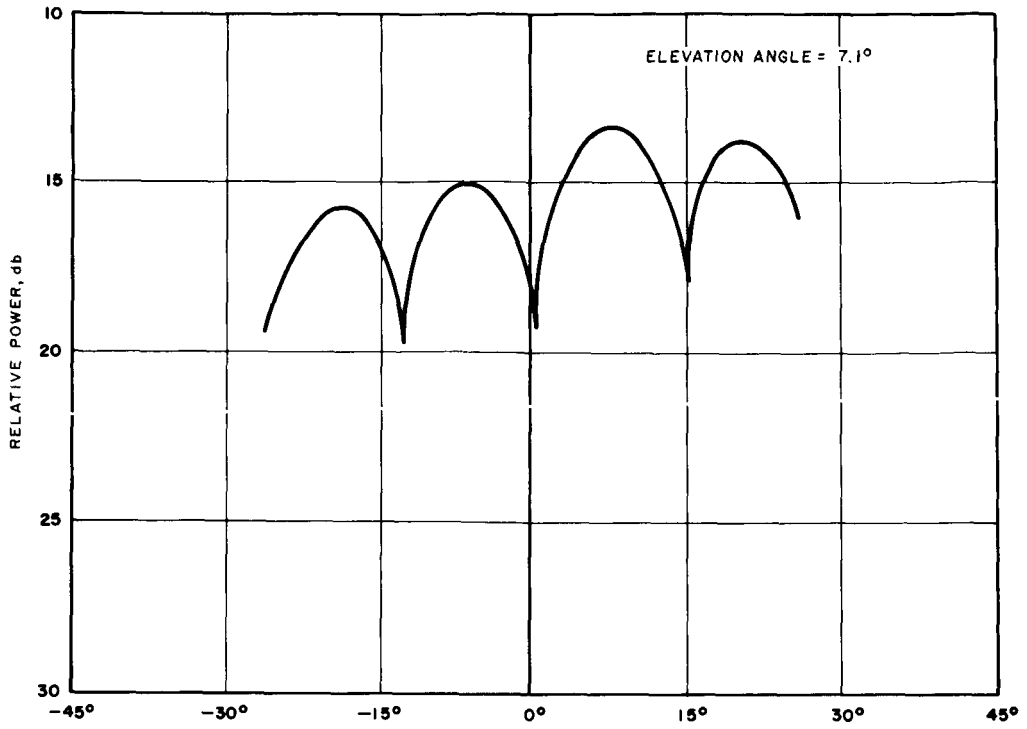

Figure 3-11. Pattern of receiving section (6 GHz) of multiple-beam breadboard measured at input of i-f amplifier with system tracking the receiving pilot.

designed into the logic, but it must be kept very small if the maximum gain from the receiving antenna is to be realized. No jitter was observed at crossover points when the patterns were recorded, so that the amount designed into the circuitry had negligible effect on the gain.

The patterns for the transmitting section of the antenna were taken with the system located 35 feet from the transmitting pilot transmitter and information receiver. A 60 MHz i-f signal was applied to the system at the input of the information i-f amplifier and the signal strength recorded at the information receiver while the system was rotated in azimuth. Patterns were taken for seven positions in elevation (four through a principal plane of the beams and three roughly halfway between principal planes). Two patterns are presented in Figure 3-12.

The ideal transmitting pattern would be constant in amplitude to ±25 degrees, at which angles the 3-db points occur; beyond ±25°

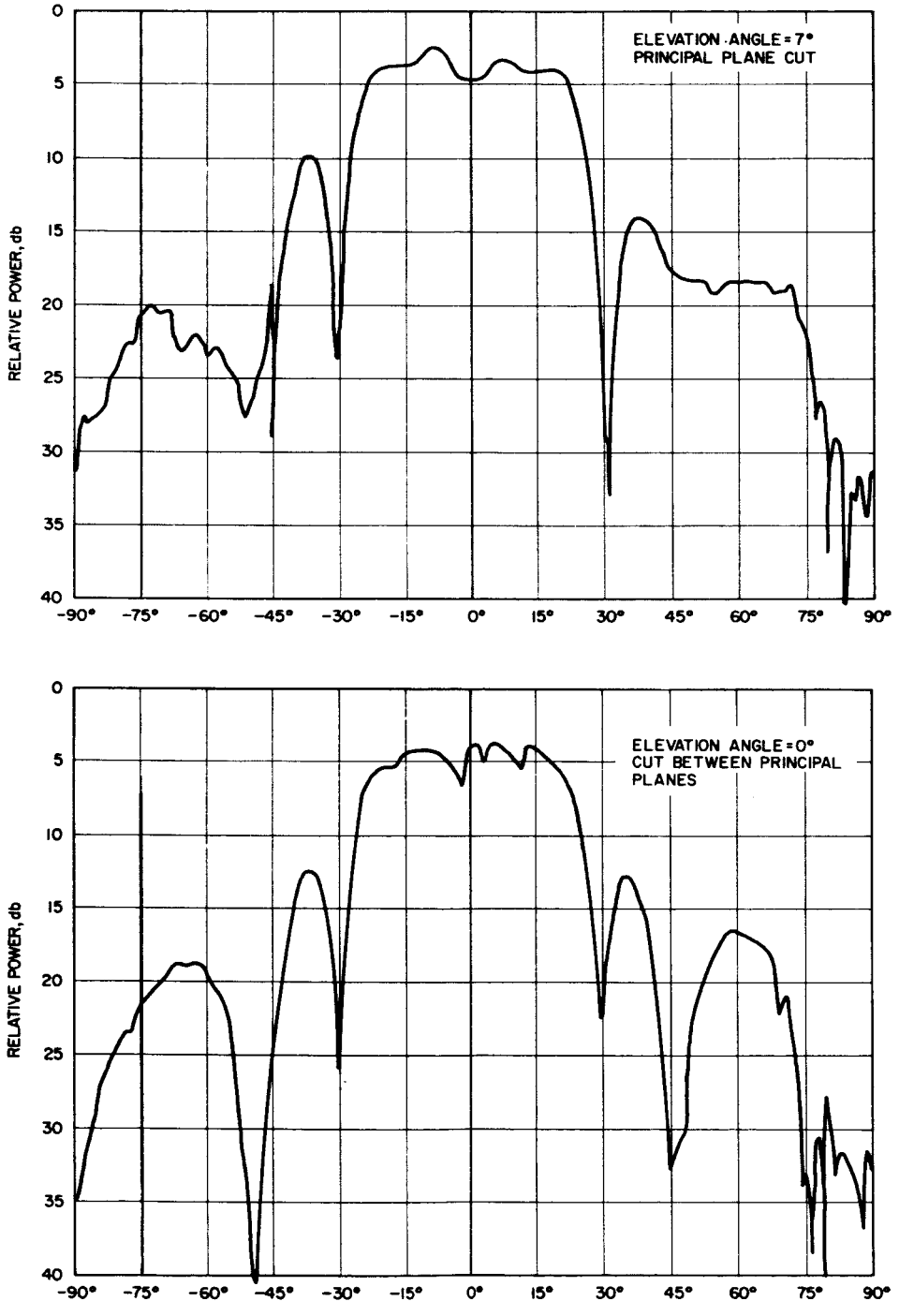

Figure 3-12. Patterns of transmitting section (4 GHz) of multiple-beam breadboard with system tracking the transmitting pilot.

the pattern amplitude would drop off very rapidly. The patterns presented in Figure 3-12 show these characteristics with some irregularities. The latter are caused by several factors: peak gain between beams is not constant, for example, but the most significant cause is probably the sidelobes and their effect on the operation of the transmitting logic. In the transmitting logic, the beams were divided into four sets with each set containing four beams. The function of the digital part of the transmitting logic was to determine the beam with the largest transmitting pilot signal for each of the four sets of beams and to switch the transmitted energy into these four beams by means of the ferrite digital switches and variable power dividers. The sets of beams can be designated A, B, C, and D with the beams arranged in elevation and azimuth as shown in Figure 3-13. If the transmitting pilot is assumed located at point P of Figure 3-13, which is in a principal plane of beams A_1, C_1, B_2, and D_2, then the patterns for these beams for the elevation of point P would be as shown in Figure 3-14.

In Figure 3-14 it will be noted that point P is located at the crossover of beams B_2 and C_1 and at the peak of the first sidelobes

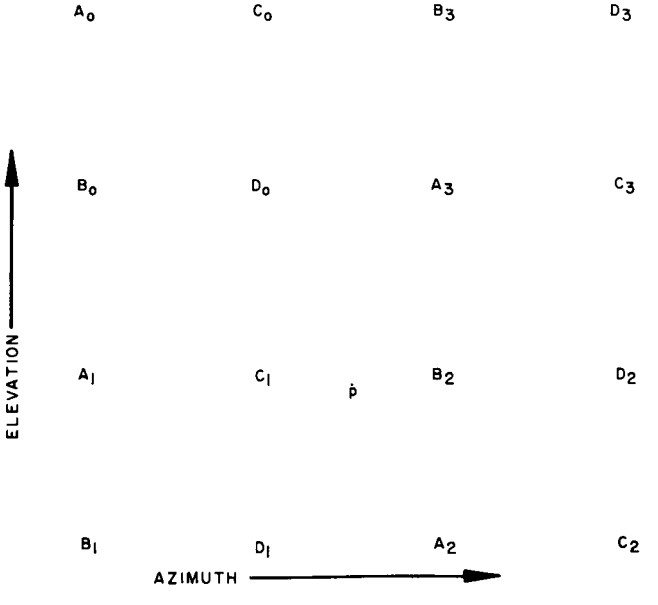

Figure 3-13. Arrangement and designation of beams.

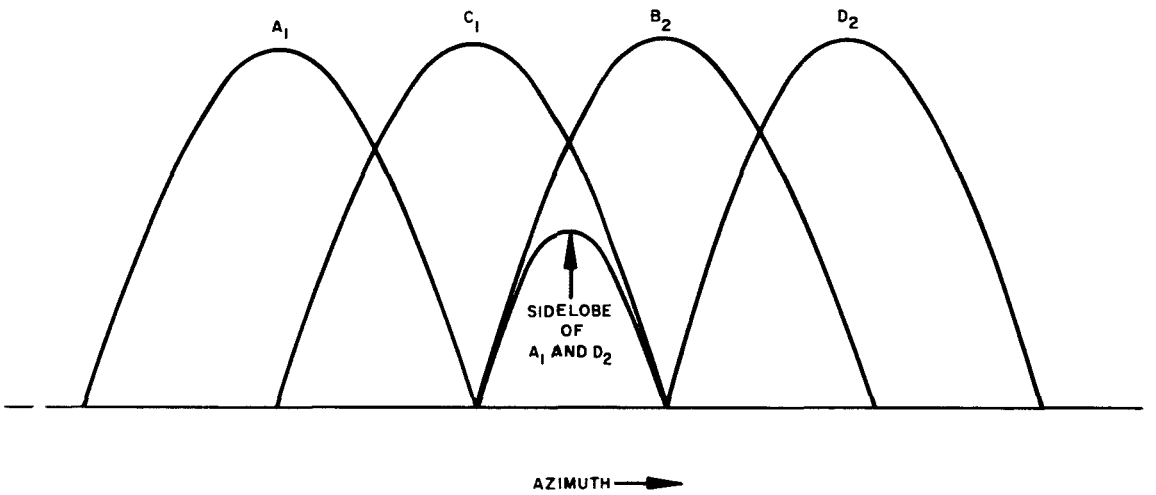

Figure 3-14. Patterns for beams A_1, C_1, B_2, and D_2 through a principal plane.

of A_1 and D_2. Since in this plane, all beams except those shown in Figure 3-14 have a null, the transmitting logic will select A_1, C_1, B_2, and D_2 and switch the transmitted energy into them. With a very low sidelobe level, the variable power dividers would be set so that all the energy was directed to beams C_1 and B_2; however, the sidelobe level is high enough to cause a significant amount of power to be directed to beams A_1 and D_2. The sidelobes do not add to the composite beam but, because of their 180° phase difference from the main beams, they actually subtract. Therefore, whenever the antenna system switches into a sidelobe, there is a noticeable dip which can be observed on the transmitting patterns.

This problem in the multiple-beam antenna system could be avoided in two ways. First, a new element design with lower sidelobes might be attempted. Second, the transmitting logic could be designed so that four adjacent beams which form a square would be selected. This design could be accomplished by dividing the beams into 9 overlapping quadrangles with each consisting of four beams. The signal levels of the four beams of each quadrangle would be added and the one with the largest sum selected. The variable power divider would then

divide the power according to the ratio of the pilot signal levels in the beams of the quadrangle selected; therefore, for the case shown in Figure 3-13 for which the transmitting pilot transmitter is located at point P, all the power would be transmitted into beams C_1 and B_2.

Patterns of the system operating with the loop closed* were taken with the system again operating 35 feet from a simulated ground receiving and transmitting pilot and an information transmitter and receiver. Since the information signal is limited by the AGC of the information i-f amplifier, these patterns are essentially those of the transmitting portion of the antenna system. One such pattern is presented in Figure 3-15.

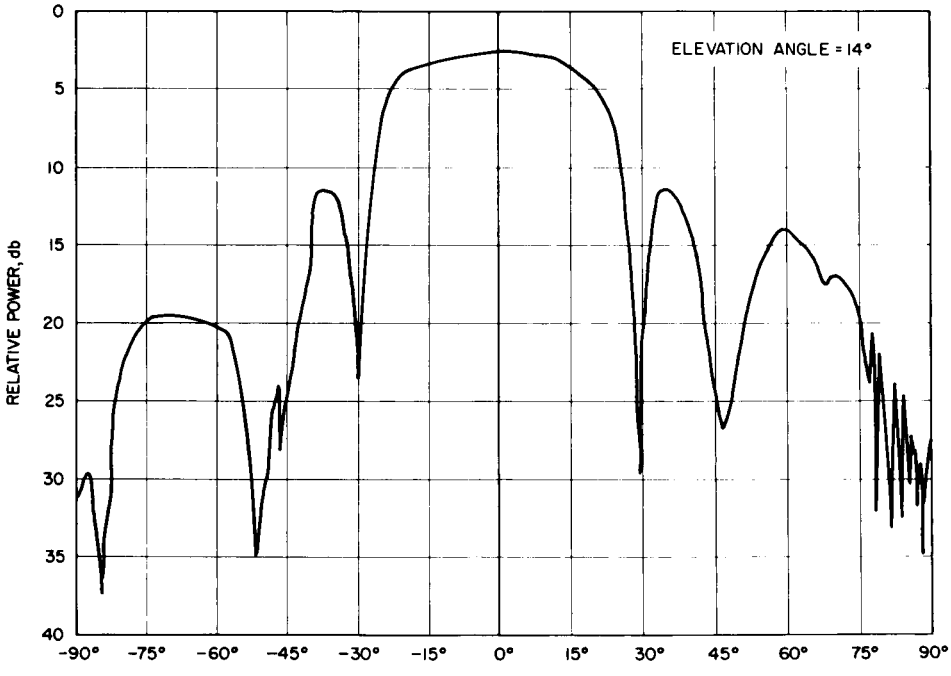

Figure 3-15. Pattern of entire multiple-beam breadboard system with system tracking both receiving and transmitting pilots.

*Closed loop means that the entire system is in operation: an information signal from a ground station is being received by the receiving array and retransmitted from the transmitting array.

3.3.2 System Signal Levels

For the signal and noise level measurements of the system the following parameters applied:

Distance of simulated ground station from the antenna system	= 35 feet
Path loss of 4.081 GHz signal	= 65.2 db
Path loss of 6.301 GHz signal	= 69.4 db
Gain of pilot antennas	= 22 db
Gain of information transmitter antenna	= 22 db
Gain of information receiver antenna	= 15 db
Power into pilot transmitter antenna for an assumed -121.5 dbw at antenna system	= -74.1 dbw
Power into information transmitter antenna for an assumed -107 dbw at antenna system	= -59.6 dbw.

The signal levels which were measured throughout the system are summarized and compared with the design objectives in Table 3-2 and in Figure 3-16.

	Design Objective (dbw)	Level Achieved (dbw)
Receiving antenna input	-107	-107
I-f buffer amplifier input	-104.5	-105
Information i-f amplifier input	-106	-110
Information i-f amplifier output	- 17.0	- 25.0
Upconverter output	- 27.0	- 34.6
TWT Input	- 29.5	- 37.1
TWT output	+ 5.5	+ 4.7
Effective radiated power	+ 23.9*	+ 23.0*

*(At peak of beam 1R1U)

Table 3-2. Signal levels of multiple-beam antenna.

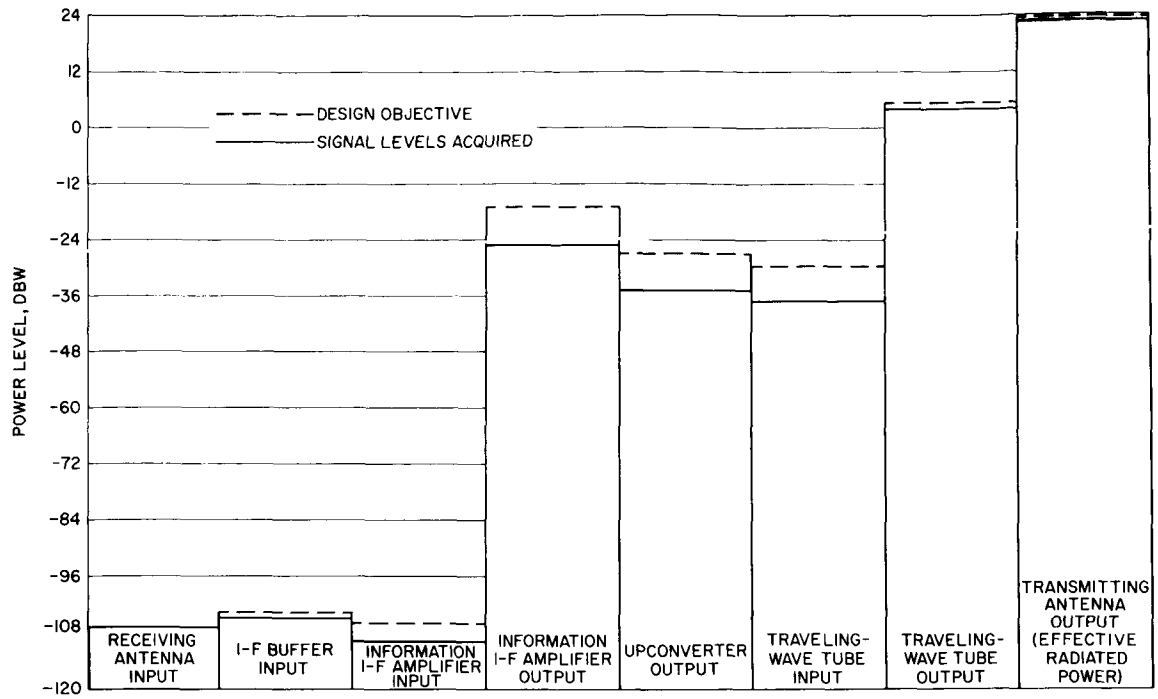

Figure 3-16. Signal levels of multiple-beam antenna.

3.3.3 System Noise Levels

The noise level of the information channel was measured by determining the minimum signal level at the information transmitter which would produce a discernible signal at the information i-f amplifier output as observed with an oscilloscope. At the information i-f amplifier output, the signal began to overcome the noise with -78 dbw at the input to the ground information transmitter located at 0^{o} elevation and 0^{o} azimuth. From this point a rough determination of the signal-to-noise ratio of the information channel at the i-f output when the incident signal strength at the receiver antenna is -107 dbw would show:

S/N measured = 78 db - 59.6 = 18.4 db

S/N (design objective) = 22 db

It can be seen that the signal-to-noise ratio at the information i-f amplifier output was about 3.6 db lower than desired. The most

significant reason for the lower figure is the 5.0 db insertion loss of the buffer i-f amplifiers and switches. This figure includes a 3-db loss because of the signal split at the buffer amplifier input. A total loss of 1.5 db had been specified in the system design.

The signal-to-noise ratio at the information i-f amplifier output for the component gains and insertion losses actually obtained for the system can be computed:

Gain of receiving antenna at balanced mixer output = 2 db

Signal level at balanced mixer output = -105 dbw

Signal level at information i-f amplifier output = -105 dbw - 5 db + 85 db = 25 dbw

Noise level at balanced mixer output is 2 db above room temperature noise = -202 dbw per cps

To compute the noise level at the output of the information i-f amplifier, the input of the buffer i-f amplifier was represented as shown in Figure 3-17. By analysis of the circuit of Figure 3-17, the mean squared noise voltage at the information buffer i-f amplifier input was found to be equal to KTB + 2.9 db. The noise figure of

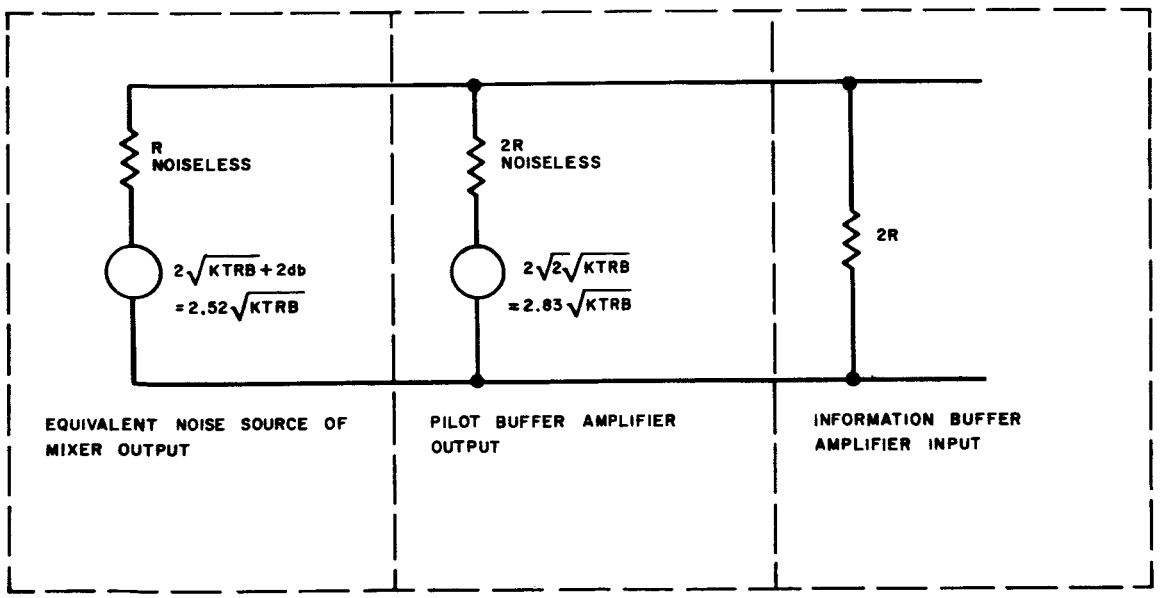

Figure 3-17. Equivalent noise source at information-buffer amplifier input.

the composite information buffer i-f switch and information i-f amplifier was

$$F = F_1 + \frac{F_2 - 1}{G} = 2 + (2-1)\ 1.58 = 3.58$$

$$F = 5.5 \text{ db}$$

Gain of composite amplifier and switch = 83 db

Noise at i-f amplifier output = (noise at input) (gain) (noise figure)
= (-204 dbw - 2.9 db + 70 db) + 83 db - 5.5 db
= -42.6 dbw

S/N (at i-f amplifier output) = 42.6 db - 25 db = 17.6 db

This signal-to-noise ratio is very near that actually realized in the system within the measuring accuracy of these signals. An improvement in the ratio at the output of the information i-f amplifier could be realized by increasing the gain of the buffer i-f amplifiers. If another system of this type were built, there would be an advantage in using mixer-i-f preamplifier units with about 20-db gain and in coupling from the preamplifiers to the i-f switches by 3-db power dividers. By using this type of configuration, the signal-to-noise ratio would be set by the preamplifier, and the appreciable amplification before the signal was split to the information channel and pilot channels would simplify design of the i-f switches. However, gain tracking would be needed between these preamplifiers.

The noise level of the pilot channels was measured by observing the video amplifier output on an oscilloscope and adjusting the power level of the pilot transmitters for a minimum discernible signal with the pilots located at 0° elevation and 0° azimuth.

Transmitting pilot power for a minimum discernible signal at the transmitting video output = -95.3 dbw

S/N (of transmitting pilot with -121.5 dbw incident power) = 95.3 db - 74.1 db = 21.2 db

Receiving pilot transmitter power for a minimum discernible signal at the receive video output	= -96.0 dbw.
S/N (of receiving pilot with -121.5 dbw incident power)	= 96 db - 74.1 db = 21.9 db

The signal-to-noise ratio specified at the video amplifier outputs was 27.5 db which is higher than the figures actually obtained by 6.3 db for the transmitting pilot and 5.6 db for the receiving pilot. (The difference in the two pilot threshold levels is probably due to inaccuracies inherent in measuring signals by observation of an oscilloscope.) The principal factor causing the signal-to-noise ratios of the pilot signals to be less than those called out for in the system design is, again, the low gain of the buffer i-f amplifiers which follows from the same reasoning used for the information channel and bandwidths of the pilot i-f amplifiers (including the filters added ahead of the amplifiers) which are about 2 MHz rather than 1 MHz as specified. The bandwidth of the pilot i-f amplifiers should be as narrow as possible even though these amplifiers are followed by video amplifiers with very narrow bandwidths because of the video detector at the i-f amplifier output. If the signal-to-noise ratio is very low at the input to this detector, the detector will degrade the signal-to-noise ratio because of a significant contribution to the noise due to noise beating with noise.

The minimum receiving pilot signal for which the receiving logic would operate properly was determined by adjusting the receiving pilot transmitter power to the lowest value for which the system will reliably switch into the proper information channel. This adjustment was done by rotating the antenna system in azimuth and observing the receiving i-f switch monitor. The power level at the receiving pilot transmitter required to enable reliable operation of the receiving logic was -80.0 dbw. Minimum incident receiving pilot power at the antenna system was -80 dbw + 22 db - 69.4 db = -127.4 dbw. At a signal level less than this figure, there was a noticeable jitter between beams when the pilot was located at the crossover point of two beams. This jitter

could be eliminated by increasing the hysteresis of the receiving logic, thus enabling the system to operate with a lower level receiving pilot.

The minimum signal for which the transmitting logic would operate properly was determined in a fashion similar to that for the receiving logic. The logic must not only determine the beams with the largest transmitting pilot signals and switch into them but also must be able to compare the relative level of the pilot signals selected.

Minimum transmit pilot power for which the digital part of the transmit logic operates properly

= -82.3 dbw (From transmitting pilot transmitter)

= -129.7 dbw (Incident power at antenna system).

Minimum transmitting pilot signal for which the transmitting logic can accurately compare signals 25 db different in level

= -69.3 dbw (From transmit pilot transmitter)

= -116.7 dbw (incident power at antenna system).

3.3.4 System Power Consumption

The power supply voltages, current, and power used were measured and are listed in Table 3-3.

	Power Supply Voltage (volts)	Current (ma)	Power (mw)
I-F Panel	+20	290	5,800
	-20	-275	5,500
Power Supply Panel	+25	330	8,250
	+12	1,035	12,960
	+12	990	11,880
	- 6	-28	168
	-12	-1,035	12,420
	-18	-570	10,260
			67,238

Power consumption exclusive of the local oscillators, traveling-wave tube, and power supplies = 67 watts

Table 3-3. Power consumption of multiple-beam system.

4.0 THE SELF-PHASING RETRODIRECTIVE ANTENNA BREADBOARD SYSTEM

One applicable retrodirective beam-steering technique forms a high-gain beam from an array of elements for a transmitting mode and uses a single wide beam from another antenna for a receiving mode. It is designed to relay information between two communicating ground stations. A station transmits an information signal at one frequency while another ground station sends a c-w pilot signal and receives the redirected information at another frequency. A breadboard implementing this concept was designed, constructed, and evaluated during Phase II of the Spacecraft Antenna Systems program. A detailed discussion of its operation and the results of performance tests are presented. It is also described physically.

4.1 SYSTEM OPERATION

The operation of the self-phasing retrodirective breadboard system is described with reference to the schematic diagram of Figure 4-1. The breadboard utilized a 16-element array (4-by-4) to form the high-gain transmitting beam and a single helical antenna as the broadbeam receiving antenna. The information signal was received at 6301 ± 5 MHz while the pilot was received at 4.159 GHz and the information retransmitted at 4081 ± 5 MHz.

4.1.1 Components and Functions

The transmitting portion of the antenna breadboard used the same 4-GHz array that was designed and used for the multiple-beam breadboard system (see Sections 2 and 3.2.1). The theoretical aperture gain of the array was 23 db with an assumed aperture efficiency and cable loss of 1-1/4 db and a 3-db element factor fall-off at the edge of the coverage. The minimum theoretical array gain was 18.75 db. Theoretical element gain was equal to 6.7 db.

The receiving portion of the breadboard system utilized one element identical with the elements of the 4-GHz array except that it

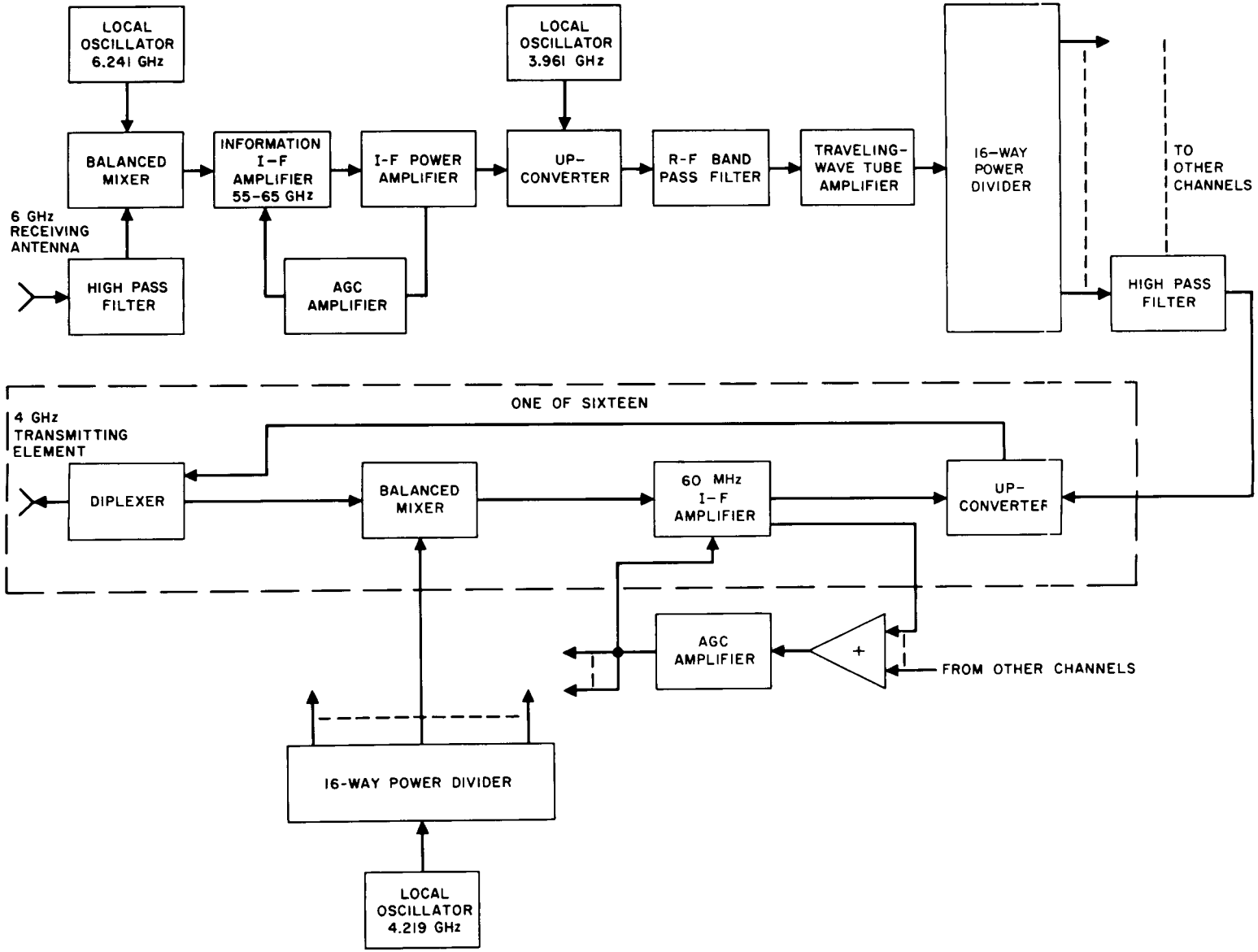

Figure 4-1. Self-phasing antenna system schematic.

was scaled in frequency to 6 GHz. Theoretical antenna gain for the receiving antenna was thus also 6.7 db.

The information which was received by the 6-GHz array passed through a high pass filter (Figure 4-1) that prevented the energy coupled from the transmitting antenna to the receiving antenna from saturating the balanced mixers. Behind the high pass filter, the information signal was down-converted to i-f at a center frequency of 60 MHz and then amplified by a high gain i-f amplifier which had a 10-MHz bandwidth.

The output from the i-f amplifier, maintained at a constant level by an AGC loop, was directed to an up-converter in which the i-f information was mixed with a local oscillator at 3.961 GHz. A band-pass filter selected the upper sideband which was directed to the input of a traveling-wave tube (TWT) amplifier. This amplifier served as an r-f power amplifier to raise the signal to a relatively high level before it was distributed to the 16 channels of the antenna system.

Distribution to the 16 channels was made by means of a 16-way strip transmission line power divider. Each output port of the divider was followed by a high pass filter to provide high isolation at 60 MHz between ports. Such high isolation was necessary since (as can be seen on the schematic of Figure 4-1) a 60-MHz signal was present at the ports of the up-converter in all 16 channels of the system.

4.1.2 Retrodirection by Phase Reversal

The pilot signal was received by an element of the 4-GHz array that had a phase term relative to some reference. The signal was mixed with the information signal present at the power divider output and transmitted with a phase term that was the negative of the pilot signal phase.

The pilot signal of 4.159 GHz which had passed through the diplexer and a local oscillator signal of 4.219 GHz were fed into a balanced mixer. The pilot signal will be denoted by $A_1 \cos(\omega_p t + \phi)$

and the local oscillator signal by $A_2 \cos(\omega_o t)$ where $\omega_o - \omega_p = 2\pi(60 \times 10^6) = \omega_{IF}$. Now if these signals are mixed and only the i-f term is retained, there results $A_3 \cos(\omega_{IF} t - \emptyset)$; therefore, the phase term of the i-f signal is the negative of that for the pilot signal. In the breadboard, this i-f signal was amplified by an i-f amplifier with a bandwidth of 1-MHz. This signal was fed to an up-converter together with the information signal of 4021 ± 5 MHz. The phase term of the up-converter output was the same as that for the i-f pilot signal since the up-converter output signal frequency was the sum of the input frequencies. The up-converter output of 4.081 GHz ± 5 MHz passed through the diplexer to an element of the 4-GHz array from which it was radiated.

The diplexers to which each element of the 4-GHz array were connected prevented the energy that was to be transmitted from the system from feeding back into the pilot receiver. They also served as band pass filters to pass only the upper sideband from the up-converter.

4.1.3 Gain Tracking

The breadboard system had a common AGC loop to provide gain tracking for the 16-pilot i-f amplifiers. Each i-f amplifier had an AGC detector output that produced a d-c voltage that was a function of the output signal level from the amplifier. The 16 AGC detector outputs went to the input of an "OR" gate. This gate was designed so that it would produce an output voltage level equal to the highest voltage level of the inputs. This level was applied to the input of the AGC amplifier. The amplifier contained a level detector so that it had zero output until the input reached the prescribed level. As the input level increased beyond this level, the AGC amplifier produced an output that controlled the gain of all 16 i-f amplifiers. Therefore, the gain of the 16 channels remained equal regardless of the relative amplitudes of the pilot signals into the loops.

A common AGC is essential if such an antenna system is to be used with something other than a planar array, for instance,

with an array of cylindrical or spherical shape. For an array for which the amplitude distribution is uniform, a common AGC would not be needed; the input signal to each amplifier is equal so that the gains in the channels are maintained equal by individual AGC's for each i-f amplifier.

4.1.4 Frequency of Pilot Signal

The frequency of the pilot signal was selected on the basis of the minimum separation allowable to permit sufficient isolation between the received pilot and the transmitted information, the maximum allowable frequency separation of the pilot signal and the transmitted signal to produce a negligible beam pointing error, and the harmonics that would be present in the loop. On the basis of these three qualifications, a pilot of frequency of 4.159 GHz was chosen.

This frequency allows sufficient separation to realize 70 db of isolation in the diplexer, and no harmonics are present that could cause oscillations in the loops.

The maximum separation in transmitted signal and pilot signal was (4.159 - 4.076) GHz = 83 MHz. When the beam was scanned 25 degrees off broadside, this frequency separation caused a beam pointing error of 0.55 degree, which was negligible since the beamwidth was about 14 degrees.

4.1.5 Signal and Noise Level Design Objectives

Design objectives for the signal and noise levels in the self-phasing antenna breadboard system are given in Table 4-1. For proper antenna performance, a phase error of 10° rms and 2-db rms amplitude error gives less than 1-db degradation in gain with a 99-percent confidence level.

4.2 PHYSICAL DESCRIPTION

The self-phasing antenna system was constructed as one unit (Figure 4-2) with the only external equipment being the power supplies

Parameter	Component Gain (db)	Minimum Antenna Gain (dbw)	Signal Level (dbw)	S/N (db)
Information Channel				
Effective radiated power			+0.75	
Theoretical peak aperture gain	23			
Aperture efficiency	-1.25			
Element factor fall-off on edge of coverage	3	18.75		
Loss when linearly polarized waves are used	3			
Number of elements (16)	12			
Power radiated per element			-30	20
Diplexer loss	3			
Up-converter loss	12.5			
Modulation input to up-converter			-14.5	20.7
Modulation power divider and high pass filter loss	13.5			
TWT gain and power out	30		-1	
Transmission filter insertion loss	3			
Up-converter conversion loss	10			
I-F amplifier gain and output level	90.3		-18	20.7
Balanced mixer conversion loss	6			
High pass filter loss	0.5	6.7		
Minimum receiving antenna gain		6.7		
Received signal level (isotropic)			-107.5	
(Continued on next page)				

Table 4-1. Signal and noise level design objectives for self-phasing breadboard.

Parameter	Component Gain (db)	Minimum Antenna Gain (dbw)	Signal Level (dbw)	S/N (db)
Pilot Channels				
Pilot signal level into up-converter			-17	28.7
Narrowband pilot i-f amplifier gain	93.3			
Balanced mixer conversion loss	6			
Diplexer insertion loss	3			
Minimum 4-GHz element gain		6.7		
Received pilot signal level (isotropic)			-108	

Table 4-1. (Continued).

and the local oscillators. All components for the system were mounted on a 48-by-22-by-1 inch plywood board with a 2-by-4 inch peripheral frame.

4.2.1 Antennas and Diplexers

The two antennas for this system were mounted on one end of the peripheral frame (see Figure 4-2). The 4-GHz transmitting antenna was the same array that was used for the multiple-beam breadboard (Section 3.2.1) and consisted of 16 helical elements mounted in a 4-by-4 arrangement on an aluminum ground plane. The ground plane was a 22-inch square plate of aluminum 1/8 inch thick. The array was mounted with the bottom edge attached to the frame so that it extended above the wooden bed in a vertical position. Mounted below was the 6-GHz receiving antenna, which consisted of a single helical element on a small square ground plane. Details of the design of the elements and the array can be found in Section 2 of this report.

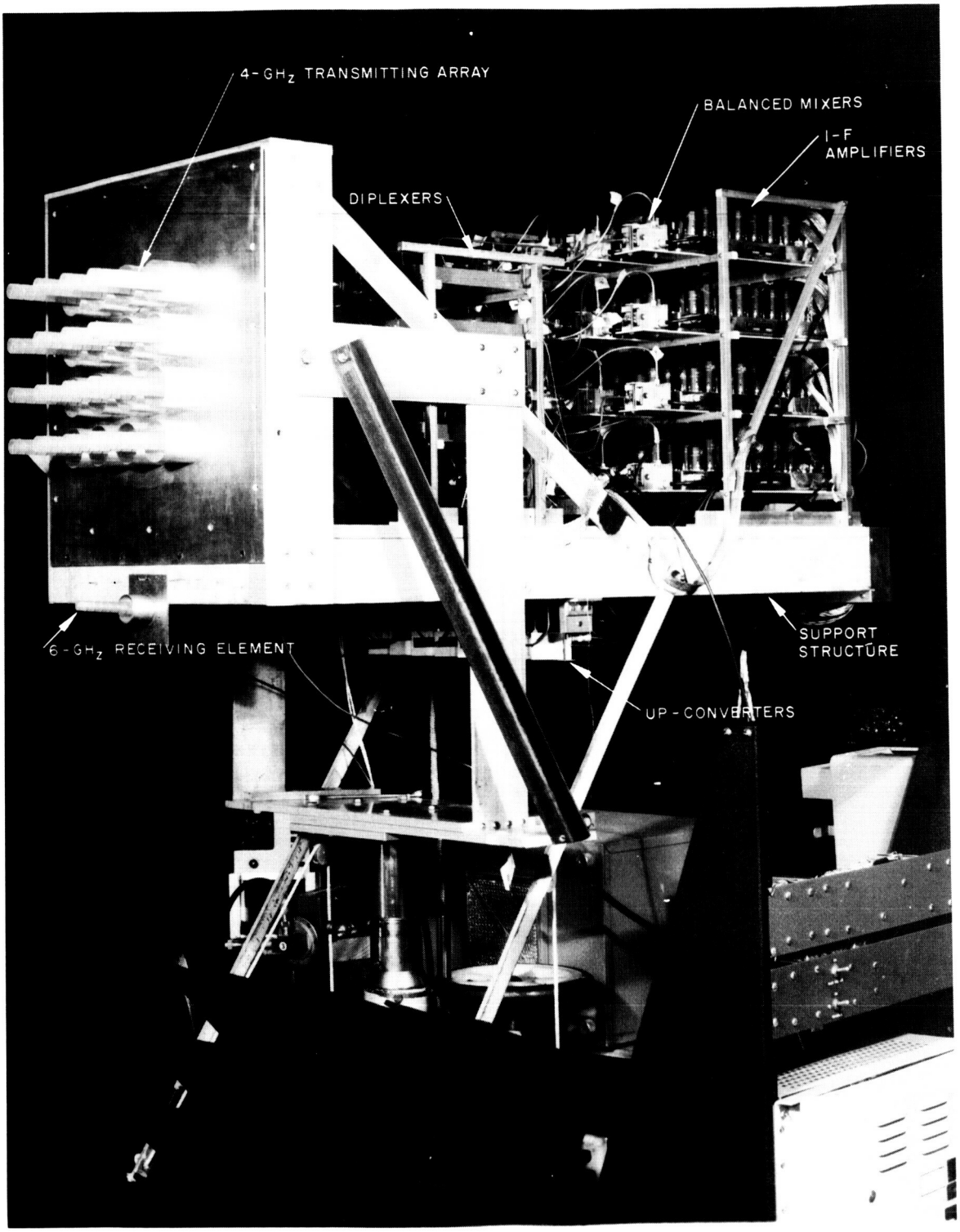

Figure 4-2. Self-phasing antenna system breadboard.

About 11 inches behind the 4-GHz array were 16 diplexers, one for each channel, stacked on an aluminum frame in an arrangement of four rows and four columns (see Figure 4-3). These were waveguide band pass filters which were 8 inches long, about 1 inch thick, and about 4 inches wide. The input ports of the diplexers were attached to the 4-GHz antenna elements with semi-rigid cables and OSM connectors.

4.2.2 Power Divider and I-f Amplifiers

Mounted in a vertical position parallel to the 4-GHz ground plane and 4-1/2 inches from the diplexers was a 16-way power divider (Figure 4-3). Behind the divider were the 16 pilot r-f mixers and i-f amplifiers. The amplifiers, each 18 inches long, were stacked like the diplexers in four rows and four columns on an aluminum frame that extended to the back of the mounting board. A balanced r-f mixer was mounted immediately in front of each i-f amplifier. The mixers were connected to the inputs of the amplifiers by means of short pieces of coaxial cable and BNC connectors. The local oscillator ports of the mixers were connected to the output of the 16-way power divider while the signal ports were connected to the output ports of the diplexers by means of semi-rigid coaxial cables.

At the back of the frame were located terminal boxes which were used to connect the power cable from each i-f amplifier to a common power cable which led to the power supplies for the system. The AGC gate and amplifier were also mounted on the rear of the frame and connected electrically to the i-f amplifiers through the terminal boxes.

4.2.3 Up-Converters

Sixteen final high-level up-converters were mounted on the bottom of the frame about half way from each end. These were approximately 2-inch cubes mounted side-by-side to form two rows that extended nearly the full width of the mounting board (Figure 4-3). The i-f ports of the up-converters were connected to the outputs of the i-f amplifiers by coaxial cables and BNC connectors. The output ports were connected to a third port of the diplexers by OSM connectors and semi-rigid coaxial

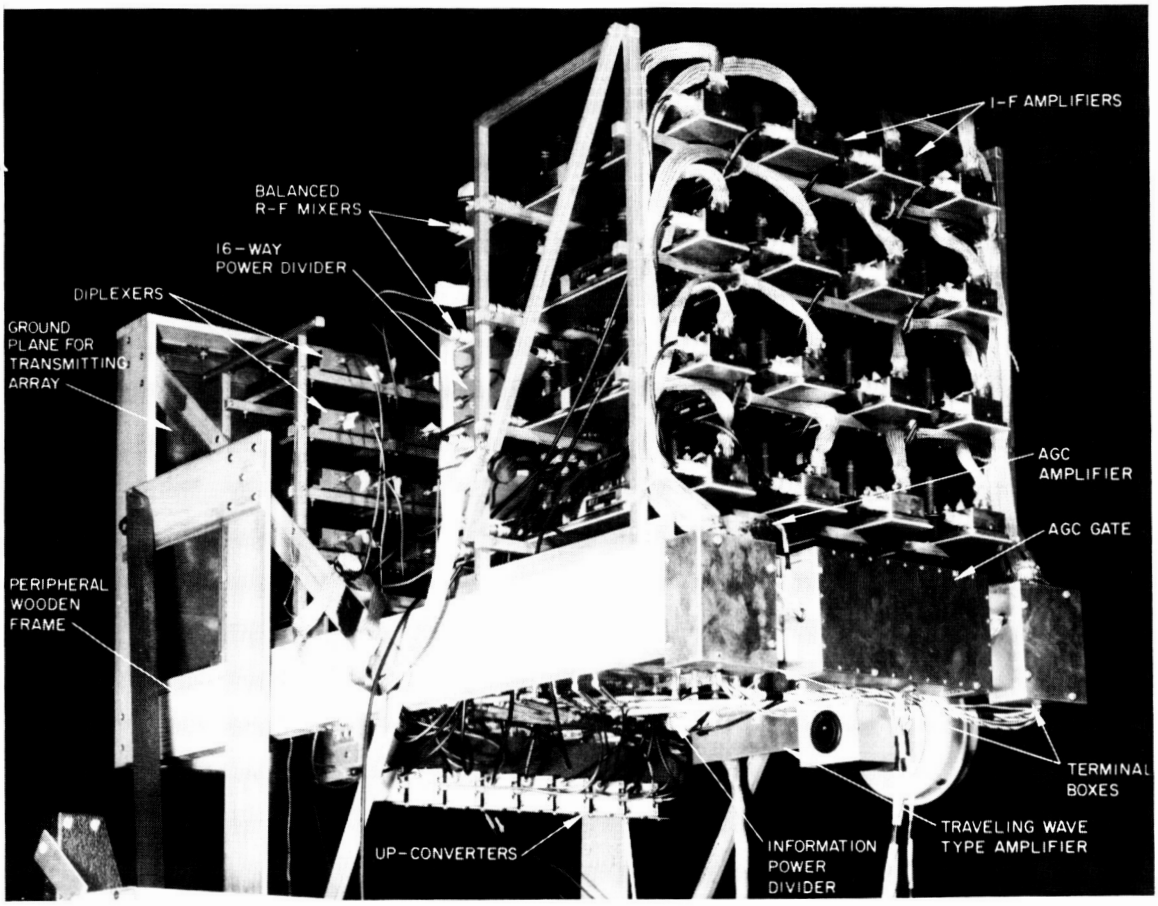

Figure 4-3. Arrangement of components in self-phasing antenna breadboard.

cables which run from the up-converters through the board to the diplexers. The third port of the up-converters was connected to an information power divider via high pass coaxial filters, semi-rigid coaxial cables, and OSM connectors. This power divider, which was about 12 inches square and 1/2 inch thick, was mounted flat against the underside of the board behind the up-converters. Mounted along one side of this power divider and connected to it was the traveling-wave tube (TWT) amplifier with its blower.

4.2.4 Information Receiving Components

All the components for the information receiver for this system were mounted on the underside of the mounting board up inside the 2-by-4 inch frame. These components were mounted behind the 6-GHz radiating element and extended to the input of the traveling-wave tube amplifier. They included a high pass filter, a balanced mixer, a wide band i-f amplifier with an AGC amplifier and power amplifier, an up-converter, and a sideband select filter.

4.3 PERFORMANCE AND EVALUATION

A thorough evaluation of the self-phasing antenna system breadboard was performed; tests included measurements of the amplitude and the phase distribution over the system bandwidth; antenna patterns for different operating modes, system signal and noise level measurements, gain measurements, and primary power consumption measurements of the antenna system (exclusive of the local oscillators, traveling-wave tube amplifier, and all power supplies).

4.3.1 Amplitude and Phase Distribution

To realize maximum gain from this type of antenna system, it was necessary to have a constant amplitude distribution for a constant phase gradient. To accomplish this distribution, the phase length through each of the sixteen channels was changed by adjustments of

the cable lengths so that the relative phase shift between the channel outputs was zero for a zero relative phase difference into the channels. The amplitude distribution was adjusted by making the gains equal through the sixteen channels. This procedure involved adjustment of the i-f amplifier gains to compensate for the insertion loss variations of the other components in the channels.

The adjustments were made for a 4.021 GHz signal from the information power dividers and then were remeasured at the edges of the information band to check for phase and gain tracking. The measurements were also made for two pilot signal levels, one for maximum pilot i-f amplifier gain and the other for a reduction of 25-db in i-f amplifier gain (a 25-db increase in the pilot signal level caused a 25-db decrease in pilot i-f amplifier gain because of the AGC). The results of these measurements are given in Table 4-2.

4.3.2 Antenna System Patterns

Patterns of the 4-GHz antenna array were taken by operating the system a distance of 12 feet 8 inches from the transmitting pilot and simulated information receiving antennas. These patterns were taken by rotating the system in azimuth with the pilot and receiving antennas fixed. Patterns were taken for eleven positions in elevation (every 5 degrees from -25 degrees to 25 degrees); the typical pattern

Information Frequency From Power Divider (GHz)	For Full I-f Gain		For 25-db I-f Gain Depression	
	Amplitude Error (rms)	Phase Error (rms)	Amplitude Error (rms)	Phase Error (rms)
4.021	0.694 db	1.98°	1.13 db	2.67°
4.016	1.6 db	3.29°	1.40 db	3.3°
4.026	1.58 db	8.18°	1.79 db	8.65°

Table 4-2. Amplitude and phase measurements of self-phasing breadboard.

shown in Figure 4-4, indicates that the variation in gain over the coverage angle was negligible and that the gain is down 3 db or less at ±25 degrees as had been predicted.

The gain of the system over the 10 MGz information bandwidth was then checked by patterns taken at three different information signal frequencies with the system locked on a pilot. These patterns (Figure 4-5) show a degradation in system gain of about 1.5 db at 4026 MHz, the upper limit of the information band. This figure does not mean that the array gain had actually fallen off at this frequency; most likely the loss was due to the insufficiently flat response characteristics of the diplexers over the bandwidth. The diplexer response curves, which are given in the Technical Report—Feasibility Models (1966) for this program, show such a characteristic clearly.

Transmitting array patterns were also taken with the bread-board system operating at the 12-foot, 8-inch distance from the pilot and information receiving antennas of the simulated ground station.

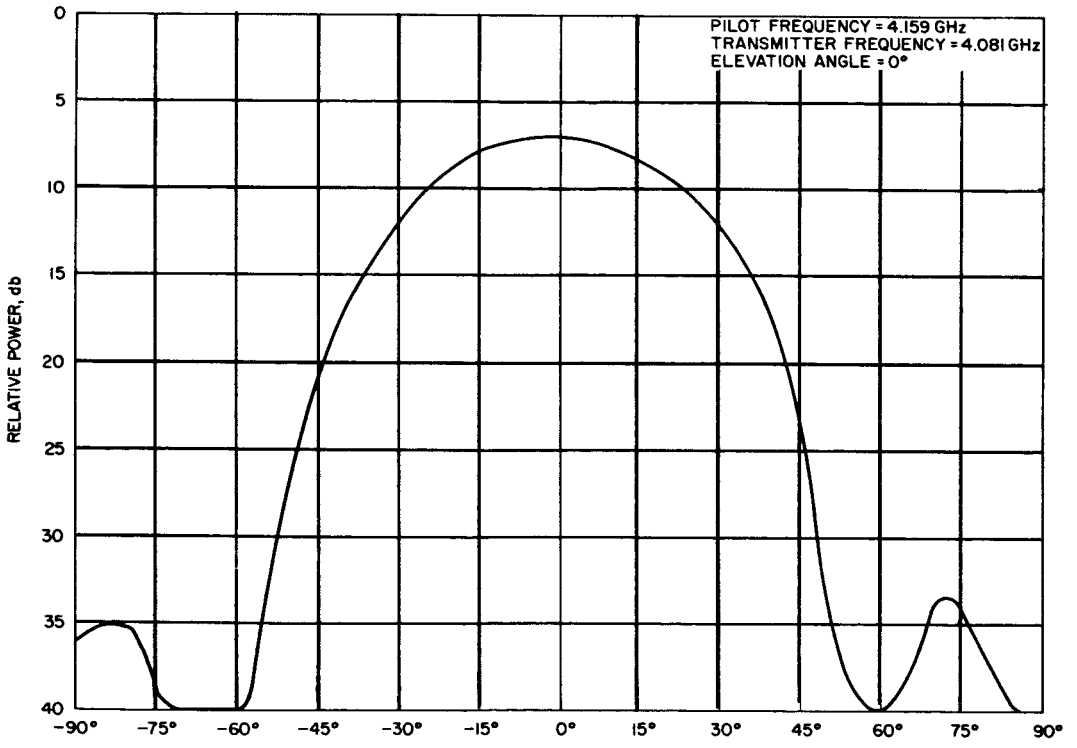

Figure 4-4. Pattern of 4-GHz transmitting array with system tracking the pilot.

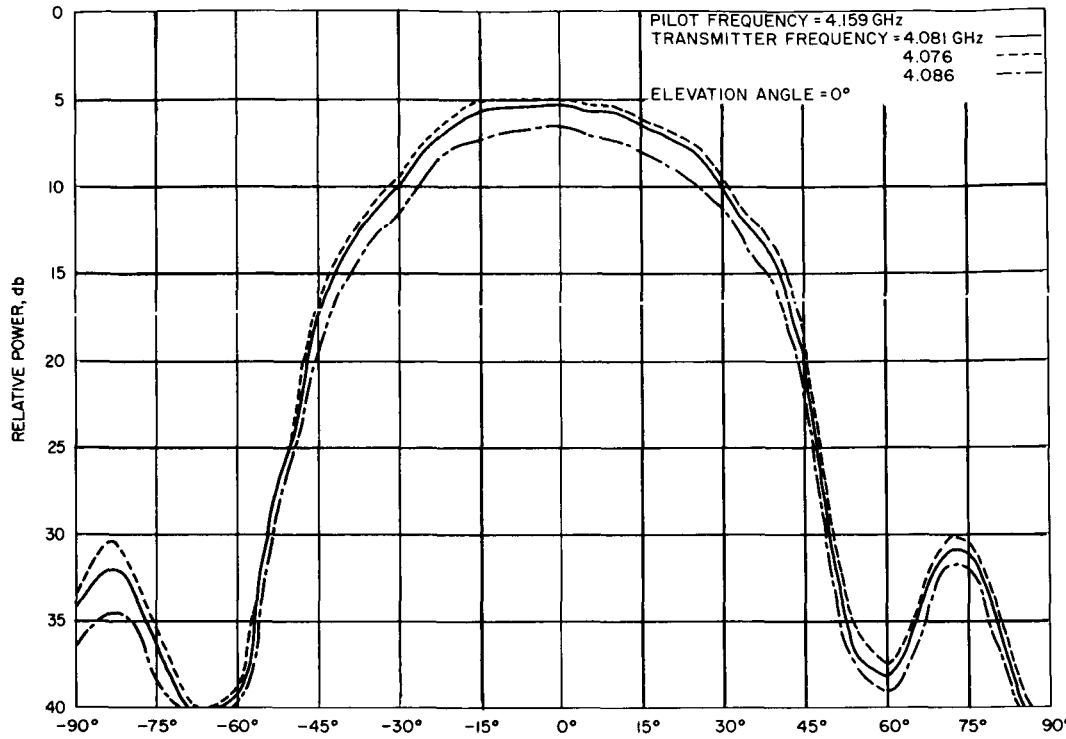

Figure 4-5. Patterns of 4-GHz transmitting array with system tracking the pilot at three transmitting frequencies.

The pilot antenna was mounted on a boom so that it could rotate with the system and remain stationary in relationship to it. Two of these patterns are presented in Figure 4-6 for elevations of 0 degrees. The pattern in Figure 4-6a was taken with the pilot located at 0 degrees azimuth, while that in Figure 4-6b was taken with the pilot located at -20 degrees azimuth. The sidelobes can be seen to be 10 db down and the beamwidth to be about 13 degrees, which were approximately the same values as those obtained with this array in the multiple-beam antenna system. When the pilot signal was at -20° azimuth, however, some beam-pointing error did occur, undoubtedly due to the element factor fall-off at the edge of the coverage angle.

Closed-loop patterns* were taken with the system rotated in azimuth. These were essentially the same as that in Figure 4-4,

*"Closed-loop" is used here to mean that the entire system is in operation: an information signal from a simulated ground station is being received by the receiving array and retransmitted from the transmitting array.

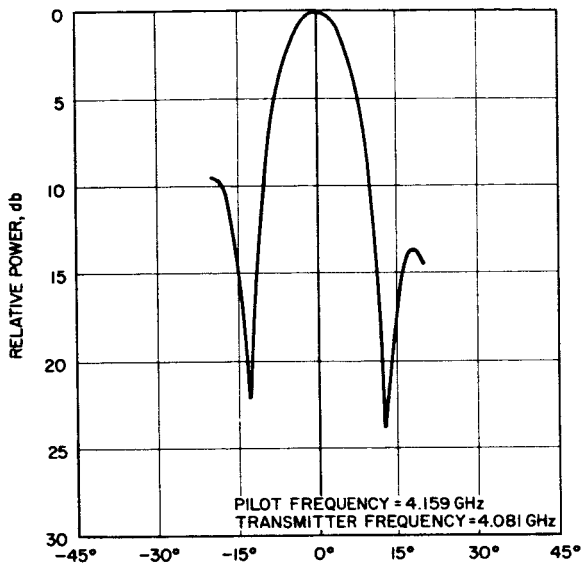

a) 0° azimuth

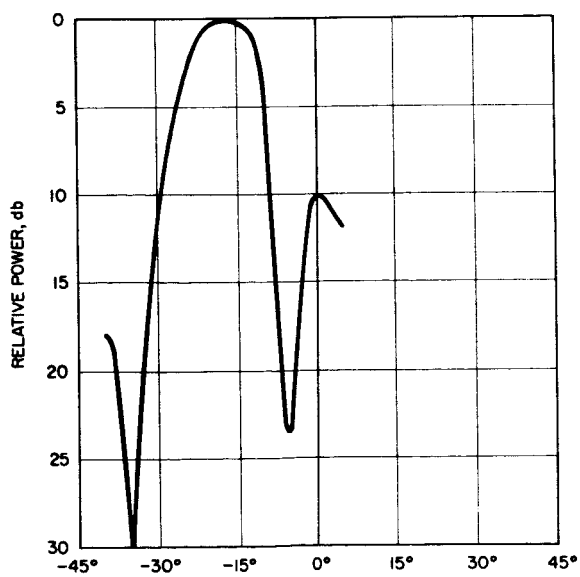

b) -20° azimuth

Figure 4-6. Patterns of 4-GHz transmitting array at 0-degree elevation with pilot stationary with respect to the antenna.

except for the superimposition of the receiving gain factor. Because of this added factor, additional suppression of the array factor occurred beyond the ± 25 degree coverage angle. One of these patterns is shown in Figure 4-7.

4.3.3 System Signal Levels

With the system operating with the appropriate pilot transmitter and ground communications transmitter, the signal levels at key points throughout the system were measured. Since there are sixteen self-phasing loops for any signal level at any point in any loop, all sixteen loops were measured and the average taken. Signal levels and component gains are given in Table 4-3 and compared with predicted values.

It will be noted that the gain of the mixer i-f amplifiers is lower than that predicted. This result is due to the adjustment of the AGC; it was set to give a lower output level from the i-f amplifiers than

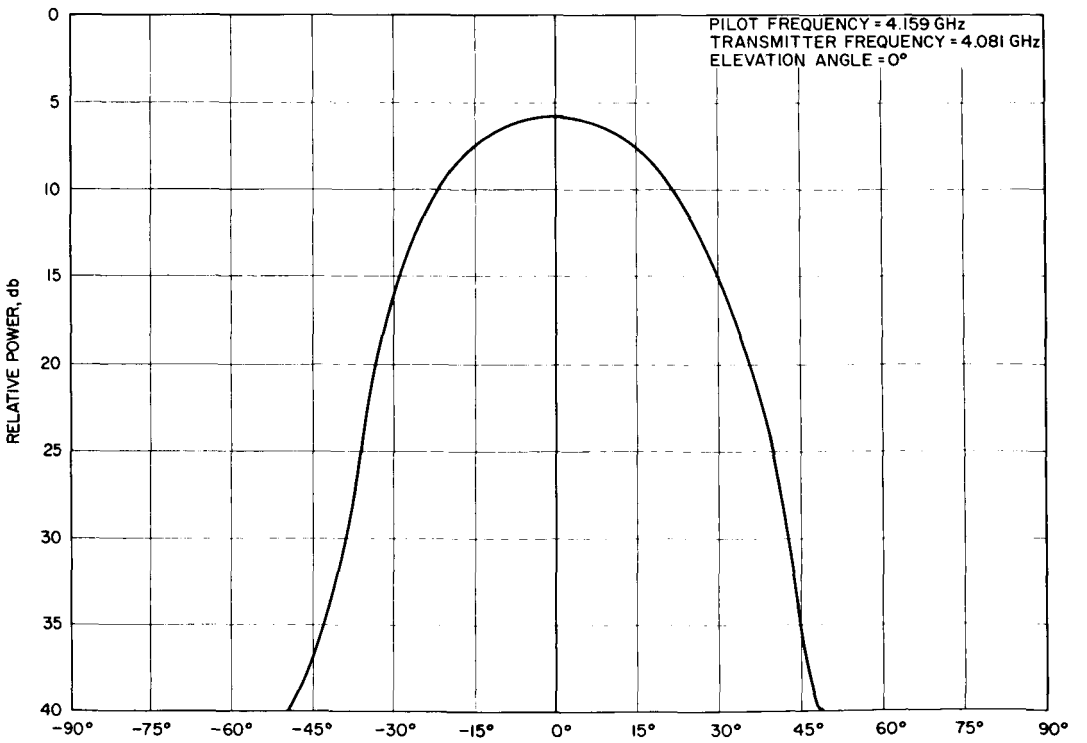

Figure 4-7. Closed-loop pattern with system tracking pilot and receiving gain factor superimposed.

Parameter	Measured Experimentally		Predicted	
	Signal Level (dbw)	Component Gain (db)	Signal Level (dbw)	Component Gain (db)
Pilot signal level at antenna (isotropic)	-108*		-108	
Pilot signal level at diplexer input	-101.3		-101.3	
Diplexer insertion loss		1.6		3
Pilot signal at input to balanced mixers	-102.9		-104.3	
Balanced mixer and pilot i-f amplifier		78.5		87.3
Pilot i-f amplifier output levels	-24.5		-17	
Information signal level into final up-converter	-14		-14.5	
Up-converter output	-43.4		-27	
Up-converter loss		29.4		12.5
Diplexer insertion loss		1.6		3.0
Power delivered to element	-45		-30	
Effective radiated power*	-13.7		+0.75	

* Experimental ERP is obtained from the power into the 4-GHz array and the array gain listed in Table 4-5 with 3 db subtracted to account for gain falloff at the edge of the coverage cone.

Table 4-3. Signal levels of self-phasing antenna.

originally specified to improve the linearity of the amplifiers and to allow enough margin to permit all loops to be adjusted for equal gain.

*Assumed level from measurement of pilot transmitter power level and path loss computation.

The most significant difference between measured and predicted component gain is the conversion loss of the up-converters. As listed in Table 4-3, the up-converter loss represents the decrease in modulated signal level during the up-conversion process. Since the two inputs to the up-converters were at different levels, the up-converter loss should really have been taken with reference to the smaller input. This procedure, however, would still have given an up-converter loss of 18.9 db. The explanation for the high loss in these devices lies in the fact that they were designed originally as low-level mixers for use on the multiple-beam antenna system. They simply do not perform efficiently as high-level up-converters, but time and money dictated the use in the self-phasing breadboard of as many components as possible from the multiple-beam system.

4.3.4 Noise Levels

The noise level of the pilot channels was measured by measuring the power at the outputs of the pilot i-f amplifiers with no pilot signals input to the system and then with an increased pilot transmitting power to provide a 3-db increase in the pilot amplifier output power. This measurement was made for each of the sixteen channels of the system. The average of the results is given in Table 4-4.

Measurement	Value
Distance of pilot transmitting antenna from antenna system	12 feet, 8 inches
Path loss	$20 \log \frac{4\pi R}{\lambda} = 56.6$ db
Pilot transmitting antenna gain	17.2 db
Power into pilot antenna for 3-db rise above noise in pilot i-f amplifier output	-97 dbw
Power at antenna system (isotropic) for 3-db rise above noise in i-f output	-97 dbw + 17.2 db - 56.6 db = 136.4 dbw
Signal-to-noise ratio at i-f amplifier output for -108 dbw at antenna system	136.4 db - 108 db = 28.4 db

Table 4-4. Averaged noise levels.

It can be seen that the signal-to-noise ratio of the pilot signal at the i-f amplifier outputs is very close to the predicted value of 29 db.

4.3.5 Gain Measurements

The gain of the 4-GHz array was measured by measuring the power fed into it and comparing these values with the power fed into a gain standard to produce the same field intensity at the information receiver. The information receiving horn was rotated in polarization to receive the maximum signal strength from the array, and another measurement was made at 90 degrees from this polarization to account for the ellipticity of the signal transmitted from the array. Values are given in Table 4-5.

The 21-db value measured for the array gain was determined for the beam at broadside. The theoretical peak aperture gain for the array was 23 db and the assumed aperture efficiency was -1.25 db to give a predicted gain of 21.75 db. Measured and predicted gain are in very close agreement.

Measurement	Value
Power into 4-GHz array	-31.7 dbw
Ellipticity of transmitted signal	1.6 db
Power into gain standard to give signal intensity equal to the largest component of the elliptical wave at information receiver	-28 dbw
Power into gain standard to give signal intensity equal to the quadrature component of elliptical wave	-29.6 dbw
Power into gain standard (sum of two components)	-25.7 dbw
Gain of gain standard	15 db
Gain of 4-GHz array	15 db + 31.7 db - 25.7 db = 21 db

Table 4-5. Measured gains.

4.3.6 System Power Consumption

Primary power consumption (exclusive of traveling-wave tube amplifier, the local oscillators, and all power supplies) is given in Table 4-6.

	Power Supply Voltage (volts)	Current (amperes)	Power (watts)
Pilot I-F Amplifiers including AGC Amplifier	150 6.3 - 10.0	1.36 33.6 - 0.0052	204.0 211.68 0.052
Information I-F Amplifier	- 20	- 0.140	2.80
Total Power Consumption			418.53 watts

Table 4-6. System power consumption.

5.0 NEW TECHNOLOGY

The transdirective concept, described in the Phase I Interim Report (Kummer and Villeneuve, 1965), is believed to be a new technique for beam-steering in self-steerable arrays. The multiple-beam breadboard antenna system represents the implementation of such a concept for the first time for satellite use. None of the components utilized is novel or unique, but the system itself is believed to be New Technology. It is described in detail in Section 3.0 of this Final Engineering Report.

The retrodirective technique by phase reversal, as implemented in the self-phasing antenna breadboard system, similarly is the first time a retrodirective self-steerable antenna system has been designed, constructed, and evaluated as a system for a satellite. Neither the technique nor the components are unique or new, but the implementation as a system for satellite use is believed to be New Technology. It is described in detail in Section 4.0 of this Final Report.

6.0 CONCLUSIONS AND RECOMMENDATIONS

6.1 PROGRAM CONCLUSIONS

The objectives of this program were the recognition of those techniques which will provide spacecraft antenna systems capable of optimum reliability and least power consumption.

6.1.1 Phases of Program

Study Phase (Phase I)

The first phase of the program consisted primarily of an intensive study of novel antenna techniques which will find application in spacecraft antenna systems. Included in this study was a review of the literature, a field survey, and an assessment of the present state-of-the-art in all electronic beam formation shaping and steering techniques. Multiple-beam formation methods, phased-locked loops, electronically self-steering antenna systems, and millimeter-wave antenna systems were studied in detail as potential parts of spacecraft systems. The study proved to be useful because a) applicable techniques were brought together and evaluated; b) specific techniques were recommended for further study; and c) the most promising techniques were selected for implementation.

Implementation Phase (Phase II)

The second phase involved the design, fabrication, and testing of two antenna system breadboards. Each system implemented a different type of electronic beam-steering technique, one the multiple-beam transdirective concept and the other a self-phasing concept. Both systems had a 10-MHz information bandwidth and used a 6000 n. mi. gravity-gradient satellite as the model for the vehicle.

The two system concepts share several advantages over other beam-steering techniques. Neither requires variable phase shifters to scan the beam as do conventional phased arrays. Their gain is not limited by the requirement that the beam cover the entire visible earth. They do not require earth sensors or preprogrammed controls. Both types of systems are applicable to nonsynchronous and synchronous gravity-gradient stabilized orbits; the self-phasing array, in addition, is applicable to unstabilized systems. In both, satellite attitude information is inherently available. Both systems, however, share the disadvantage of requiring a pilot signal to be generated at the earth receiving station (or a command signal at the earth transmitter for the multiple-beam transdirective command mode).

6.1.2 Breadboards

The transdirective breadboard was a multiple-beam antenna system that used beam-forming matrices in conjunction with planar arrays to position the beams in space. The breadboard system utilized two 4-by-4 arrays, one for transmitting and one for receiving. The receiving array had 16 overlapping beams with discrete beam positions; the transmitting beam could be continuously scanned by the use of four adjacent beams appropriately weighted to form one composite beam. The breadboard was operated by pilot signals, although the concept can be made to operate equally as well on command. The components used for this system were all state-of-the-art, and no unusual difficulties in circuit design were encountered. The logic proved to be complex, using, for example, over 1000 transistors.

The transdirective breadboard performed as designed, and patterns obtained for this system were quite satisfactory. The system switched beams at the beam crossover as predicted with no jitter between beams. The gain of the receiving array, measured at the beam ports of the beam-forming matrix, was 15 db minimum. The transmitting logic properly selected the four beams with the largest transmit pilot via the transmit switch, and the relative power into the four beams was controlled by the analog logic and variable power dividers to form a

composite beam. This beam accurately tracked the transmit pilot with about a 2-db variation in gain over the cone of coverage except for 1 db to 3 db dips which were caused when the logic selected a sidelobe of one of the beams. These dips could easily be eliminated, however, by a redesign of the transmitting logic. Gain for the transmitting array was 17.4 db minimum as measured at the beam ports of the transmitting beam-forming matrix.

This program proved the feasibility of the transdirective concept for spacecraft antenna system application. This type of system can be built very light in weight and of low power consumption in a 4-by-4 version such as the breadboard. High gain on transmit can be achieved by the use of the digital transmit switch and variable power dividers which eliminate an 8-db dip from peak gain at the diagonal crossovers of four beams. For the breadboard, discrete beam positions were used for the receiving array; however, a continuously scanning beam could be obtained on receive by utilizing four beams to form one composite beam as is done for the transmitting array. This arrangement would raise the -8 db points to -2 db from peak gain.

The transdirective breadboard utilized a 4-by-4 beam-forming matrix as one of its major components. Conceptually, such matrices can be built to any size, but in practice, after a point the increase in losses with size are appreciable compared with the desired increases in gain with size. Extension of the transdirective concept to larger antennas necessitates building matrices larger than the 4-by-4 matrix used in the breadboard. At present, it appears that a matrix larger than 8-by-8 is not too practical without appreciable matrix developmental effort, and even an 8-by-8 introduces severe receiver front end losses.

In addition to their weight and loss problems, the beam-forming matrices utilize large numbers of couplers or hybrids which further increase the complexity and bulk. Other additional components in the system include electronically controlled r-f switches and very complex switch control circuitry. Variable power dividers may even be required instead of switches between the beams with additional circuitry and

control circuitry to insure smooth transfer, since the minimum useful signal is determined by the gain at the beam switch-over point. Because of the large numbers of components and the complexity of many, failures in the transdirective array may be variable in catastrophic terms, depending on which component failed. The concept does, however, lend itself readily to control by command which could be an important asset for some applications. Further, the r-f components (the matrix or the lens) are inherently reliable, and satellite attitude information is inherently available in such a system.

The self-phasing breadboard utilized a 4-by-4 array for transmitting and a single helical element for receiving. A pilot signal was received by the elements of the array which provided the phase information for the self-phasing array. Phasing was accomplished by a mixing technique to automatically point a beam back in the direction of the pilot signal. The breadboard proved the feasibility of this type of system for spacecraft application. It operated satisfactorily in simulated tracking tests, and the patterns taken were very good with no dips or degradation in gain over the desired coverage angle. The gain at scan angles of $\pm 25^{\circ}$ was down about 3 db from peak as was expected. Measured gain of the 4-by-4 array was 18-db minimum. The phase and gain tracking was 8° rms and 1.6 db rms between modules. No problems were encountered in this regard.

The self-phasing system is modular in form so that any given system could be extended to any number of elements; thus this concept has growth potential. Additionally, because the modules are independent, failure of one is not catastrophic. No switches or switching controls or logic circuitry, as such, is required in the system. Elements can be placed on any shaped surface and are not restricted to planar surfaces as are most phased arrays, including the transdirective system.

All components for the self-phasing system are state-of-the-art except for final r-f amplifiers that would operate at the satellite transmitting frequency. These amplifiers, which would boost the

effective radiated power and would significantly improve the efficiency of a self-phasing system, would have to be developed for a flight-qualified system. Another drawback of the self-phasing system is that an N element array requires N phase-matched modules, and each module requires a complete receiver and transmitter.

6.2 RECOMMENDATIONS

6.2.1 Study Phase

It is recommended that the study phase of this program be continued. The continuing program would be aimed toward three objectives:

(a) A continuous updating, evaluation, and assessment of new electronically and mechanically steered arrays. Realistic missions would be chosen for application of pertinent techniques.

(b) A continuous updating of components both for application to the present engineering models of the self-steering arrays and for application to the newer techniques studied in item (a).

(c) A reevaluation and implementation of the breadboards and engineering models for applications other than presently contemplated. In the preceding study, it was pointed out that the self-steering arrays could be applied to spin-stabilized vehicles. Design changes and specific implementation of both the transdirective and, especially, the self-phasing arrays should be studied and implemented with the present breadboards.

(d) A study of the implementation of steering techniques at millimeter waves. See 6.3.5.

6.2.2 Implementation

Engineering Model

Evaluation of the two antenna systems proved that both techniques were feasible for spacecraft antenna system application. As pointed

out in section 6.1.2, each system has distinct advantages and disadvantages. It is recommended that both models be implemented into engineering models. As an example of what might be achieved, a synchronous orbit, gravity-gradient stabilized satellite is taken as the model. A 30-degree coverage is assumed. Two independent 125-MHz information channels are assumed. Gain is realized on transmit and receive with a generation of four independent beams. An 8-by-8 two-dimensional array is employed. In the next several paragraphs the characteristics of these models will be projected:

Multiple-beam Transdirective Array

1) Components are nearly all proved, except for the matrix which should be straightforward.
2) System is readily adaptable to either command or pilot or to both on transmit and/or receive mode as well.
3) Total number of additional components is nearly proportional to the number of additional channels.
4) System is adaptable to multiple beams.
5) System does not require phase coherence of phase-locked loops.
6) Phase coherence is required in the continuous scan mode, that is, on transmit mode from the variable power dividers to radiating elements.
7) System requires a traveling-wave tube on transmitting portion, but no phase coherence is required.
8) Insertion losses (gain loss) are high.
9) An 8-by-8 system will meet minimum gain of 24 db with a theoretical aperture gain of 34 db.
10) System will provide 33 dbw or more ERP. *
11) Weight of 8-by-8 dual channel system is about 175 pounds.
12) Failure is variable in catastrophic terms.

*ERP, the effective radiated power, is the gain of the array times the total r-f power into the array.

Self-Phasing Array

1) Components are close to state-of-the-art except for final r-f amplifiers. R-f amplifiers can be expected to be within the state-of-the-art and able to provide 100 mw power within the next 2-3 years at 2 GHz but not at 8 GHz. Tunnel-diode amplifiers are a possible solution; but present ones do not have sufficient power. Multiplier chains can also be used, but their phase coherence and tracking properties are not known. Heterodyning is relatively easy for arrays with small numbers of elements, but with arrays of 64 or more elements, phase coherency becomes a more difficult problem. It is possible to use a self-phasing array without these components with somewhat less efficiency and ERP. A high level upconverter and high level driver replace the low level upconverter and r-f amplifier. With 64 modules the minimum transmit and receive gains will be 30 db.
2) System operates on pilot signals from desired beam directions.
3) Total number of additional components is nearly proportional to the number of additional channels.
4) System is adaptable to multiple beams.
5) System requires phase coherence on receive and transmit.
6) System requires high-power local oscillator(s).
7) Insertion losses (gain losses) are low.
8) A 64 (8-by-8) module system will meet a minimum gain of 30 db with a theoretical aperture gain of 34 db.
9) The effective radiated power will be about 25 dbw without final r-f amplifiers.
10) Weight of 8-by-8 system is 175 pounds.
11) No major catastrophic failures should occur.

As a result of the evaluation of both types of techniques, it is recommended that an engineering model of an 8-by-8, high-gain, multilobe, electronically steerable antenna system of the self-phased type be given first priority. This recommendation was based on the following conclusions:

1) The self-phasing system appears to offer a large growth potential for future applications because it is modular in concept; a 64-element unit is readily extended to any reasonable number of elements.
2) The self-phasing system is suitable for use with any type of stabilization, gravity-gradient, spin, or even no stabilization.
3) The self-phasing system can be used not only on satellites but also on spacecraft and space probes as well.
4) The self-phasing system can be mounted on surfaces of almost any shape. It is not restricted to planar or cylindrical surfaces.
5) The self-phasing system requires no programming of its pointing direction; it automatically points in the direction of the pilot signals.
6) The system has a very high reliability since the failure of a few channels does not appreciably degrade the system performance and does not introduce any holes in the pattern coverage.

6.3 APPLICATIONS OF SELF-STEERING TECHNIQUES TO MILLIMETER WAVES

A brief evaluation was made of the feasibility of extending the self-steering techniques, studied and implemented on this program, into the higher frequencies, from 10 to 100 GHz. This part of the spectrum, expecially the millimeter wavelengths (30 to 100 GHz), has seen a tremendous increase in activity in the last few years and this activity will continue. As the available allocations at the lower (cm)

frequencies are filled, it will become necessary to exploit higher frequencies -- the millimeter-waves.

Before presentation of the evaluation, a summary is given of both radio-wave propagation characteristics and antenna design considerations at the millimeter wavelengths. The information is drawn chiefly from the Phase I Interim Report (Kummer and Villeneuve, 1965). Components for the millimeter wavelengths are covered in considerable detail in Section 7 of that report. For the purposes of this report, it should suffice to note that r-f components such as circulators, isolators, switches, and filters become smaller for the higher frequencies, but their losses increase with increasing frequency. Crystal diodes and down-converters have an increase in noise figure, and transmitter power becomes more difficult to generate.

6.3.1 Propagation Characteristics

a) Increasing attenuation due to atmospheric absorption

Attenuation increases as the frequency increases, although low-loss frequencies (called windows) exist around 35 and 94 GHz. Attenuation will be lowest for vertical incidence and highest for propagation at low elevations tangent to the surface. (Straiton and Tolbert, 1963). Attenuation peaks occur at 25 GHz (1.25 cm) and at 60 GHz (5 mm), frequencies that find appropriate use in very short range systems for which privacy is desired. They can also be utilized to reduce interference between earth and satellites if employed in satellite-satellite systems.

Some of the estimated effects of atmospheric absorption are shown in Table 6-1. The values given for the various atmospheric conditions should be added to those listed in the first line for clear weather. For example, at 35 GHz the assumed atmospheric loss is

For clear weather path at 10^{o} above horizon	1.2 db
With light fog, add another	0.6 db
Total Loss about	2 db

Characteristics of Atmosphere	Attenuation at 35 Gc for Various Elevation Angles (db)			Attenuation at 94 Gc for Various Elevation Angles (db)		
	5°	10°	90° (Zenith)	5°	10°	90° (Zenith)
Clear weather	2.5	1.2	0.25	10	5	<1
Fog: visibility 2000 feet ($0.032\ g/M^3$)	1.2	0.6	0.1	5.7	2.9	0.5
Fog: visibility 400 feet ($0.32\ g/M^3$)	7.4	3.8	0.7	57	29	5.0
Fog: visibility 100 feet ($2.3\ g/M^3$)	63	32	5.5	>100	>100	40
Light rainfall: 1 mm/hr	11.4	5.7	1.0	40	20	<4
Moderate rainfall: 4 mm/hr	57	29	5	100	70	12.5
Heavy rainfall: 16 mm/hr	>100	>100	17.5	>100	>100	50

Table 6-1. Effects of atmospheric absorption.

The actual values, of course, depend on the location, elevation, and local weather of the terminal.

Researchers have pointed out that the attenuation by rain at millimeter wavelengths restricts the use of these frequencies for reliable earth-space communication. However, they also point out that no measurements of attenuation by rain have been published in the United States for a source located beyond the troposphere (URSI National Committee Report, 1964). Since the millimeter frequencies must eventually be utilized, it is expected that more intensive studies and measurements will have to be undertaken to determine the

radiowave propagation characteristics between earth and space with special emphasis on attenuation, multipath fading, usable bandwidths, and scintillations. At the present time, however, it is reasonable to conclude that earth-satellite communications will be restricted to the lower radio frequencies if reliable communications are to be maintained between an arbitrary point on the earth and space (Haydon, 1960; Perlman et al., 1959).

b) Path loss calculations

Antenna parameters vary with frequency as can be seen in calculations of the path losses. In these calculations, it is assumed that the usual free space transmission formula applies and that excess path loss has been neglected.

$$P_R = P_T \frac{G_T G_R \lambda_2}{(4 \pi R)^2} \tag{6-1}$$

For a satellite-to-satellite system it is reasonable to assume antennas of equal gain; thus,

$$G_T = G_R$$

and if $G_T = G_R$, then

$$G_T = G_R = G \tag{6-2}$$

For a constant ratio of P_R to P_T,

$$G^2 \lambda^2 = \text{constant}.$$

This relationship means that the required antenna gain is directly proportional to frequency. For a constant efficiency and given frequency, the antenna gain is proportional to the area of the aperture. For this particular system, the antenna area is inversely proportional to frequency.

6.3.2 Antenna Considerations

High gain and narrow beamwidths can be achieved at the millimeter frequencies with antennas of physically small sizes. The absolute accuracies with which the antenna must be fabricated increase in proportion to the frequency, however. Heat losses increase as well, because of the increasing ohmic losses. For earth-to-satellite systems, other parameters must also be taken into account, such as a fixed satellite antenna size, transmitter power, weight, etc. The antenna is not the only factor affecting the weight of the system. As was discussed in the Phase I report (Kummer and Villeneuve, 1965), for electronically steered antennas, including those which are self-steering, the weight of the electronics does not change appreciably as the r-f frequency into one module is increased. Rather, the weight directly depends on the number of modules. For a constant angle of coverage, the weight would increase directly as the gain.

6.3.3 Specific Satellite Self-Steering Systems

a) Discrete Beam (Transdirective)

The heart of the multiple-beam system at the lower frequencies is a beam-forming matrix. These matrices are composed of line lengths and 3-db directional couplers made of strip transmission lines. All the components are carefully adjusted for proper phasing. A two-dimensional matrix of 8-by-8 ports can be projected to 10 GHz with reasonable assurance of success, both in terms of phasing and acceptable loss (3 db or less). It is estimated, however, that the technique cannot be extended much beyond 10 GHz. Problems include both increasingly tight tolerances and increasing losses.

The transdirective concept is applicable at the higher millimeter frequencies with optical equivalents such as one or two-dimensional lenses. Large one-dimensional (cylindrical) lenses made of quartz have been fabricated, tested, and evaluated. A lens 18 inches in diameter was tested at 56 GHz. It has a half-power beamwidth of one degree, which corresponds to an 80 percent use of the aperture; gain has not yet been measured. Smaller lenses of the same shape have also

been shown to be very efficient at these frequencies. The problem with the quartz lenses is their weight: a 10-inch diameter lens of spherical shape would weigh 73 pounds. Lightweight lenses (density 0.4) are being investigated and are showing promise (Mosaic, 1965). Development must also include feeds, isolators, and other r-f components. Some are available or can be developed for space application (Kummer and Villeneuve, 1965). While these components will become smaller, a problem that remains is the logic circuitry which will remain nearly unchanged.

Some of the specific implementations of scanning techniques applicable to the transdirective concept at the millimeter wavelengths are discussed in the Phase 1 report. Newer implementations include digitally scanned systems that utilize lenses and miniaturized ferrite switches, such as the one pictured in Figure 6-1. This switch consists of a ferrite core and metal matching post fitted into a waveguide aperture. Several ferrite materials and configurations were

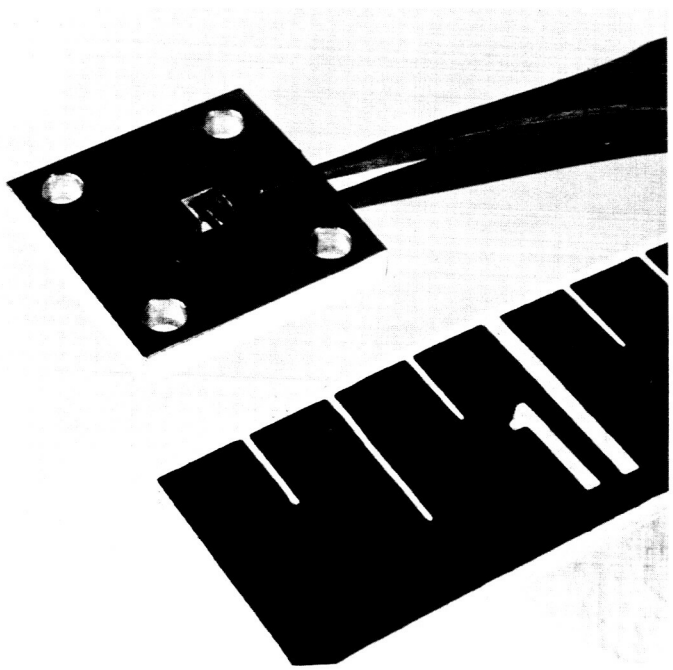

Figure 6-1. Miniaturized ferrite switch for digitally scanned millimeter-wave system.

tested with an external magnetic field in the vicinity of the ferrite slab. Typical switching ratios of 30 db with a forward insertion loss of 0.2 db were achieved at 34 GHz. Higher switching ratios were obtained but with a corresponding increase in forward loss. Careful selection of ferrite material and careful design of the matching post should provide a loss in the switched state greater than 40 db with an 0.1 db forward loss.

A ferrite switch can be used with a digital scanner in a configuration such as that discussed in the Phase 1 report (see Figure 6-2), but the range of scanning is limited to about 120 degrees with this type of arrangement. The array of switched apertures tends to block the aperture for large scan angles. The feed structure can be rearranged, however, in a configuration such as that sketched in Figure 6-3 to produce 360 degrees of scanning with either circular or linear polarization.

b) Self-Phased Arrays

The self-phasing techniques can be extended to 100 GHz but at the expense of loss and degradation in signal-to-noise on receive. These degrations can be expected at the present because mixers with noise figures comparable to those at centimeter wavelengths are not available. It should be pointed out that the degradation will occur equally in any single-port receiving system that utilizes these mixers. Thus, the self-phasing systems will be competitive with the mechanically scanned systems on receive. However, on transmit, there will be degradations due to the lack of efficient up-converters and the unavailability of solid-state millimeter-wave amplifiers.

6.3.4 Conclusions

The transdirective and self-phasing techniques developed on this program can be extended to millimeter waves. However, to make these systems attractive for application to space communications, special components for the high frequencies must be developed.

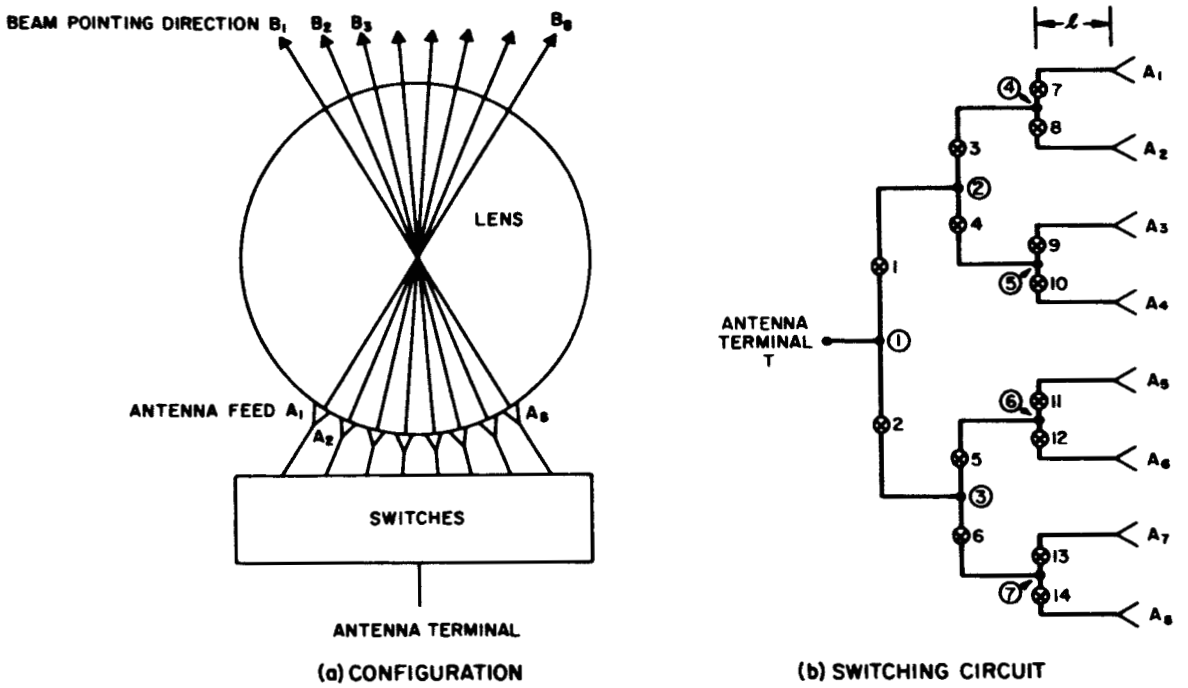

$A_1 \ldots A_8$	FEEDS DISTRIBUTED OVER SURFACE OF SPHERE OR ALONG PERIPHERY OF CYLINDRICAL LENS
$B_1 \ldots B_8$	BEAM POINTING DIRECTIONS FOR FEED $A_1 - A_8$, RESPECTIVELY
⊗1. ... ⊗14	SWITCHES
①, ②, ... ⑧	JUNCTIONS

ANTENNA FEED CONNECTED	SWITCHES ACTUATED
A_1	2, 4, 8
A_2	2, 4, 7
A_3	2, 3, 10
A_4	2, 3, 9
A_5	1, 6, 12
A_6	1, 6, 11
A_7	1, 5, 14
A_8	1, 5, 13

Figure 6-2. Multiple feed scanning antenna utilizing switches.

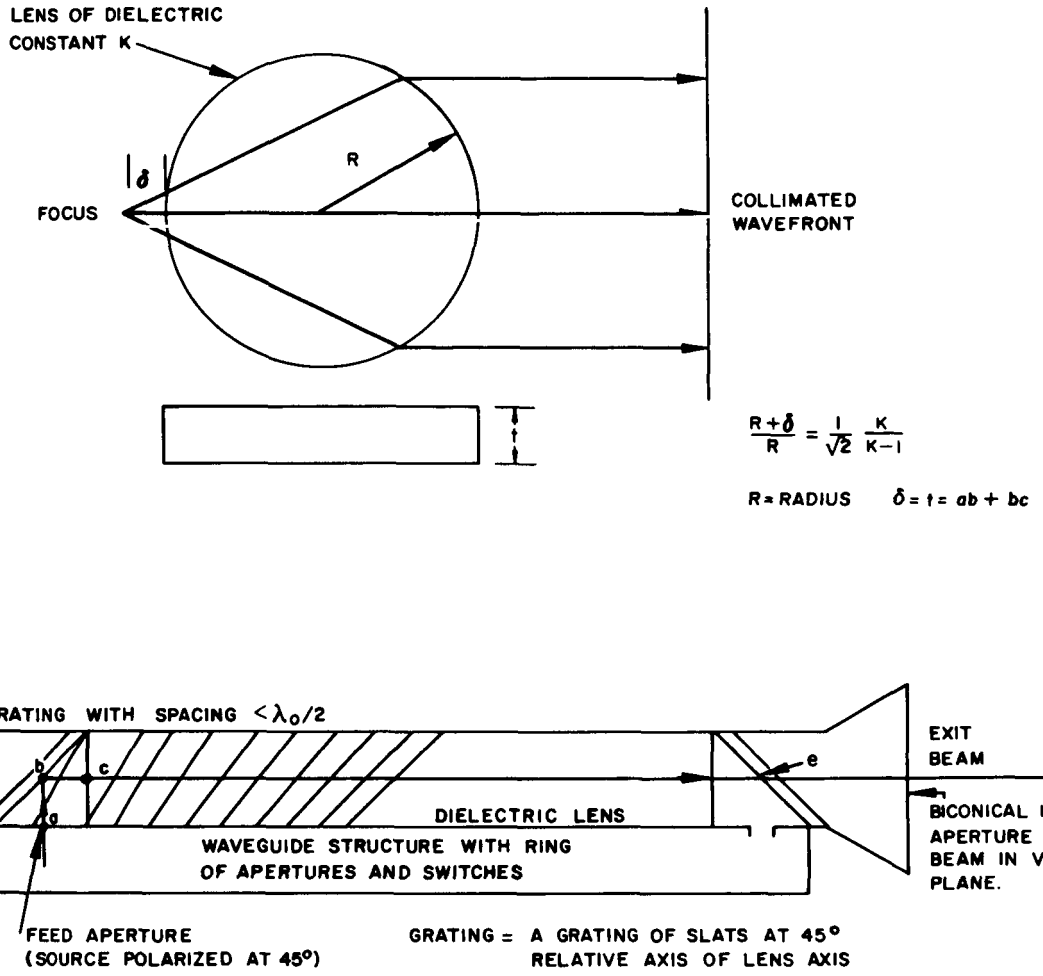

Figure 6-3. Alternative multiple feed scanning configuration producing 360 degrees of scan.

The most applicable electronic technique is the discrete beam array that utilizes some implementation of the transdirective electronics. Lens antennas should be used as the beam-forming element.

The second technique is the mechanically scanned feed in back of a lens. A mechanically scanned planar array would be a third choice.

Self-phasing arrays would be applicable on receive but not on transmit at these frequencies.

6.3.5 Recommendations

It is recommended that the millimeter-wave techniques be studied intensively and be evaluated for spacecraft applications. Particular attention should be paid to the fact that this region is a transition between the array (discrete) and continuous (optical) aperture techniques. The optimum combination of techniques from both disciplines should be exploited.

Critical areas to be investigated include:

(1) The realization of high gain from physically small apertures without excessive loss.

(2) The pointing and steering of these arrays in a particular direction in space.

(3) The implementation of steering techniques which obviate the need for accurate stabilization and which use efficient components.

(4) The models of satellite systems which emphasize the satellite to satellite communication.

7.0 REFERENCES

Haydon, J. W. (1960). Optimum frequencies for outer space communication, NBS J. Res. 64D, No. 2, 105-109.

Kummer, W. N., and A. T. Villeneuve (1965). Spacecraft Antenna Systems, Interim Engineering Report on Contract NAS 5-3545 (Phase 1 - Final Report), No. P65-35, Hughes Aircraft Company, Culver City, California.

Mosaic Radar Study Program (1965). Quarterly Progress Report No. P66-43, Hughes Aircraft Company, Culver City, California.

Perlman, S., et al. (1959). Concerning optimum frequencies for space communications, IRE Trans. CS-7, 167.

Straiton, A. W., and C. W. Talbert (1963). Factors affecting earth-satellite millimeter wavelength communications, IEEE Trans MTT-11, 296.

Technical Report - Feasibility Models (1966). Spacecraft Antenna Systems (Contract NAS 5-3545), Report No. P66-48, Hughes Aircraft Company, Culver City, California.

URSI National Committee Report (1964). Tropospheric propagation affecting space communications. Commision II. NBS J. Res., Radio Science 68D, 558.